UNIVERSITY OF THESSALY


DOCTORAL THESIS

# Study and development of algorithms for managing and optimizing wireless resources in environments of multiple technologies

Author:
Kostas Chounos

Supervisor:
Assoc. Prof. Athanasios Korakis

Dissertation Committee:
Assoc. Prof. Athanasios Korakis
Prof. Leandros Tassiulas
Assoc. Prof. Antonios Argyriou

*A thesis submitted in fulfillment of the requirements for the degree of Doctor of Philosophy*

*in the*

Department of Electrical and Computer Engineering

November 16, 2021

# Declaration of Authorship

I, Kostas Chounos, declare that this thesis titled, "Study and development of algorithms for managing and optimizing wireless resources in environments of multiple technologies" and the work presented in it are my own. I confirm that:

- This work was done wholly or mainly while in candidature for a research degree at this University.
- Where any part of this thesis has previously been submitted for a degree or any other qualification at this University or any other institution, this has been clearly stated.
- Where I have consulted the published work of others, this is always clearly attributed.
- Where I have quoted from the work of others, the source is always given. With the exception of such quotations, this thesis is entirely my own work.
- I have acknowledged all main sources of help.
- Where the thesis is based on work done by myself jointly with others, I have made clear exactly what was done by others and what I have contributed myself.

Signed: _____

Date: _____

*"Life is like a marathon:*
*You should start strong, but it is imperative to finish even stronger."*

ΠΑΝΕΠΙΣΤΗΜΙΟ ΘΕΣΣΑΛΙΑΣ

# Περίληψη

Τμήμα Ηλεκτρολόγων Μηχανικών και Μηχανικών Υπολογιστών

Διδακτορικό Δίπλωμα Ειδίκευσης

**“Μελέτη και Ανάπτυξη Αλγορίθμων Διαχείρισης & Βελτιστοποίησης Ασύρματων Πόρων σε Περιβάλλοντα Ύπαρξης Πολλαπλών Προτύπων”**

Κώστας Χούνος

Λόγω των ριζικών αλλαγών στην καθημερινότητα μας, μια απότομη αύξηση της παγκόσμιας ασύρματης συνδεσιμότητας έχει παρατηρηθεί τα τελευταία χρόνια. Επομένως, τα παραδοσιακά δίκτυα μεγάλης εμβέλειας (macro-cells) είναι πλέον ανεπαρκή να εξυπηρετήσουν αποτελεσματικά τις απαιτήσεις των χρηστών τους. Αυτό οδήγησε στην παράλληλη ανάπτυξη μικρότερων και πυκνότερων ετερογενών κυψελών (Heterogeneous networks), η οποία προτείνεται ευρέως στο πλαίσιο των δικτύων 5ης γενιάς (5G). Επιπρόσθετα, εκεί εμφανίζονται οι έννοιες του «softwarization» και «cloudification», επιτρέποντας έτσι την εκμετάλλευση όλων των διαθέσιμων δικτυακών πόρων (radio resources) με ενιαίο τρόπο. Εκ πρώτης όψεως, τα παραπάνω φαντάζουν ιδανική λύση για το φαινόμενο έλλειψης πόρων (capacity crunch). Παρόλα αυτά, αρκετή προσοχή πρέπει να δοθεί, καθώς η πλειοψηφία των πυκνά τοποθετημένων ετερογενών κυψελών (ultra-dense HetNets) στα δίκτυα 5G περιέχει τεχνολογίες και πρότυπα που χρησιμοποιούν τις ίδιες περιορισμένες ζώνες συχνοτήτων. Εκτός αυτού, ελάχιστος έως καθόλου συντονισμός υπάρχει μεταξύ αυτών των προτύπων στα επίπεδα προτεραιότητας μεταδόσεων και συνύπαρξης. Επομένως, μεγάλη ποσότητα απρόβλεπτων παρεμβολών δημιουργείται, γεγονός που οδηγεί σε αμφισβητήσιμη απόδοση σε αυτά τα περιβάλλοντα. Τέλος, αφενός μεν ο χειρισμός των ασύρματων δικτυακών πόρων ως υπηρεσία (radio as a service) μπορεί να οδηγήσει σε πιο αποτελεσματική χρήση πόρων και σε σύγκριση με την στατική κατανομή φάσματος. Αφετέρου, αυτό αυξάνει κατά πολύ την πολυπλοκότητα όσον αφορά την ενορχήστρωση του δικτύου.

Για να αντιμετωπιστεί αποτελεσματικά η έλλειψη φάσματος, απαιτείται προσεκτικός δικτυακός σχεδιασμός και ευέλικτη διαχείριση πόρων. Στόχος αυτής της διδακτορικής διατριβής είναι η ανάπτυξη και παρουσίαση νέων μοντέλων και μηχανισμών, τα οποία βελτιώνουν την αξιοποίηση των πόρων σε σύγχρονα ασύρματα συστήματα πολλαπλών προτύπων. Αρχικά, η παρούσα διατριβή, ασχολείται με τον εντοπισμό και την αποφυγή παρεμβολών στα ευρέως διαδεδομένα συστήματα IEEE 802.11 (Wi-Fi). Δεδομένου ότι το πρότυπο Wi-Fi κατέχει σημαντικό ρόλο στα δίκτυα 5G, η διατριβή αυτή παρουσιάζει αναλυτικά πως η ορθή φασματική ανάλυση μπορεί να ενισχύσει την απόδοση του δικτύου κάτω από σχήματα επιλογής σταθμού βάσης, επιλογής καναλιών και πρόβλεψης παρεμβολών στο μέλλον. Επιπρόσθετα, η διατριβή αυτή εστιάζει και στην δυναμική μίσθωση και τιμολόγηση των ασυρμάτων πόρων δικτύωσης σε περιβάλλοντα 5G. Για τον λόγο αυτό, δημιουργούνται τα προσχέδια για μια οντότητα που έχει ως σκοπό την δυναμική τιμολόγηση του διαθέσιμου φάσματος. Τέλος, αξίζει να σημειωθεί, ότι όλα τα μοντέλα και οι μηχανισμοί που αναπτύχθηκαν στο πλαίσιο αυτής της διατριβής έχουν αξιολογηθεί πειραματικά σε πραγματικές ασύρματες υποδομές (wireless testbeds).

UNIVERSITY OF THESSALY

# Abstract

Department of Electrical and Computer Engineering

Doctor of Philosophy

**"Study and development of algorithms for managing and optimizing wireless resources in environments of multiple technologies"**

by Kostas Chounos

Due to the radical changes in our daily habits, a persistent raise of global wireless traffic has been observed during the past years. Consequently, the traditional macrocell networks, are now incapable of serving their users requirements efficiently. This led to the parallel deployment of smaller and denser heterogeneous cells, which is vastly proposed in the context of 5G architectures. Additionally, the principles of softwarization and cloudification are widely applied in those architectures, thus enabling the exploitation of all the available radio resources in a unified way. At first glance, using the aforementioned techniques may seem an ideal solution to the capacity crunch phenomenon. However, the majority of the densely deployed heterogeneous cells in 5G networks are operating under the same limited spectrum bands, with little or no coordination at all. Therefore, large amount of unpredicted interference is present, which leads to questionable performance at these environments. Additionally, on the one hand, treating the radio resources as a service may result in a more efficient resource utilization, compared to the static spectrum allocation. On the other hand, this also increases greatly the complexity in terms of network orchestration.

To effectively eliminate the capacity shortage, the careful network planning and the agile resource management are now considered essential. The aim of this doctoral thesis is to develop and present novel frameworks that improve the resource utilization in modern heterogeneous wireless systems. Initially, this dissertation deals with the interference detection and avoidance at the widely deployed IEEE 802.11 systems. As the Wi-Fi standard is playing a significant role in 5G networks, this thesis analytically presents how the increased spectral awareness can boost network performance under user association, channel selection and interference prediction schemes. Last but not least, this thesis also focuses on dynamic leasing and pricing of networking resources in 5G multi-tenancy environments. The blueprints for a dynamic Policy and Charging Control core network entity are created under the use of Service Level Agreements. It is worth to be noted that all the frameworks developed in the context of this thesis have been experimentally evaluated in real wireless testbeds.

# *Acknowledgements*

Upon the completion of this thesis , I would sincerely like to express my deep gratitude to several people. They generously provided guidance and support during these years and in such way contributed significantly to the completion of my PhD studies.

First and foremost, I would like to thank my supervisor Assoc. Prof. Thanasis Korakis, as well as Prof. Leandros Tassiulas, for the trust and guidance they gave to me during the past years. The great opportunity I was offered to deal with contemporary research topics, holds great importance at my personal evolution in the University of Thessaly. Additionally, I would like to thank Assoc. Prof. Antonios Argyriou who was involved as a member of the dissertation committee. Of course, special thanks also to Assoc. Prof. Iordanis Koutsopoulos, Assoc. Prof. Gerasimos Potamianos, Prof. Spyros Lalis and Prof. Symeon Papavassiliou for accepting to serve in the examination committee of my thesis.

Furthermore, I would like to express my gratitude to all current and past NITlab members, for the smooth and pleasant cooperation we had. Separately, I would like to thank Ilias Syrigos, Virgilios Passas, Yiannis Zografopoulos and Panagiotis Skrimponis, with whom, we have shared many pleasant experiences during the past years. Moreover, many thanks to Apostolos Apostolaras, George Iosifidis, Nikos Makris, Stratos Keranidis, Giannis Kazdaridis and Kostas Choumas, who shared their research insight and in such way continuously encouraged me to keep going. Of course, apart from the lab colleagues, special thanks also to Evmorfia, Akis, Nikos, Dimitris, Lia, Evi, Thanasis and all of my close friends who provided everyday support and motivation.

Last but not least, there are no words to express the love and gratitude for my family. None of what I have achieved until today would be possible without their support. More specifically, Christos my father, an engineer who strongly motivated me from young age to deal calmly with all problems arised. Rena, my mother, who taught me to be persistent and honest, even when it comes with a great cost. Panagiotis, my elder brother and running partner, who continuously encouraged me to maximize the efforts and exceed my goals. Elli, my wife, who generously gave me love, courage and support from the first day we met. This thesis is specially dedicated to them...

# *Publications*

The ideas as well as the algorithms, figures and results of this thesis, are part of the following publications:

- **Journals**

  **[J1:]** K. Chounos, P. Karamichailidis, N. Makris and T. Korakis. **"Unlicensed Spectrum Forecasting: An Interference Umbrella based on Channel Analysis and Machine Learning"**, *(revised and resubmitted for publication) to IEEE Transactions on Network Science and Engineering*, 2021, IEEE

- **Conferences**

  **[C1:]** K. Chounos, A. Apostolaras and T. Korakis **"A Dynamic Pricing and Leasing Module for 5G Networks"**, *in the proceedings of IEEE 5G World Forum (5GWF), 2020, IEEE*

  **[C2:]** A. Apostolaras, K. Chounos, L. Tassiulas and T. Korakis **"Servicing Inelasticity, Leasing Resources and Pricing in 5G Networks"**, *in the proceedings of International Symposium on Modeling and Optimization in Mobile, Ad Hoc, and Wireless Networks (WiOPT), 2020, IEEE / IFIP*

  **[C3:]** K. Chounos, N. Makris and T. Korakis **"Enabling Distributed Spectral Awareness for Disaggregated 5G Ultra-Dense HetNets"**, *in the proceedings of IEEE 5G World Forum (5GWF), 2019, IEEE*

  **[C4:]** K. Chounos, S. Keranidis, A. Apostolaras and T. Korakis **"Fast Spectral Assessment for Handover Decisions in 5G Networks"**, *in the proceedings of IEEE Consumer Communications & Networking Conference (CCNC), 2019, IEEE*

  **[C5:]** K. Chounos, S. Keranidis, T. Korakis and L. Tassiulas **"Characterizing the impact of interference through spectral analysis on commercial 802.11 devices"**, *in the proceedings of IEEE International Conference on Communications (ICC), 2017, IEEE*

Furthermore, there were research efforts within the same or previous periods, led to the following publications which are not directly correlated with this thesis:

- **Journals**

  **[J1:]** A. Apostolaras, G. Iosifidis, K. Chounos, T. Korakis and L. Tassiulas **"A Mechanism for Mobile Data Offloading to Wireless Mesh Networks"**, *IEEE Transactions on Wireless Communications*, 2016, IEEE

- **Conferences**

**[C1:]** D. Syrivelis, G. Iosifidis, D. Delimpasis, K. Chounos, T. Korakis and L. Tassiulas **"Bits and coins: Supporting collaborative consumption of mobile internet"**, *in the proceedings of IEEE International Conference on Computer Communications (INFOCOM), 2015, IEEE*

**[C2:]** A. Apostolaras, G. Iosifidis, K. Chounos, T. Korakis and L. Tassiulas **"C2M: Mobile data offloading to mesh networks"**, *in the proceedings of IEEE Global Communications Conference (GLOBECOM), 2014, IEEE*

**[C3:]** S. Keranidis, V. Passas, K. Chounos, W. Liu, T. Korakis, I. Koutsopoulos, I. Moerman and L. Tassiulas, **"Online Assessment of Sensing Performance in Experimental Spectrum Sensing Platforms"**, *in the proceedings of ACM Workshop on Wireless Network Testbeds, Experimental evaluation & CHaracterization (WiNTECH), 2014, ACM*

- **Demos**

**[D1:]** S. Keranidis, K. Chounos, T. Korakis, I. Koutsopoulos, and L. Tassiulas, **"Enabling AGILE Spectrum Adaptation in Commercial 802.11 WLAN Deployments"**, *in the proceedings of the Annual International Conference on Mobile Computing and Networking (MobiCom), 2014, ACM*

**[D2:]** V. Passas, K. Chounos, S. Keranidis, W. Liu, L. Hollevoet, T. Korakis, I. Koutsopoulos, I. Moerman, L. Tassiulas, **"Online Evaluation of Sensing Characteristics for Radio Platforms in the CREW Federated Testbed"**, *in the proceedings of the Annual International Conference on Mobile Computing and Networking (MobiCom), 2013, ACM*

# Contents

# List of Figures

# List of Tables

# List of Abbreviations

| | |
|---|---|
| **5G-NR** | 5G New-Radio |
| **ABS** | Almost Blank Sub-frames |
| **ACS** | Automatic Channel Selection |
| **ANDSF** | Access network discovery and selection function |
| **AP** | Access Point |
| **B2B** | Business to Business |
| **C-DU** | Coordinated Distributed Units |
| **CCA** | Clear Channel Assessment |
| **CHF** | 5G Charging Function |
| **CoMP** | Coordinated Multipoint |
| **COTS** | Commercial of the self |
| **CSA** | Channel Switch Announcement |
| **CSMA-CA** | Carrier's sense and multiple access - Collision Avoidance |
| **CU** | Central Unit |
| **CW** | Contention Window |
| **DC** | Duty Cycle |
| **DCF** | Distributed Coordination Function |
| **DCS** | Dynamic Channel Selection |
| **DenseNets** | Dense Networks |
| **DIFS** | DCF Interframe Spaces |
| **DL** | Downlink |
| **DoF** | Degree of Freedom |
| **DU** | Distributed Unit |
| **eCIC** | enhanced InterCell Interference Control |
| **ED** | Energy Detection |
| **EPC** | Envolved Packet Core |
| **FDD** | Frequency Division Duplexing |
| **FFT** | Fast Fourier Transfer |
| **GI** | Gurard Interval |
| **GRU** | Gated Reccurent Unit |
| **HetNets** | Heterogeneous Networks |
| **ICIC** | InterCell Interference Control |
| **InP** | Infrastructure Provider |
| **INT** | Interferer |
| **ISM** | Industrial, Scientific, and Medical (Unlicensed Frequency Bands) |
| **KPI** | Key Performance Inidicator |
| **LSTM** | Long short-term Memory |
| **LTE** | Long Term Evolution |
| **LTE-U** | LTE in Unlicensed spectrum |
| **LWAAP** | LTE-WLAN Aggregation Adaptation Protocol |
| **MCS** | Modulation and Coding Scheme |
| **ML** | Machine Learning |

| | |
|---|---|
| **MNO** | Mobile Network Operator |
| **NAV** | Network Allocation Vectror |
| **NF** | Network Functions |
| **NFV** | Network Functions Virtualization |
| **OFDM** | Orthogonal Frequency-division Multiplexing |
| **O-RAN** | Open RAN |
| **PBCH** | Physical Broadcast Channel |
| **PDCP** | Packet Data Convergence Protocol |
| **PCC** | Policy Charging Control |
| **PCF** | 5G Policy Charging Function |
| **PCRF** | Policy Control and Charging Rules Function |
| **PDR** | Packet Delivery Ratio |
| **PSD** | Power Spectral Density |
| **QoE** | Quality of Experience |
| **QoS** | Quality of Service |
| **RAN** | Radio Access Network |
| **RLC** | Radio Link Control |
| **RSSI** | Received Signal Strength Indicator |
| **RNN** | Recurrent Neural Network |
| **RNTIs** | Radio Network Temporary Identifiers |
| **S** | Spectral Sample |
| **SAE** | System Architecture Evolution |
| **SBA** | Service Based Architecture |
| **SC** | Sub-Carriers |
| **SDN** | Software Defined Network |
| **SDR** | Software Defined Radio |
| **SG** | Specifications Group |
| **SIFS** | Short Interframe Spaces |
| **SISO** | Single Input Single Output |
| **SLA** | Service Level Agreement |
| **SNR** | Signal to Noise Ratio |
| **SP** | Scanning Period |
| **SS** | Spatial Streams |
| **SUT** | System Under Test |
| **UE** | User Equipment |
| **UP** | Uplink |
| **URLLC** | Ultra Reliable and Low latency Communications |
| **VNF** | Virtual Network Function |
| **WLANSP** | Wireles LAN Selection Policy |

*Dedicated to my beloved family and friends…*

# Chapter 1

# Introduction

## 1.1 Motivation - Problem Statement

The ever-increasing need for continuous wireless connectivity observed in recent years, drastically formats the landscape of the communication systems given so far. Suffocating levels of congestion are noted at wireless infrastructures, which will be further increased. Indicatively, as it is stated at the latest Cisco [1] global forecast the 4G mobile connections will grow from 4.9 billion in 2020 to 6.0 billion until 2023. Additionally, regarding the 5G connections, they officially appeared on the scene in 2020 and will grow over 100-fold from about 13 million to 1.4 billion. In such way, by the end of 2023, there will be 11% devices and connections with 5G capabilities enabled. In parallel with cellular technologies, significant data demand increment is expected at the unlicensed spectrum bands as well. The IEEE 802.11 (Wi-Fi), can be given as the most typical example of an unlicensed spectrum protocol, which is widely deployed nowadays. There, a nearly a two-fold increment of global public Wi-Fi hotspots will take place between 2020 and 2023, with 11% of them supporting the recently established Wi-Fi 6 (IEEE 802.11ax).

As the 5G networks are emerging under several new use case scenarios [2, 3, 4], the Ultra Reliable and Low latency Communications (URLLC) [5], with wireless links reaching up to Gbps speeds are highly anticipated. However, the deployed monolithic long-scale cellular infrastructures, gradually proved inadequate to serve the increased wireless data demands efficiently. In such way, the vast majority of the upcoming 5G topologies, complementary deploy smaller and denser heterogeneous wireless cells. There, both the introduction of new devices (5G New-Radio) [6, 7] in several bands (cm/mm-Wave), alongside with the existing sub-6GHz technologies like LTE and Wi-Fi, are strategically used [8, 9, 10] for overcoming the capacity crunch problem. It is worth to be noted that after 3GPP's Release 17 [11], the integration of non-3GPP cells like Wi-Fi, will be officially part of the cellular networks at 5G. Therefore, huge emphasis is being lately given to the softwarization and virtualization according to which, all the available heterogeneous Radio Access Networks (RANs) can be aggregated at the cloud (Cloud-RAN) [12, 13], for increasing the overall wireless capacity needed by novel data-hungry user applications. Thus, the tight coordination of new-introduced with preexisting wireless standards, is considered essential in modern 5G and beyond architectures.

In an economic point of view, the base station cloudification and the joint integration of heterogeneous technologies in a unified way, will reduce significantly the

Capital expenditures (CAPEX) as well as the Operating expenses (OPEX) costs. Additionally, the symmetrical use of common physical infrastructures for more than one competitive Mobile Network Operators (MNOs) and Infrastructure Providers (InPs), will be supported under the use of Service Based Architectures (SBAs). To this end, the rise of 5G technology is also expected to create new collaboration opportunities among operators and enable new Business to Business (B2B) models [14, 15, 16]. Although this could be extremely tempting, as more efficient use of the available spectrum is expected, several challenges may arise. Distinct separation as well as proper orchestration and resource management, are essential for achieving smooth operation at 5G networks. The concept of network slicing [17] has been recently introduced in 5G architectures, which practically enables the partitioning of physical resources in independent logical networks. However, as 5G architectures strongly involve technologies which operate at the unlicensed spectrum with opportunistic access, both the isolation and the performance guarantees may be extremely challenging.

## 1.2 Thesis Synopsis - Contributions

Aim of this doctoral thesis is to present, analyze and experimentally evaluate the proposed models as well the developed frameworks. In brief, the proposed solutions are intend to utilize the limited available spectrum in a more efficient way and boost the achieved performance at the end users (UEs). It is worth to be noted that emphasis is given at protocols, which utilize either unlicensed or licensed spectrum frequencies for their operation. The fundamental questions that we try to answer in the context of this doctoral thesis are the following:

1. How can the precise detection of uncontrolled interference be achieved in the unlicensed Wi-Fi spectrum?
2. How should a UE extract sophisticated non-3GPP (Wi-Fi) association decisions in 5G environments?
3. How should the non-3GPP (Wi-Fi) Distributed Units (DUs) dynamically adjust their operating channels?
4. How can the future interference levels be predicted in the unlicensed Wi-Fi channels?
5. How can the performance of each wireless link (Wi-Fi) be precisely estimated by actively gathering several wireless metrics?
6. How can the resources be dynamically priced at 5G multi-tenancy environments?

The remainder of this thesis is stated below.

Initially, this dissertation focuses on examining standards, which use the unlicensed (ISM) bands as a home for their transmissions. Particularly, the widely deployed IEEE 802.11, which holds a key role at 5G networks is taken into consideration. In theory, the opportunistic channel access given at the ISM bands results in full

medium utilization and high performance. However, the denser wireless deployments in parallel with the constantly increasing data demands and number of wireless users, largely reduce the transmission opportunities. Practically, the ISM bands are now characterized by strong contention and high levels of uncontrolled interference. Therefore, proper ways are investigated in order to perceive and avoid the catastrophic interference in these challenging unpredicted environments. The comprehensive awareness achieved through spectrum sensing [18], tends to be the most prevalent way to accomplish that, resulting more efficient resource management [19, 20] and increased performance as well.

- **Spectrum Occupancy evaluation:** Initially, Chapter 2 contains a novel mechanism which perceives and quantifies the interference levels in the unlicensed spectrum. The proposed framework, exploits spectral measurements which extracted from the PHY-layer of commercial 802.11 chipsets for evaluating the spectral conditions in real-time. Based on a generic metric (Duty Cycle) and through energy detection, the proposed mechanism is capable of detecting not only Wi-Fi transmissions, but non-IEEE 802.11 interference as well. Finally, extensive experiments showcase the high detection accuracy achieved from the proposed scheme under several topologies and scenarios.

- **Spectrum Aware WLAN Roaming Selection:** In Chapter 3, a novel UE-driven scheme for optimal Wi-Fi association decisions is presented and experimentally evaluated, in the context of the 5G architectures. In contrast with the conventional approach (RSSI based) which is defined at IEEE 802.11 protocol, the proposed framework complementary considers the spectrum conditions at both Access Point (AP) and UE sides. In such way, the detection of spectrum anomalies like hidden terminal effects can be quantified, as the least normalized capacity for each available AP-UE link is calculated from the proposed model. Finally, the proper function of the proposed solution is confirmed through testbed experimentation.

- **Dynamic Wi-Fi Channel (Re)configuration for DUs:** A network architecture with heterogeneous basestations complying with the Cloud-RAN concept, is considered in the context of Chapter 4. There, multi-technology links are deployed for serving end users through two different paths (LTE and Wi-Fi). Bearing in mind the challenging spectral conditions given at the ISM bands, the proposed framework, describes a scheme for enabling dynamic channel selection and configuration at non-3GPP Distributed Units (DUs). Through dedicated signaling between the different participating units and the cloud located part of a base station, the most efficient frequency is selected on a real-time basis. Significantly higher performance noted for the Wi-Fi DUs during extensive experimentation and when the proposed mechanism is applied.

- **Interference Prediction and Link Performance Estimation:** As analytically demonstrated in previous chapters, the augmented spectral awareness strongly improves the network performance under several use cases. Although the utilization of Duty Cycle metric significantly determines the spectrum decisions taken so far, its exclusive use, may not reveal the exact transmission opportunities given in Wi-Fi frequencies. Thus, a novel entity (Monitor DU) which extends the architectural design given at Chapter 4, is introduced and evaluated in the context of Chapter 5. Through the active collection of several

additional wireless metrics (airtime, number of active terminals), the accurate performance for any given IEEE 802.11 link at the areas of supervision is calculated. More specifically, Long-term utilization predictions are exported through Machine Learning, regarding the next 2-hours in a minute accuracy. Furthermore, the exact throughput calculation is extracted through short-term predictions, and when the current conditions are largely differentiated from the long-term predictions. Finally, it is thoroughly proven that the proposed framework covers comprehensively the cases of both IEEE 802.11 and non interference, in Indoor and Outdoor uncontrolled experimental environments.

Furthermore, this thesis deals also with protocols which may also use licensed portions of spectrum. In contrast with the opportunistic channel access given at the unlicensed spectrum, there straightforward ways like frequency and time divisions [21, 22, 23], are established for sharing the available resources. As a result, distinct separation and isolation of the radio resources, as well as interference elimination are achieved at those bands. Thus, the expected Quality of Service (QoS) - Quality of Experience (QoE) [24, 25, 26] for each user, can be negotiated and ensured in advance among the network entities. However, the static spectrum allocation from MNOs which was widely applied until now, often lead to non-optimal resource utilization. To this end, 5G networks roll out the software-defined radio access network (SD-RAN) concept, through softwarization and cloudification. In such way, the aligned use of shared physical radio resources from multiple MNOs is now enabled. Hence, proper ways for dynamically managing and pricing the available network resources, are now investigated at 5G application scenarios.

- **Dynamic Resource Pricing and Leasing for 5G Networks:** In the context of Chapter 6, a novel framework for enabling dynamic Policy and Charging Rules in modern 5G multi-tenancy environments, is designed and presented. Based on our proposed theoretical work [27] and through recent technological advances, in this chapter the blueprints for a Policy and Charging Control (PCC) core network entity that it can dynamically coordinate pricing and leasing decisions are developed. The interactions between an Infrastructure Provider (InP) and MNOs are modeled as a Service Level Agreements (SLAs) and the dynamic charging rules are implemented as an extension of the 5G Policy Charging Function (PCF). Thus, the MNOs are able to instantiate tailored slices with adaptive pricing schemes, when their resources are insufficient to serve the connected users (UEs). Furthermore, extensive testbed experimentation showcases proper functioning of the proposed framework, under both UDP and TCP additional traffic demands.

Finally, Chapter 7 concludes this thesis by summarizing all the research contributions presented. Additionally, several extensions are described as potential future work.

# Chapter 2

# Spectrum Occupancy Evaluation

**Contents**



Performance experienced by end-users supporting the popular 802.11 protocol is significantly degraded in densely populated urban areas, mainly due to the extensive spectrum sharing and the resulting 802.11 impairments such as "hidden-terminals", overlapping channel interference, etc. Moreover, as the unlicensed spectrum is also home for other wireless technologies and a large range of RF devices, the experienced channel conditions further deteriorate due to cross-technology interference. While the various resulting phenomena can be efficiently mitigated by isolating affected links from interference sources over spectrum, 802.11 networks currently lack unified mechanisms for characterizing the impact of different interference sources across the available channel configurations. In this context, we take advantage of spectral measurements available at the PHY-layer of commercial 802.11 equipment, in order to develop a highly accurate spectral analysis mechanism that is able to quantify the impact of interference on WLAN performance. The developed distributed mechanism concurrently operates on all network nodes and characterizes the band of interest with minimal overhead. Through the implementation of our approach on commercial 802.11n chipsets and its detailed experimental evaluation, we showcase its applicability in characterizing the impact of spectrum congestion and interference in a unified way, towards driving efficient spectrum adaptation decisions.

## 2.1 Introduction

The wide adoption of wireless networking technologies in everyday life scenarios has created unprecedented levels of congestion in unlicensed frequency bands. Core factors impacting spectrum congestion include the ever-increasing density of WLAN deployments, along with the limited availability of non-overlapping channels and the uncoordinated management of common setups. In this context, it is rather common for 802.11 networks to experience extensive sharing of spectrum resources with

collocated links, thus providing fertile ground for the appearance of common 802.11 problems such as "hidden-terminals", channel overlapping etc. Consequently, the network performance experienced by 802.11 end-users in high density deployments is significantly degraded. Additionally, spectrum in unlicensed bands is also being heavily utilized by other wireless protocols (e.g., Bluetooth, Zigbee) and a large range of RF devices (e.g. cordless phones, security cameras), or even Microwave ovens. Several research approaches like [28, 29] have shown that non-Wi-Fi devices appear rather frequently and with fairly high signal strengths, resulting in strong cross-technology interference. Considering also that the concept of LTE in Unlicensed spectrum (LTE-U), originally proposed by Qualcomm in [30], and officially included from the release 13 of LTE standard [31], we clearly understand that the unlicensed spectrum will keep becoming increasingly crowded with diverse technologies. In addition, as the integration of Wi-Fi access in the cellular network is expected beyond 3GPP Release 17 [11] for 5G-NR, serious doubts about the achieved performance on these networks may arise.

The aforementioned interference sources pose even more critical impact on deployments supporting the latest wireless standard versions, which adopt channels of wider width. More specifically, IEEE 802.11n [32] supports up to 40 MHz channels and the IEEE 802.11ac [33], as well as next-gen IEEE 802.11ax [34], further increase the channel width up to 160 MHz, in an effort to improve the achievable data rates. Nonetheless, while the throughput performance of high SNR links nearly doubles when doubling the configured bandwidth, this property no longer holds in the presence of interference as presented in [35], thus showing that fixed application of wider channel widths (as followed by 802.11n) is not the optimal solution. Towards achieving fair spectrum sharing with legacy devices and avoiding cross-technology interference, the 802.11ac protocol allows channel bandwidth to be determined on a frame-by-frame basis. In spite of the extra protection mechanisms that 802.11ac features for combating interference, detailed experimental results provided in the recent studies [36, 37] showcased that performance is prone to both 802.11 and heterogeneous transmissions on secondary channels. Taking into account the above, we clearly understand that careful interference management needs to be applied in accordance with planned selection of primary channels, in order to take advantage of the excess capacity that larger channel widths are able to offer.

In this chapter, we propose a spectrum evaluation approach that is able to quantify the impact of various interference sources on WLAN performance in a unified way. The offered wide applicability and ease of deployment consist the proposed solution ideal for careful planning of channel assignments, as well as for driving efficient spectrum adaptation decisions for 802.11ac and beyond networks in the long term.

## 2.2 Related Work

A large body of research studies has focused on accurately characterizing the spectrum utilization in ISM bands. The works in [38, 39] presented detailed spectrum occupancy evaluations of the ISM band over diverse scenarios, by utilizing high precision devices like spectrum analyzers. The authors in [40] developed a frequency adaptation algorithm that aims at maximizing the achievable capacity and implemented their approach on a Software Defined Radio platform. On the other hand,

the work in [28] presented the innovative Airshark system that builds on the spectral analysis capabilities of commodity Wi-Fi hardware to provide identification of cross-technology interfering devices. Trying to address the common 802.11 problematic scenarios of "hidden and exposed terminals", the works in [41, 35] proposed approaches that resolve identified link conflicts through centralized scheduling, thus being applicable only to centrally managed WLANs.

Except from the aforementioned research approaches, several commercial frameworks provide ways of quantifying spectrum usage in ISM bands. More specifically, the Ubiquiti Air View [42] system enables extraction of useful information about spectrum usage and representation through Power Spectral Density (PSD) and Waterfall graphs. The Air Magnet system [43] provides more sophisticated capabilities, such as interference classification and Duty cycle evaluation. The most comprehensive solution appears to be the Cisco MERAKI framework [44], which supports quantification of both 802.11 and heterogeneous spectrum utilization and utilizes these data to configure updated channel configurations in an automated way. The common downside of all the above commercial frameworks is that they either prerequisite the use of additional hardware or induce network downtime, while the measurements collection process is running.

## 2.3 Contributions

In this chapter, we propose and develop a spectrum occupancy evaluation framework that relies on spectral measurements to quantify the impact of interference on the performance of 802.11 links. The key novelty of the proposed solution is that it takes advantage from the inherent spectrum sensing capabilities of commercial 802.11 hardware, thus providing for rapid deployment on existing 802.11 equipment. Identification of 802.11 link conflicts is executed in a distributed way through detailed interpretation of spectral measurements at both the transmitter and receiver sides of each link. Building the proposed mechanism on generic metrics that interpret raw spectral data, we offer the ability to detect transmissions of non-802.11 devices, consisting our solution aware of cross-technology interference as well. Through extensive experimentation in realistic testbed deployments and across a wide range of interference sources and scenarios, we verified the perceived spectrum evaluation accuracy along with the wide applicability of the proposed solution. Finally, at the end this chapter some initial experimental measurements are given, regarding the overhead injected from the proposed mechanism and under a generic configuration set.

## 2.4 Proposed System

Through this chapter, we build on the inherent spectrum sensing capabilities of 802.11 hardware to develop a spectral analysis mechanism that is able to quantify the impact of interfering transmissions to 802.11 links. Considering that the link of interest uses a specific central frequency $\mathcal{F}_c$ and channel bandwidth $\mathcal{BW}$, we propose to quantify spectrum utilization between frequencies $F_c$ - $BW/2$ and $F_c$ + $BW/2$ at both the transmitter and receiver to associate this information with the channel conditions experienced at each side.

### 2.4.1 802.11 Basics

According to the standard, 802.11 transceivers first employ the CSMA/CA procedure before initializing transmissions, in order to detect whether the detected Power level on $\mathcal{F}_c$ exceeds specified thresholds [45]. In the case where the detected power exceeds the Energy Detection (ED) threshold the medium is directly declared as busy, while in the case of power exceeding the lower Clear Channel Assessment (CCA) threshold and only if the 802.11 signal preamble is successfully decoded, the medium is defined to be busy. In both cases, transmissions are postponed to avoid collisions, while throughput performance is degraded proportionally to the amount of captured channel access time. On the other hand, if none of the above cases is satisfied, the medium is declared as idle and transmissions are allowed. However, the resulting throughput might still be degraded in the case that transmitted frames collide with other transmissions that are detected at high power levels at the receiver side. In this case, the probability of collisions depends on the amount of time captured by interfering nodes [46].

Based on the above observations, we aim at evaluating the amount of channel time captured at both the transmitter and receiver ends, in order to characterize how interference affects the protocol operation. To this aim, we employ the scanning capabilities of OFDM compatible hardware, as the 802.11 implements the OFDM scheme since the introduction of 802.11a and its posterior g, n and ac amendments. OFDM compatible receivers [47] feature hardware dedicated in implementing the Fast Fourier Transfer (FFT) algorithm, in order to convert received OFDM signals from time to frequency domain and feed data to the corresponding channel subcarriers $\mathcal{SC}$. This process includes the collection of a spectral sample $\mathcal{S}$ collected on $\mathcal{F}_c$, comprising the Power level received on each one of the $\mathcal{SC}$, and denoted by $\mathcal{P}(i, \mathcal{S}, \mathcal{F}_c)$, i $\in \mathcal{SC}$.

### 2.4.2 Spectrum Occupancy Evaluation

For the purposes of our evaluation, we decided to use the notion of *Duty Cycle* ($\mathcal{DC}$) as the core metric for describing the percentage of time in which the Power of the considered spectrum fragment exceeds a specific Power Threshold $\mathcal{P}_{\mathcal{TH}}$. We use $\mathcal{P}(\mathcal{S}, \mathcal{F}_c, \mathcal{BW})$ to denote the power of Spectral Sample $\mathcal{S}$ that has been collected on the central frequency $\mathcal{F}_c$, characterises a total bandwidth of $\mathcal{BW}$ MHz wide spectrum and calculated it as:

$$\mathcal{P}(\mathcal{S}, \mathcal{F}_c, \mathcal{BW}) = \sum_{i}^{\mathcal{SC}} \mathcal{P}(i, \mathcal{S}, \mathcal{F}_c) \tag{2.1}$$

where $P(i, \mathcal{S})$ denotes the power at each corresponding subcarrier of spectral sample $\mathcal{S}$. We also use $\mathcal{N}_S$ to denote the amount of samples that have been collected during the scanning process and correspond to a given $\mathcal{F}_c$. As our solution considers varying $\mathcal{BW}$ levels, we use $\mathcal{DC}(\mathcal{F}_c, \mathcal{BW})$ to denote the *Duty Cycle* of the spectrum part between frequencies $F_c$ - $BW/2$ and $F_c$ + $BW/2$ and calculate it as follows:

$$\mathcal{DC}(\mathcal{F}_c, \mathcal{BW}) = \frac{1}{\mathcal{N}_S} \sum_{S=1}^{\mathcal{N}_S} on(\mathcal{P}(\mathcal{S}, \mathcal{F}_c, \mathcal{BW}), \mathcal{P}_{\mathcal{TH}}) \tag{2.2}$$

where the function $on(\mathcal{P}(\mathcal{S},\mathcal{F}_c,\mathcal{BW}),\mathcal{P}_{\mathcal{TH}})$ is equal to 1 if the $\mathcal{P}(\mathcal{S},\mathcal{F}_c,\mathcal{BW})$ of the spectral sample under consideration exceeds the $\mathcal{P}_{\mathcal{TH}}$ threshold, and 0 otherwise.

There is a huge amount of works related with the definition of appropriate detection thresholds. However, as our system follows the standard 802.11 CSMA implementation, the CCA and ED thresholds as specified for each protocol version play the key role in performance (Table 2.1).

TABLE 2.1: IEEE 802.11 CCA and ED Thresholds.

| ***Channel Width*** | CCA (primary) | CCA (non-primary) | ED |
|---|---|---|---|
| ***20MHz(n)(ac)*** | -82dBm | -72dBm | -62dBm |
| ***40MHz(n)(ac)*** | -79dBm | -72dBm | -59dBm |
| ***80MHz(ac))*** | -76dBm | -69dBm | -56dBm |

More specifically, when estimating channel conditions at the transmitter side, we need to consider either the CCA for evaluating the amount of captured channel time by decodable 802.11 transmissions or the lower ED threshold for non-decodable 802.11 or non-802.11 transmissions. On the other hand, at the receiver side our evaluation takes into account only the higher CCA threshold as any signal exceeding this value is potential interference.

### 2.4.3 Implementation

Several commercial 802.11 devices (supporting the n and ac standards) developed by major vendors of wireless products, such as Qualcomm and Intel, provide access to raw spectral samples through interfaces implemented in Open-Source drivers (ath9k [48], iwlwifi [49], and ath10k [50], etc.). In this context, we employ the commercial Qualcomm AR9380 802.11n compatible chipset [51] that is 3x3 MIMO and supports the 20 MHz and 40 MHz channel widths and control it over the ath9k driver. The default ath9k implementation supports a background scanning mechanism at the station mode of operation, which scans the list of available 20 MHz channels for discover neighboring APs. Collection of spectral samples runs also in parallel over the list of channels accessed through the background scanning. The AR9380 remains on each channel for the scanning interval of $\sim$50 ms and supports the maximum sampling rate of $\sim$100 KSps, featuring also a relatively low channel switching delay of $\sim$1-2 ms.

In order to scan the 2.4 GHz ISM[1] band of interest that is 80 MHz wide, we need to manually execute it at least 4 times for steps of 20 MHz. Through tests, we observed that the AR9380 is able to efficiently store up to 250 spectral samples per scanned channel. While the sample collection procedure might end much sooner than the scanning interval, given the configured sampling rate and number of samples, the card will still remain on the channel. In order to decrease the overall overhead of the scanning operation, we decided to decrease the channel interval from 50 ms down to 15 ms, taking into account that the maximum signal under consideration would be the emission of MW ovens that lasts $\sim$ 8.8 ms. Moreover, we configured the sampling rate of 16.67 KSps, so that the collected samples are equally distributed over the

[1]It is worth to be noted, that all IEEE 802.11 mechanisms proposed in this thesis, are applicable for both 2.4 and 5GHz Wi-Fi bands.

scanning interval of 15 ms. Having significantly reduced the overall scanning overhead, we also decided to scan in steps of 10 MHz, so that we decrease the spectrum separation between the configured $\mathcal{F}_c$ and the detected signals. Thus we require 7 operations starting from frequency 2412 MHz and ending on 2470 MHz for covering the 80 MHz. Through extra driver modifications, we ported the above procedure at the AP side as well and also configured it to take place simultaneously at both sides, by utilizing Beacon timestamps for synchronization. The collected spectral samples across the whole band are subsequently fed to an external program written in C that interprets them in detailed Received Signal and Duty Cycle measurements, as described through equations (2.1) and (2.2). This chapter's implementation is based on 802.11n, thus we use the corresponding CCA and ED thresholds of -82 dBm and -62 dBm. We also verified the successful operation of our solution on the 802.11ac Qualcomm AR9880 chipset using ath10k driver. Finally, the spectral capabilities for all aforementioned wireless adapters are listed at Table 2.2.

TABLE 2.2: Atheros Chipset Sensing Capabilities

| **Bandwidth / Sub-carriers (MHz) ($\mathcal{SC}$)** | **Chipset Type** | |
|---|---|---|
| | ***AR9380*** | ***AR9880 / AR9880-BR4A v2*** |
| 20/56 | ✓ | ✓ |
| 40/128 | ✓ | ✓ |
| 80/256 | ✗ | ✓ |

It is worth to be noted that, throughout this dissertation all the experiments executed with spectral samples of 20MHz $\mathcal{BW}$ and 56 $\mathcal{SC}$. In such way, we are able to export detailed spectrum occupancy results for 20-160MHz channels, without losing useful information.

## 2.5 Initial Experiments

The detailed experimental evaluation that follows has been executed on the NITOS [52] indoor testbed that provides a wide range of wireless hardware in an interference-free environment. This first set of experiments focuses on validating the spectrum evaluation accuracy of the proposed mechanism across both 802.11 and cross-technology signals.

### 2.5.1 802.11 signal detection

The experimental setup includes four different 802.11n 20 MHz links ranging from high-SNR to low-SNR, which are also configured across five different Transmission Power values to transmit backlogged traffic using MCS 0. We use an extra node that operates in Monitor mode and an external Python script to log the RSSI of all received packets and compare it with the average Received Signal as estimated through equation (2.1) over the spectral data captured at the same node. In Fig. 2.1, we observe the perceived accuracy of our Received Signal estimation across a wide range of link SNRs. More specifically, we observe that the measurements obtained

from the Monitor interface, fully converge with those exported from the proposed framework.

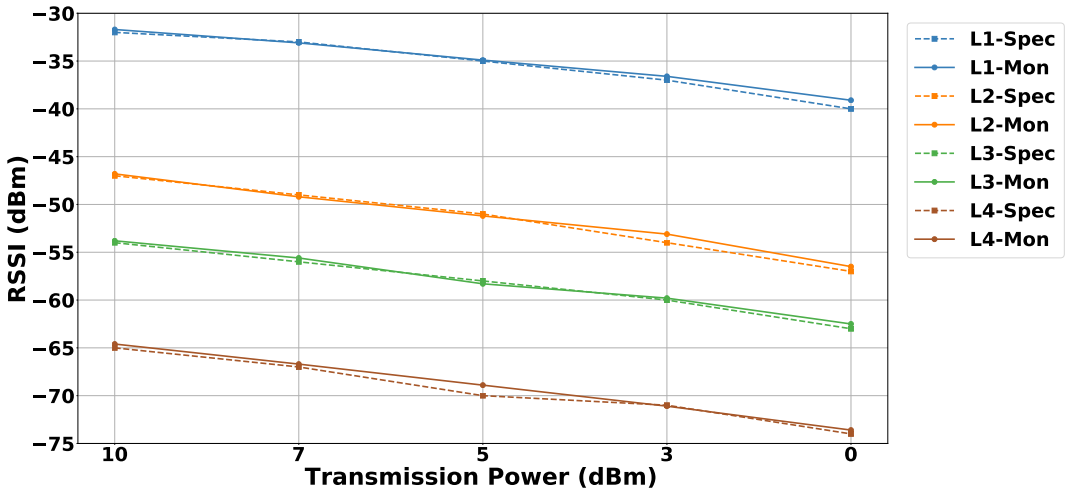


FIGURE 2.1: RSSI Detection Accuracy

Next, we focus solely on the high-SNR link and configure it to use 5 different MCS configurations (0, 3, 7, 10, 13) and also four different application-layer traffic loads to vary the occupied channel airtime. The same node is used to sniff all transmitted packets and calculate the occupied channel time through the Python script by aggregating the duration of each captured frame. Fig. 2.2 presents the collected results and verifies the accuracy of the $\mathcal{DC}$ estimation. More specifically, we observe that for the MCS 0 scenario the $\mathcal{DC}$ closely approximates the channel airtime, while the deviation slightly increases for higher MCSs with the maximum value measured to be $\sim$11% for the highest traffic load of MCS 7. Having verified the accuracy of detecting 802.11 transmissions, we next proceed by experimenting with signals of heterogeneous technologies.

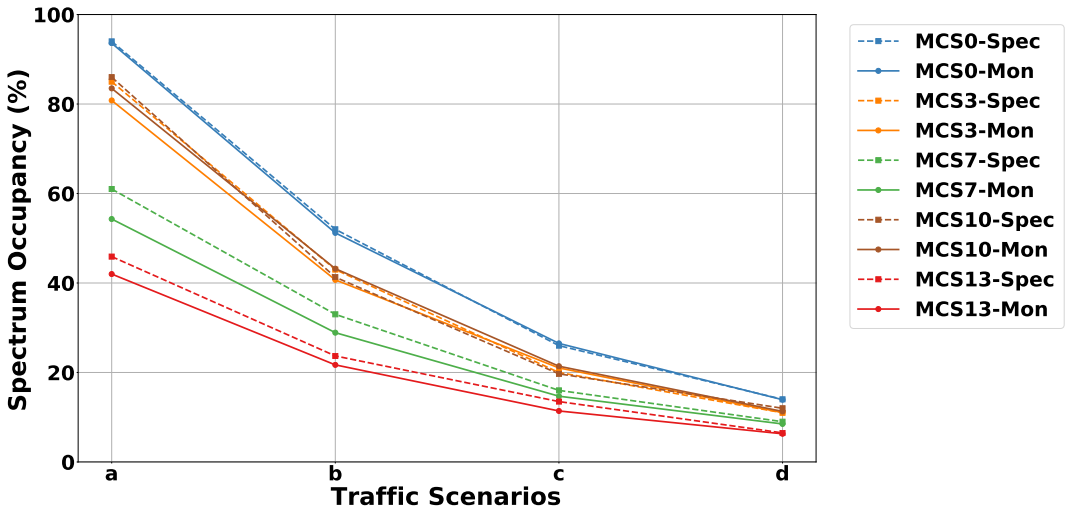


FIGURE 2.2: Airtime Detection Accuracy

### 2.5.2 Cross-technology signal detection

For this purpose, we generate transmissions through different types of RF hardware to characterize the resulting PSD and $\mathcal{DC}$ evaluation over the 2.4 GHz band. More specifically, we use an 802.11n link that transmits saturated traffic at MCS 7, a Bluetooth 4.0 dongle, while we also configure a USRP B210 [53] to emulate the signal transmitted by a Microwave oven and an LTE-U femtocell. To setup the LTE-U eNodeB device, we use the opensource srsLTE framework [54]. During the operation of each different device, we plot the PSD as captured by our sensing mechanism in Figures 2.3(a), 2.4(a), 2.5(a) and 2.6(a), while Figures 2.3(b), 2.4(b), 2.5(b) and 2.6(b) depict the $\mathcal{DC}$ evaluation.

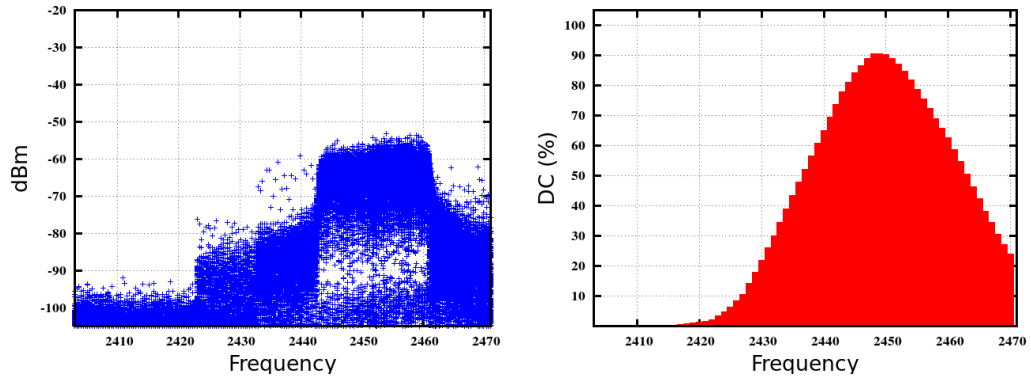


(a) 802.11n 20MHz - PSD (b) 802.11n 20MHz - DC

FIGURE 2.3: IEEE 802.11n 20MHz Captured Transmission

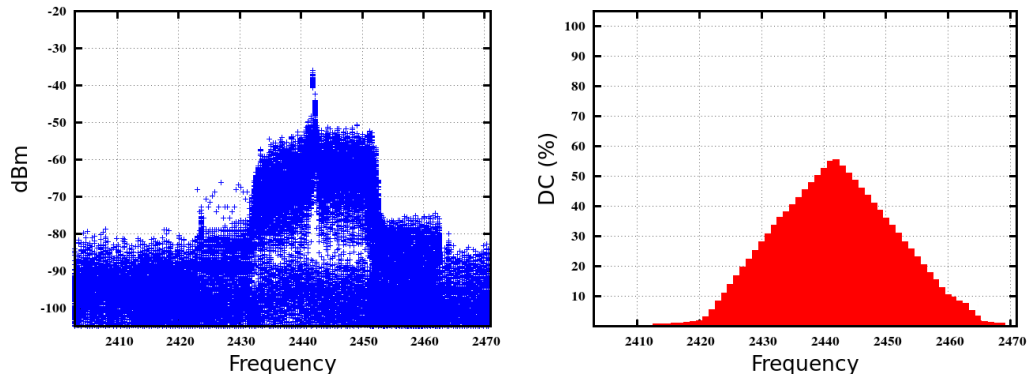


(a) Microwave Oven - PSD (b) Microwave Oven - DC

FIGURE 2.4: Microwave Oven Captured Emission

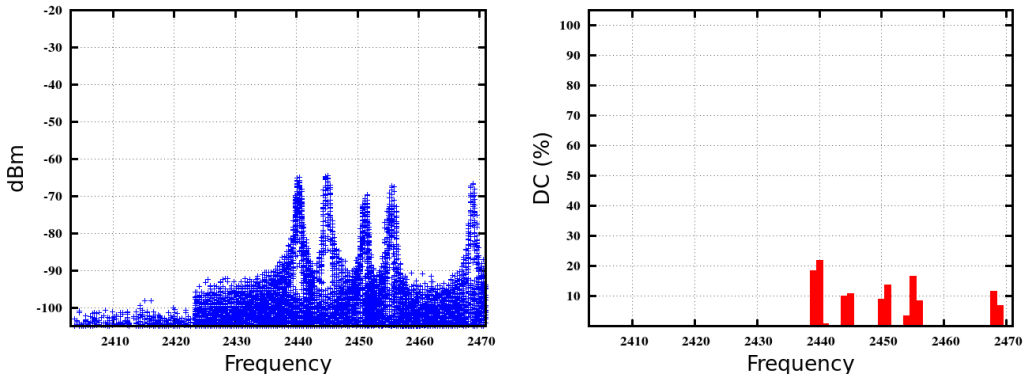


(a) Bluetooth 4.0 - PSD (b) Bluetooth 4.0 - DC

FIGURE 2.5: Bluetooth 4.0 Captured Transmission

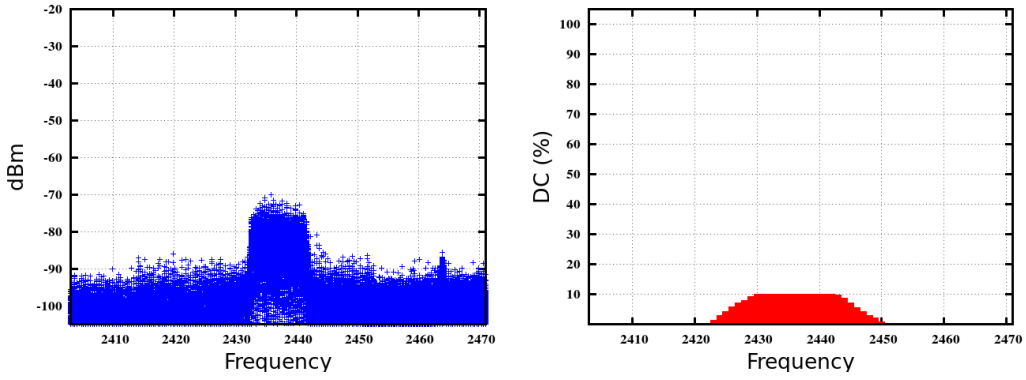


(a) LTE-U - PSD (b) LTE-U - DC

FIGURE 2.6: LTE-U Captured Transmission

We clearly observe the high spectrum utilization (∼90%) that 802.11n links are able to achieve at high AMPDU aggregation sizes, along with the precise detection of the $\mathcal{DC}$ of microwave ovens that typically emit high RF energy in 2.44-2.47 GHz frequencies with $\mathcal{DC}$ of ∼50%, as mentioned in [28]. Moreover, we are also able to capture transmissions of the Bluetooth that performs frequency hopping and efficiently detect spectrum fragments, on which the frequency hopping devices operate less frequently. In Fig. 2.5(b), we depict the $\mathcal{DC}$ evaluation when considering channels of 1 MHz width, as channels 20 MHz presented zero $\mathcal{DC}$. Our observations agree with other cross-technology interference related studies [28, 29] that characterize Bluetooth as a light interference source that only minimally affects the performance of 802.11 links, due to its relatively low transmission power. The emulated LTE-U device implements the eNodeB, utilizing 10 MHz of bandwidth and transmitting System Information Broadcasting messages over the Physical Broadcast Channel (PBCH) [31]. Though the $\mathcal{DC}$ evaluation, we notice the remarkably high signaling overhead of ∼10% that is used by LTE systems for broadcasting purposes.

## 2.6 Experimental Evaluation

In this section we present a thorough analysis of 802.11 problematic scenarios through the proposed approach. We deploy our mechanism on an 802.11n link (referred as System under Test - SUT) and use another 802.11n link as the interference source (referred as Interferer - INT). More specifically, we experiment with "hidden-terminal" and adjacent channel interference scenarios. Taking advantage of detailed statistics exposed by the ath9k driver, we also log the MAC layer Packet Delivery Ratio (PDR) performance, for aiding in interpretation of experimental results.

### 2.6.1 Hidden-terminals

For the purposes of this experiment, we configure two links that appear to be hidden to each other. More specifically, the INT link appears to be hidden to the transmitter of the SUT link while the receiver is directly impacted by INT transmissions. We verify this claim, by ensuring that the SUT transmitter cannot decode any frames of the INT link when sniffing in Monitor mode. On the other hand, the INT link is constantly not affected by the SUT transmissions, thus enabling us to focus solely on analyzing the performance of the SUT link. We configure the SUT to use the fixed MCS 0, while generating different scenarios for the INT link by using both MCS 0 and MCS 7 and varying the injected application layer traffic load as well.

By applying our spectrum evaluation mechanism, we first verify that the INT link appears hidden to the SUT transmitter as it detects zero $\mathcal{DC}$. However, the throughput results of Fig. 2.7 present remarkably low performance especially under high traffic conditions for the INT link. Fig. 2.9 presenting the $\mathcal{DC}$ as measured at the SUT receiver, clearly highlights that the performance degradation is only attributed to receiver side interference, which is also verified by the low PDR, as shown in Fig. 2.8. Taking a closer look at the results, we observe that the $\mathcal{DC}$ evaluation is inversely proportional and complementary to the throughput and PDR performance, across the range of tested scenarios. This is expected as in this setup every collision event results in frame losses only for the SUT link and as a result affects PDR and throughput proportionally. The key outcome of this experiment is that even difficult to handle 802.11 impairments can be easily identified through joint interpretation of spectral measurements at both the transmitter and receiver sides.

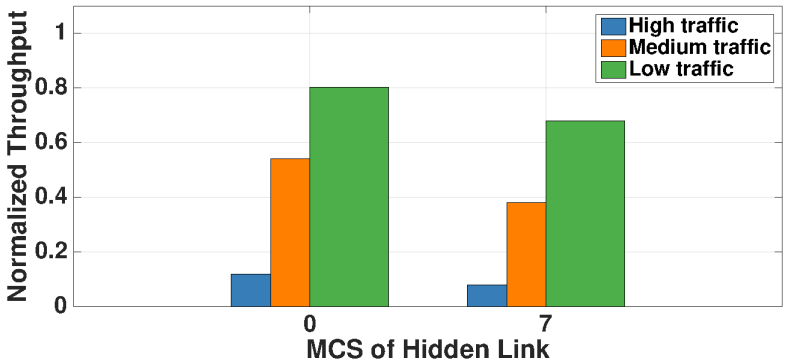


FIGURE 2.7: Hidden-Terminal Scenarios - Throughput Performance of SUT Link

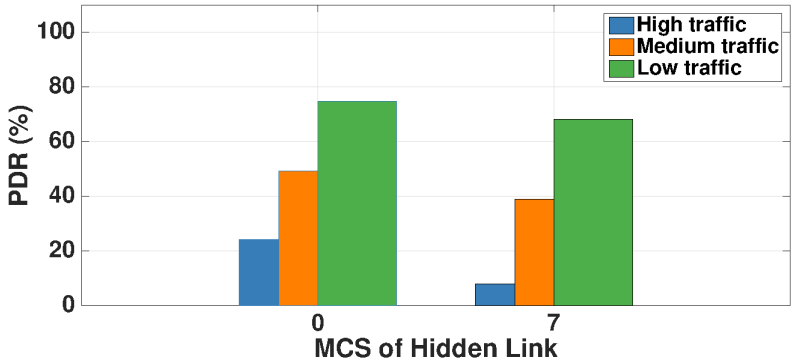


FIGURE 2.8: Hidden-Terminal Scenarios - PDR Performance of SUT Link

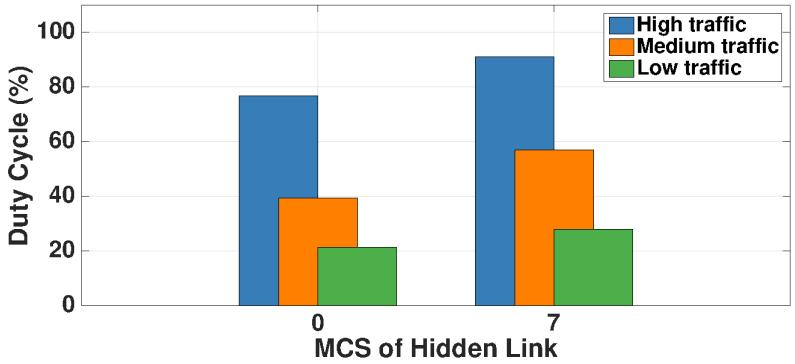


FIGURE 2.9: Hidden-Terminal Scenarios - DC of SUT Link

### 2.6.2 Overlapping channel interference

In this experiment, we use two high-SNR 802.11n links with closely spaced (∼5m) transmitter-receiver pairs. By measuring both link strengths, we remark that the SUT link approximates the -37 dBm and the INT link the -45 dBm. Since both links are able to sense each other's transmissions, the medium is fairly shared when operating on the same channel, thus highlighting the impact of channel contention. Next, we gradually tune the frequency of one link (INT) in steps of 5 MHz to increase the frequency offset between their central frequencies.

Fig. 2.10 and 2.11 depict the performance of both the SUT and INT links in terms of throughput and PDR accordingly, while Fig. 2.12 shows the $\mathcal{DC}$ measurements as evaluated at the transmitter of each link. Due to the close proximity between the transmitter-receiver pair of both links, their $\mathcal{DC}$ measurements appear to be identical and for this reason we present only the transmitter side evaluation. Focusing on the case where the same frequency is configured, we observe that both links detect $\mathcal{DC}$ values close to 90% and approximately equally share throughput. This observation comes due to the fact that during the spectral data collection procedure, lasting for 15 ms, the contending link experiences undisturbed access to the medium, thus resulting in high $\mathcal{DC}$ measurements.

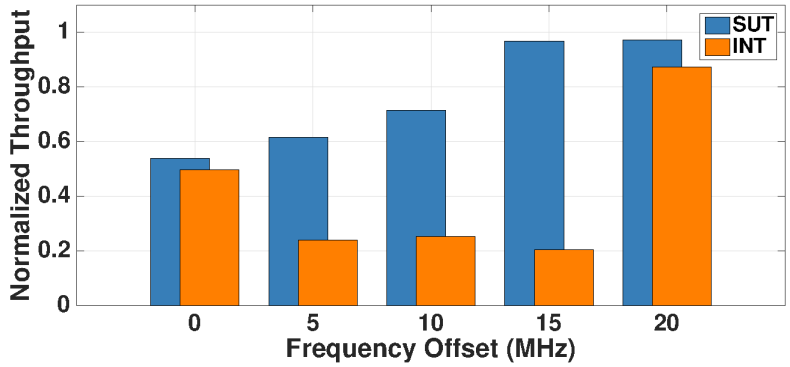


FIGURE 2.10: Adjacent channel interference scenarios - Throughput

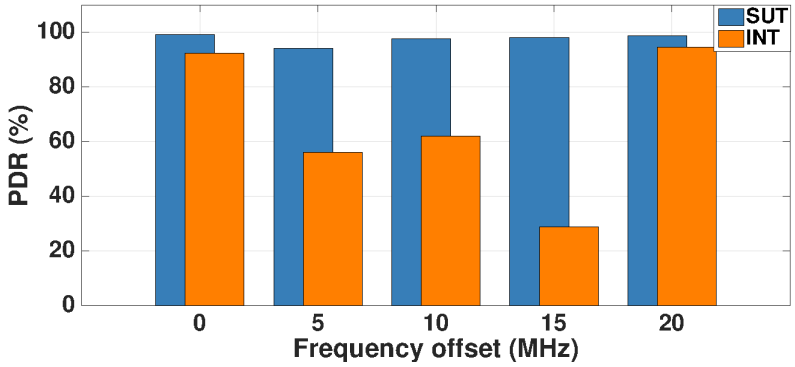


FIGURE 2.11: Adjacent channel interference scenarios - PDR

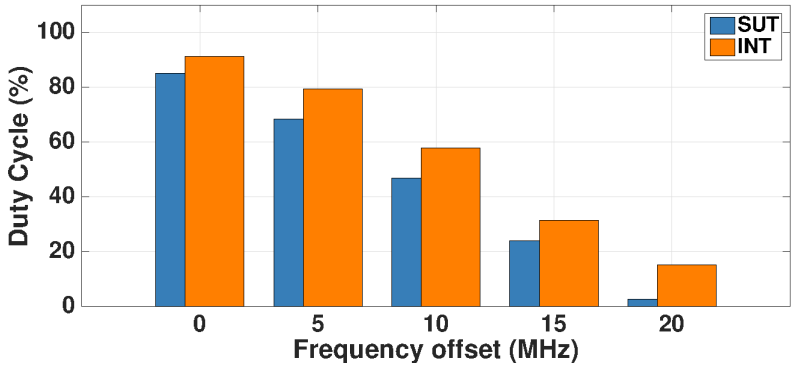


FIGURE 2.12: Adjacent channel interference scenarios - Transmitter DC

In scenarios of increasing frequency offset separation (moving from 5 MHz to 15 MHz), the $\mathcal{DC}$ evaluation shows that the links no longer share the medium equally, estimating higher performance for the SUT link that detects lower $\mathcal{DC}$ values. Moreover, we observe that the SUT link gradually improves the obtained throughput as the impact of overlapping channel interference decreases. On the other hand, the INT link achieves constantly much lower throughput compared to SUT, while it also detects decreasing $\mathcal{DC}$ values between 5 MHz to 15 MHz separation. In the case of

20 MHz channel separation (theoretically no overlap), both links experience nearly isolated operation reaching close to maximum nominal throughput. Concluding, we observed that the proposed spectrum evaluation procedure enabled both links to detect ongoing transmissions on overlapping channels and quantify the impact of adjacent channel interference to understand whether it affects them or not. However, we remark that the joint impact of "capture effect" further complicates the channel sharing process, and motivates further investigation.

### 2.6.3 Outdoor experiments

In this experiment, we deploy our spectrum sensing solution in an outdoor located densely populated area, in the city center of Volos, Greece. The surrounding area consists of offices, cafes and residences. The monitoring device is placed on the 3rd floor of an open space offices building that faces a park. We collect spectral measurements every 5 seconds and evaluate the utilization through the $\mathcal{DC}$ metric on a 24/7 basis. Fig. 2.13 and 2.14 correspond to measurements collected over 4 weeks and illustrate the maximum spectrum occupancy per hour of day and the average occupancy over channels 1-11 accordingly.

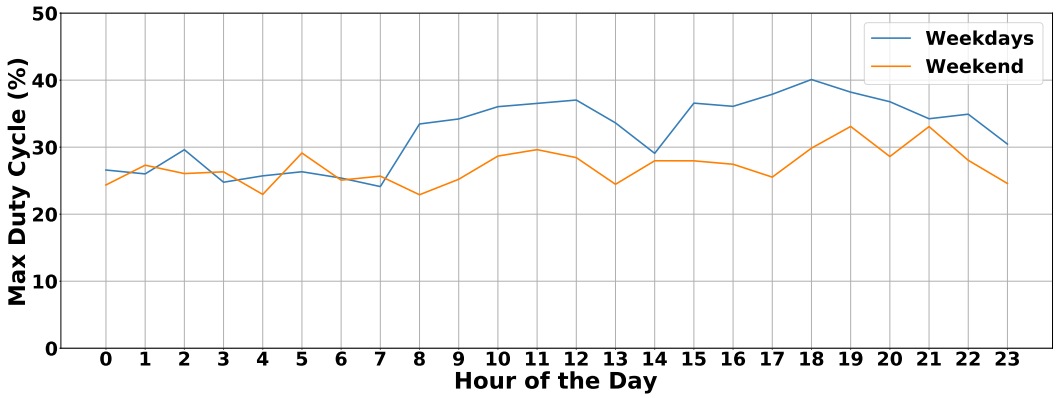


FIGURE 2.13: Outdoor Environments - Maximum Spectrum Occupancy over time

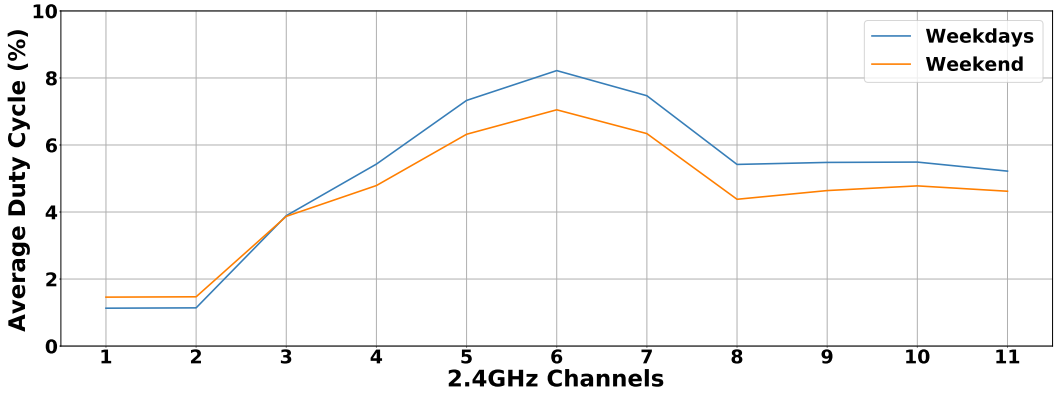


FIGURE 2.14: Outdoor Environments - Average Spectrum Occupancy per channel of the 2.4 GHz band

We can see that the lowest utilization appears between 00:00-08:00, while much higher values are observed between 08:00-23:00. In addition, lower utilization is indicated during the weekends, in comparison with weekdays. Results presented in Fig. 2.14 demonstrate unequal distribution of traffic across channels, with channels 5-7 being far more utilized than channels 1 and 2. These measurements showcase the advantage of employing the proposed solution for planning of channel assignments.

### 2.6.4 Overhead Consideration

Parameters affecting the overall induced overhead include the number of central frequencies to be scanned, the scanning interval and scanning period (SP), as well as the overhead injected during channel switching. Having described the exact values configured in our implementation (Section 2.4.3), in this experiment we vary the period over which scanning procedures are executed that exerts crucial influence on the system performance between 100ms and 5 sec.

TABLE 2.3: Indicative Throughput Demands

| *Scenario* | Bandwidth |
|---|---|
| ***Video call Standard quality - Bi-directional (Vc1)*** | 400 Kbps |
| ***Video call High Definition - Bi-directional (Vc2)*** | 1.2 Mbps |
| ***Video Streaming Standard quality (Vs1)*** | 3 Mbps |
| ***High definition Video (Vs2)*** | 5 Mbps |
| ***Ultra High definition Video (Vs3)*** | 25 Mbps |

To evaluate the injected overhead, we experiment with 5 different common traffic scenarios corresponding to VoIP calls and HD Video Streaming presented in Table 2.3. The bandwidth requirements have been carefully selected to match the requirements specified by Skype [55] and Netflix [56] accordingly. Considering that during the overall band scanning procedure, our implementation provides intervals for regular traffic exchange, we do not expect higher layer protocols to be remarkably impacted by the introduced mechanism. Fig. 2.15 illustrates the nominal throughput obtained in each scenario and clearly shows that even extreme scanning period values of 100 ms only minimally impact performance. Based on the obtained results, we observe SP values between 1 and 5 sec that can provide the ideal trade-off between frequency of channel conditions updating and protocol overhead. For the sake of clarity, we remark that all the experiments presented prior to this section used the SP of 7 secs, in order to make sure that the scanning frequency did not affect the obtained results. It is also worth to be noted that detailed overhead versus detection accuracy measurements are also listed at Chapter 3 (Section 3.4.1).

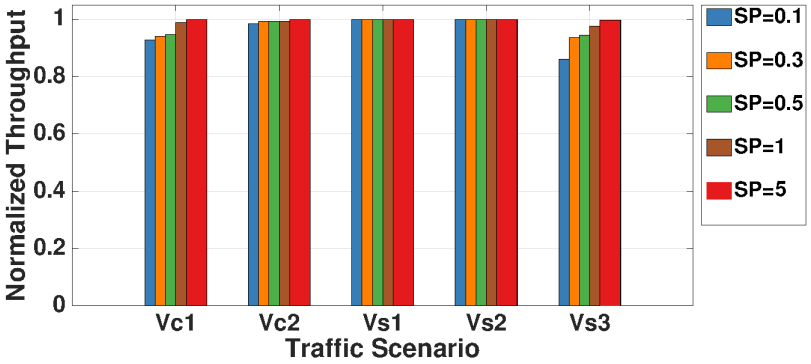


FIGURE 2.15: Overhead evaluation

## 2.7 Conclusions

In this chapter, we presented a comprehensive framework that relies on spectrum analysis for quantifying the interference impact on 802.11 links. The proposed mechanism takes advantage of PHY-layer measurements available on standard compliant 802.11 hardware. An extensive experimental study of the proposed system's operation under different types of interference and spectral phenomena was presented. At the following chapters, we keep the proposed mechanism as a basis for user association, channel selection and interference prediction / estimation schemes. In such way, we are able to observe and examine the gains of spectral aware decisions, in the context of 5G network architectures.

# Chapter 3

# Spectrum Aware non-3GPP Roaming Selection for UEs

**Contents**



In this chapter, a UE-driven light-weight mechanism for fast handover decisions and efficient WLAN selection in the context of 5G networks will be presented. As the network deployments are expected to be denser and the mobile user will be offered a multitude of alternative short coverage range options to have her mobile traffic served, her roaming decision will be performance critical. While the current 3GPP standardization considers the use of network performance statistics of nearby WLANs for the UE-driven roaming selection to address the uncertainty of the shared wireless medium, their collection and processing inevitably affects the mobile user performance and inserts an accuracy-performance tradeoff. A spectrum assessment framework is introduced, that is based on commercial hardware and open-source software, to evaluate the conditions on the nearby WLANs and let the UE to infer their performance with minimum overhead by jointly relying on Duty Cycle evaluation and the RSSI metrics. Our ready-to-be deployed solution leverages the use of off-the-shelf equipment similarly with Chapter 2 and enables fast decision procedures for the WLAN selection with low collection and processing overhead. The proposed mechanism is evaluated by conducting testbed experiments. The results reveal performance gains in terms of UE's achieved throughput when enabling the proposed framework to infer the spectral WLAN conditions and decide for the AP to roam.

## 3.1 Introduction

### 3.1.1 Motivation

While mobile data offloading to wireless LANs seems to offer a promising solution against the so called capacity crunch problem[1] of cellular networks, its potential is

[1] According to Cisco VNI[1], the proliferation of smart devices and the corresponding unprecedented data demand, have resulted only for 2018 in a significant increase of 64% in global mobile data

currently limited by the uncertainty of the shared wireless medium and the low-performance WLAN selection mechanisms that are used to enable the intercommunication between 3GPP and non-3GPP RANs. Notwithstanding the existing standardized interworking solutions between 3GPP-enabled and Wi-Fi access networks [57, 58], their usage have failed to exhibit the full interworking potential for networking efficiency, and merely achieved a relatively sufficient level of performance for delayed services[59]. As the cell and WLAN selection procedures are UE-initiated, each UE's decision for roaming is limited by the insufficient knowledge for the performance and conditions in the nearby WLANs. However, a sophisticated mechanism that could provide frequent and accurate network state information from the nearby WLANs for even more accurate assessment, although meticulous, would heavily affect the throughput and latency performance due to the extra incurred burden for exchanging network state information messages.

Currently, the ANDSF (Access network discovery and selection function) and WLAN selection policy [58, 60] mechanisms provide a standardized functionality for network discovery and non-3GPP RAN selection and allows a UE obtain network/channel status information and AP parameters from the nearby eNBs or APs (e.g. RSSI, channel load), however, it does not specify how the UE should leverage this information to select the preferable point of service. So far the existing solutions implementing the ANDSF functionality cannot achieve the maximum performance gain, as this would require complex and cumbersome coordination and frequent and real-time communication of control signaling and information between the different nearby RANs. Moreover, the standard WLANSP (Wireles LAN Selection Policy) procedures are merely based on approaches for AP selection relying on the RSSI measurements ignoring well-known problems such as hidden terminal leading to undesirable RAN selection and poor performance.

Nevertheless, the fast and rapid selection of the most appropriate Wi-Fi RAN for a UE to roam is one of the major challenges for efficient resource management and fast speed communications. Additionally, it is expected to provide the capability for smooth and seamless transitions between different RAN technologies, in 5G next generation networks. As the small cell and dense network deployments of heterogeneous RAN technologies are expected to overlap in the rural areas, the mobile user will be able to simultaneous connect and dis-connect to different eNBs, or Wi-Fi APs in order to communicate and receive service.

Furthermore, the tight integration of next generation cellular networks LTE-A-Pro with new radio interfaces to meet the 5G requirements for fast and low-latency communications renders solutions for simultaneous multi-connectivity and rapid handover highly attractive in order to enable faster mobility and common resource management.

### 3.1.2 Contribution

In this chapter, we present a novel UE-driven decision mechanism for handovers and efficient WLAN selection in 5G networks. In Fig. 3.1 a representative use case scenario is shown. Different WLANs characterized by different RSSI levels are co-located in the vicinity of a 3GPP LTE cell and offer alternative point of services.

traffic as compared with 2017. Moreover, this demand is expected to be further raised from 11 to 49 Exabytes per month until 2021.

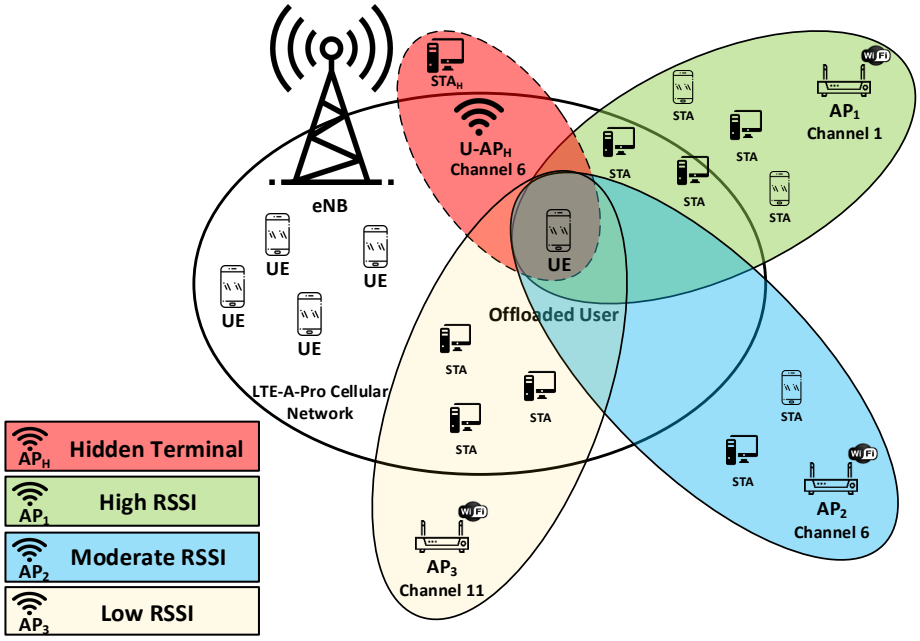


FIGURE 3.1: An LTE-A macrocell serving mobile users that are partially in the range of different WLANs. The offloaded user decides the WLAN to roam. Relying her choice on the different RSSIs that she experiences is inadequate to infer the WLANs performance conditions and reach an accurate decision.

Upon taking a roaming decision, the UE considers apart from RSSI also the perceived spectral conditions, in order to export optimal association decisions. To this end, the contributions of this chapter can be summarized as follows:

- *Assessment of the Wireless Spectrum Occupancy:* The proposed system enables a UE to elaborate and assess the perceived wireless spectrum conditions (under the use of Duty Cycle metric which introduced in Chapter 2), from the nearby Wi-Fi networks and take them also into its consideration for its WLAN association decision. Particularly, a UE[2] jointly considers the channel utilization that it detects and the received signal strength RSSI from the available AP candidates.
- *Light-weight Mechanism:* In comparison to other works [61] for contention and traffic-load aware user association that require tight coordination and cumbersome exchange of channel state quality information between APs in the first-hop and second-hop neighbor, our mechanism requires minimum signaling overhead which tends to be the appropriate solution for fast handovers in the 5G domain.
- *A ready-to-be deployed Solution:* Finally, we propose a roaming decision framework for 5G communication systems that is based completely on conventional IEEE 802.11 hardware and leverages open source software. Our solution is ready-to-be deployed in commercial off-the-shelf devices, which strongly encourages its wide applicability in future communication networks without additional deployment costs.

[2]We use also the term STA to refer to the UE that has been offloaded to the Wi-Fi network.

- *Performance Evaluation:* We evaluate the above roaming decision framework using real hardware experimentation. We conducted extensive experiments in the NITOS testbed[52], and we showed that our decision framework can assist UEs for accurate WLAN selection when roaming with a minimum scanning overhead.

The rest of this chapter is organized as follows. In Section 3.2, we present prior related work. Next in Section 3.3, we present the proposed framework and describe in detail all its software and hardware components. Furthermore, in Section 3.4 we conduct extensive experimentation in NITOS wireless testbed [52] to prove the validity of the proposed framework and to assess its performance in various network settings. Finally in Section 3.5, concludes the chapter.

## 3.2 Related

Seamless interoperability with fast handover between cellular and Wi-Fi networks pose significant challenges for alternative network discovery, persistent connectivity and traffic management. To this end, 3GPP defined the ANDSF, an entity within an evolved packet core (EPC) of the system architecture evolution (SAE) for 3GPP compliant wireless networks, that is leveraged to assist UEs to discover non-3GPP access networks (e.g. Wi-Fi mesh networks) and assist in handover and offloading operation.

ANDSF offers the standard interface to operators in order to enable device-based policies for network discovery and access network selection policies to the UE. Unlike the static approach, that was adopted primarily in 3G networks, and utilized roaming lists, ANDSF is a dynamically adaptive solution for 4G & 5G network deployments of fast changing mobile environments in which rules and metrics evaluation determines which network to select based on particular objectives (usually defined by the operators and combined with pricing schemes [62]). The management of toggling between the access networks is both device dependent and network assisted using policies communicated to the user. In this way, ANDSF enables the operator to influence Wi-Fi network usage and balance traffic to provide enhanced QoS. Moreover, the tighter integration of Wi-Fi networks with the LTE-A-Pro as expected in the 5G era.

Intense research effort has been conducted in cellular systems for the alleviation of the capacity crunch problem, where the vast majority of the approaches steer the offloaded data to Wireless Local Area Networks (WLANs). There through, several works denote the significant energy and performance gains that could be obtained, when the offloading mechanisms are applied. More specifically, the authors in [59] present a solid experimental study for 3G networks, where the well known "on-the-spot" and "delayed" offloading schemes are evaluated in terms of efficiency and energy savings. Furthermore, other approaches [63] focus more on the trade-off between achieved performance and additional delay, in the offloaded links. Therefore, these works clearly denote how the Quality of Service (QoS) is considered in the offload case studies until now. By taking it a step further, the authors in [59], [64] declare how the delayed offloading schemes apart from energy savings, could also create financial benefits/profits for both mobile users and operators.

While mobile data offloading from cellular to Wi-Fi networks appears to be an ideal solution for addressing the current cellular networks capacity crunch problem, on the other hand, significant performance drains are also observed lately in the commonly used IEEE 802.11 links, which are leveraged to convey and serve the offloaded data. Both the tremendous wireless data demands and the lack of available spectrum, make the WLANs highly susceptible environments for efficient transmissions. This problem is further intensified as the ISM bands of 2.4GHz are also home for a large variety of protocols and RF devices. More specifically, in this limited spectrum portion multiple sources of light (IEEE 802.15.1 Bluetooth, IEEE 802.15.4 ZigBee) and heavy radio interference (caused by Microwave Ovens, Wireless Cameras), largely affect the performance of IEEE 802.11 links. As expected, the great variations on wireless channel conditions may arise the obvious question of how the performance QoS is guaranteed in these links.

An important amount of work have proven that both the intense coexistence of multi-protocol RF devices [65, 66, 67] and the rapidly interchangeable channel conditions greatly affect Wi-Fi performance. Additionally, strong emphasis has been given within the identification and selection of the proper networks for data offloading. More specifically, until now several approaches [68, 69, 70, 71] investigate some of the practical and theoretical aspects associated with the WLAN's selection, condition and estimated capacity respectively.

Nevertheless, there is a noticeable lack of proposed works which take into account the performance fluctuations could arise from channel's external interference. In particular, Nguyen et al. [69] propose an offloading scheme with dynamic AP selection, based on both received signal strength (RSSI) and channel load metric exposed from APs in IEEE 802.11k networks. However, effects like hidden terminals which frequently occurred in dense Wi-Fi environments and largely affect the WLAN performance, are not considered in the aforementioned approaches so far.

## 3.3 Framework

Alongside with the increased expansion of wireless applications in recent years, the consequent lack of available spectrum became a hazardous threat for the communication performance in wireless networks. As a result, the unlicensed frequency bands (ISM) are currently over utilized, mainly due to the widely deployed IEEE 802.11 infrastructures in a small portion of wireless spectrum. Moreover, the unregulated transmissions from non-Wi-Fi devices deteriorate the problem of the already reduced performance. Thereby, spectrum awareness in IEEE 802.11 systems gained a lot of research [28, 67, 72, 73] and industrial [43, 44] interest. Based on this mindset, we exclusively take advantage of PHY-layer spectral measurements that could be exported from commercial chipsets, in order to develop our proposed spectrum awareness decision framework.

### 3.3.1 Hardware

To assess and evaluate our framework's performance, we have leveraged NITOS wireless testbed [52] to conduct extensive experimentation. There, a large variety of

wireless and wired resources are available to the experimenter remotely for evaluating experimental prototype implementations. As mentioned above, in this chapter we exclusively take advantage of Atheros commercial chipsets for facilitating the current spectrum analysis, similarly with the framework proposed at Chapter 2. Particularly, we employ the testbed's wireless nodes to act as the offloaded users and STAs in the available IEEE 802.11 networks. These nodes are equipped either with AR9380 or AR9880 PCI-e interfaces. Additionally, we use off-the-shelf TP-Link AC1750 dual band routers to act as APs. These routers include both AR9380 and AR9880-BR4A v2 wireless adapters, which are also directly compatible with the proposed spectral awareness mechanism and all IEEE 802.11 a/b/g/n/ac standards. The detailed spectrum sensing capabilities for these wireless adapters are analytcally stated at Chapter 2 (Tabel 2.2).

### 3.3.2 Enabling Spectrum Awareness

Undoubtedly, the primary objective for any spectrum aware framework could not be other than the fast and precise recognition of channel's conditions. Therefore, a proper way for quantifying the percentage of active transmissions should be adopted. Based on previously proposed approaches [67] we use the widely adopted Duty Cycle ($\mathcal{DC}$) metric and thus, we are able to discover in real time the presence of interference sources as analytically proved at Chapter 2. More specifically, the proposed framework could be distinctly separated into the following phases:

**Phase 1.** *Collecting Spectral Measurements:* Initially, we have to trigger the wireless adapter for initializing the spectrum sense procedure. During this phase, the wireless interface collects raw spectral samples based on the user's requested parameters. As part of this chapter, we scan the spectrum under inspection using 20MHz non overlapping channels with central frequency $\mathcal{F}_c$ and using 56 FFT subcarriers ($\mathcal{SC}$) resolution (The 1st Configuration Setting as shown in Table 2.2). Thereafter, each spectrum instance obtained in 20MHz/56$\mathcal{SC}$ forms a spectral sample ($\mathcal{S}$). Moreover, to achieve higher detection accuracy, we collect $|\mathcal{N}_s| = 250$ spectral samples for every channel scanned. ($\mathcal{N}_s$ denotes the set of samples that have been collected during the scanning process and correspond to a given central frequency $\mathcal{F}_c$). Bearing in mind that during this phase the wireless adapter will temporarily be out of conventional order, the aforementioned spectral parameters should be carefully adjusted. In such way, the framework's overhead will be reduced as much as possible and without losing valuable spectrum information. In addition to the initial measurements given at Section 2.6.4, further extensive overhead experiments under various configurations are given in Section 3.4.

**Phase 2.** *Inferring Spectrum Utilization:* After the completion of the first phase, all the collected spectral measurements have already been reported to the device through the Linux proc filesystem. At this state and without any further processing, no useful information could be inferred about the percentage of the spectrum utilization. In order to do so, a user space algorithm has been developed, to convert the raw measurements to Duty Cycle utilization per frequency. The Duty Cycle (equation 2.2) is a metric that describes the percentage of time in which the power of the considered spectrum fragment exceeds a specific power threshold $\mathcal{P}_{\mathcal{TH}}$. Based on the IEEE 802.11 standard for each wireless adapter involved, we use the appropriate

CCA and ED power thresholds (Table 2.1), for setting properly the $\mathcal{P}_{\mathcal{TH}}$ and discover the amount of the harmful emissions given at the ISM bands. Thus inferring accurate results with regards to precise utilization of the frequency / frequencies. It is worth to be noted that the developed framework (Shell and C scripts) is applicable without additional software/hardware modifications and works under all IEEE 802.11 standard versions.

**Phase 3.** *Roaming Selection:* According to the 3GPP standard procedures, the roaming decision is initiated by the UE when it detects that the current communication conditions (within the cell or the AP where it has been associated with) are not sufficient to attain the desired communication performance for the data service that it has requested. For that reason, the UE periodically elaborates various types of measurements and statistical information, which could be provided by the WLAN selection policy or the ANDSF component[3]. According to [57, 60], WLANSP offers to the UE the following list of selection criteria: *CriteriaPriority, HomeNetworkIndication, PreferredRoamingPartnerList. MinBackhaulThreshold, MaximumBSSLoadValue, RequiredProtoPortTuple,PreferredSSIDList, SPExclusionList.* while the ANDSF may provide also access network discovery information, WLAN selection information, ePDG configuration information, inter-system mobility policy, the inter-system routing policies and the inter-APN routing policies.

### Spectrum Aware WLAN Roaming Selection

The collected measurements regarding the Wi-Fi APs statistics, in the case where the APs belong to a list of *trusted non-3GPP* networks could be passed to the EPC network and further processed by the ANDSF and WLANSP functionalities. Thus updating the criteria list and the corresponding parameters. In the case of *untrusted non-3GPP* networks, this info could be injected in the beacon packets. In this chapter, we assume that all the available AP candidates are listed as *trusted non-3GPP* networks. Moreover, there exist a set of $\mathcal{A}$ of $|A|$ access points and a set $\mathcal{U}$ of $|U|$ user equipment devices.

Our WLAN selection mechanism assesses the WLAN performance conditions by inferring jointly from the perceived spectrum occupancy and the RSSI measurements. By holding the trusted APs list and receiving the Wi-Fi beacon frames, a UE can initialize the roaming procedure. Initially, each UE $u \in \mathcal{U}$ should be aware of its local spectral conditions, thus it performs Phases 1 and 2 only for the frequencies $\mathcal{F}_c$ which are used by the trusted available APs in its vicinity. We use $\mathcal{DC}_u(\mathcal{F}_c) \in \{0,1\}$ to denote the $\mathcal{DC}$ percentage that has been sensed and exported by the UE $u \in \mathcal{U}$ on a given frequency $\mathcal{F}_c$. Respectively, we periodically activate Phases 1 and 2 at the AP $a \in \mathcal{A}$ side and we export the corresponding $\mathcal{DC}$ value $\mathcal{DC}_a(\mathcal{F}_c) \in \{0,1\}$ only for its operating frequency $\mathcal{F}_c$[4]. Moreover, through the beacon frames the UE is able to retrieve the RSSI values $\mathcal{RSSI}_a$ for each listed available AP candidate. As a result, the predicted modulation and coding scheme ($\mathcal{MCS}_{ua}$) between UE $u \in \mathcal{U}$ and each candidate AP $a \in \mathcal{A}$ can be exported through Table 3.1. Then, using the

[3]The UE may retain and use this ANDSF and WLANSP information until new or updated information is received.

[4]The collected $\mathcal{DC}$ metric can be passed in the UE either using the WLANSP and ANDSF mechanism or a beacon frame.

TABLE 3.1: IEEE 802.11n Sensitivity Thresholds

| MCS (1-4 Spatial Streams) | ***20MHz*** | ***40MHz*** |
|---|---|---|
| | values in (dBm) | |
| 0 / 8 / 16 / 24 | -82 | -79 |
| 1 / 9 / 17 / 25 | -79 | -76 |
| 2 / 10 / 18 / 26 | -77 | -74 |
| 3 / 11 / 19 / 27 | -74 | -71 |
| 4 / 12 / 20 / 28 | -70 | -67 |
| 5 / 13 / 21 / 29 | -66 | -63 |
| 6 / 14 / 22 / 30 | -65 | -62 |
| 7 / 15 / 23 / 31 | -64 | -61 |

mapping table[5] that shows the corresponding theoretical rate which is mapped to a particular MCS, we can derive an estimation of the throughput. In this context, the least normalized capacity $C_{ua}$ (Mbps) between a UE $u$ and each available AP $a$ can be calculated by applying Eq. (3.1).

$$C_{ua} = (1 - \mathcal{DC}_{\max}) * \mathcal{C}_{Th}, \tag{3.1}$$

where $\mathcal{DC}_{max} := \max\{\mathcal{DC}_u(\mathcal{F}_c), \mathcal{DC}_a(\mathcal{F}_c)\}$ represents the worst case scenario of the occupied spectrum, as this is perceived either in the UE or AP side. Therefore, $(1 - \mathcal{DC}_{\max})$ represents the remaining spectrum. Additionally, $\mathcal{C}_{Th}$ is the theoretical data rate that could be achieved as this is derived from the predicted $\mathcal{MCS}_{ua}$. In this way, the UE $u$ takes the roaming decision to an AP $a$, relying on the calculated normalized capacity values by selecting the AP $a^* \in \mathcal{A}$ that offers the maximum capacity potential. That is:

$$a^* = \max_{a \in \mathcal{A}} C_{ua} \tag{3.2}$$

## 3.4 Evaluation

In this section, extensive experiments were conducted in order to highlight the proposed framework's superiority. All the scenarios were implemented and tested in NITOS wireless testbeds [52]. Specifically, the indoor isolated testbed was used for implementing the examined topologies. Although the proposed framework deals directly with external interference, the uncontrolled presence would produce inconclusive results.

### 3.4.1 Initial Experiments

Primarily, we deem essential to measure the total overhead added in the wireless chipset, every time the proposed framework is executed. The purpose of this experimental scenario is to highlight the performance drains (Mbps), compared with

[5]Table listed in http://mcsindex.com/ is derived from IEEE 802.11-2012 Standard - Sections 18.3.10.2 (802.11a OFDM), 19.5.2 (802.11g ERP), 20.3.21.1 (802.11n HT) and maps RSSI values to MCS indexes for the purpose of determining the data rates.

the detection accuracy of the proposed framework. This particular experimental scenario contains two wireless transmissions, which will take place in the 2.4GHz ISM band. Initially, we use USRP B210 [53] in order to emulate a microwave oven's emission, which corresponds to 50% of channel's utilization. We use channel 1 (2412MHz) as the center frequency of microwave's emulated transmission and a bandwidth of 20MHz. Additionally, we set a high RSSI 20MHz wide IEEE 802.11n link, in which the proposed mechanism will be applied. We set the Wi-Fi link intentionally at channel 11 (2462MHz) in order to be completely isolated from microwave oven's interference. Then, we initialize a Wi-Fi transmission and more specifically, we create three scenarios of 50, 100 and 150Mbps of unidirectional UDP traffic from AP to STA. In such way, we are able to examine the overhead occured from the proposed framework, under saturated UDP traffic demands.

Additionally, the experimental results were produced by examining the following parameters: (a) the time spent $t_{scan}$ on scanning a particular frequency $\mathcal{F}_c$ and (b) the Scanning Period (SP), which represents how often the AP/UE triggers the proposed framework and thus refreshes its spectral awareness. Initially, we set $t_{scan}$ (10ms, 20ms and 50ms). In addition, for a different number of SP ranging from $SP = 100ms$ to $SP = 5000ms$, we have also run the same execution. In Figures 3.2, 3.3 and 3.4 ,we show the averaged experimental results, after conducting the aforementioned scenario 10 times for all parameter combinations. There, we can observe that the more frequent (low $SP$) the proposed framework is executed, the higher performance drains occur. Additionally, the larger performance decays appear when the adapter scans the channel for $t_{scan} = 50ms$ comparing to $t_{scan} = 20ms$ or $t_{scan} = 10ms$. This is immediately explained as during the scan time the wireless adapter can not transmit or receive packets. Moreover, measurements with higher $\mathcal{DC}$ accuracy occur when the wireless adapter spends more scanning time on a frequency $\mathcal{F}_c$. More specifically, the exported $\mathcal{DC}$ values from the framework at 2412MHz (microwave's emulated transmission) were 44,82%, 48,43% and 49,97% when the adapter scans the $\mathcal{F}_c$ for $t_{scan}$ =10, 20 and 50ms, accordingly. As noted above, the microwave transmission occupied half of the channel's capacity, and thus the expected $\mathcal{DC}$ percentage should be 50%.

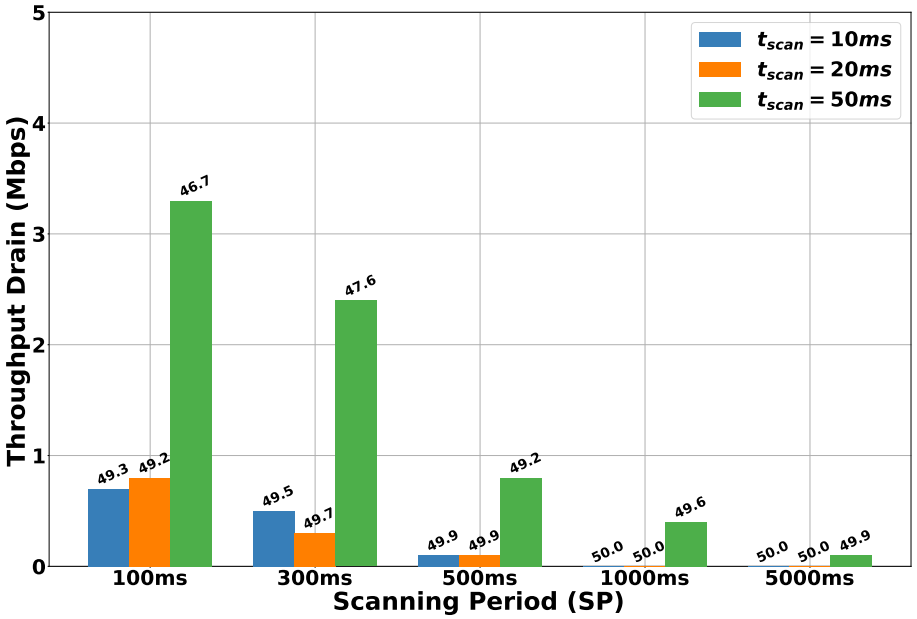


FIGURE 3.2: Performance Drains (Demand 50Mbps UDP)

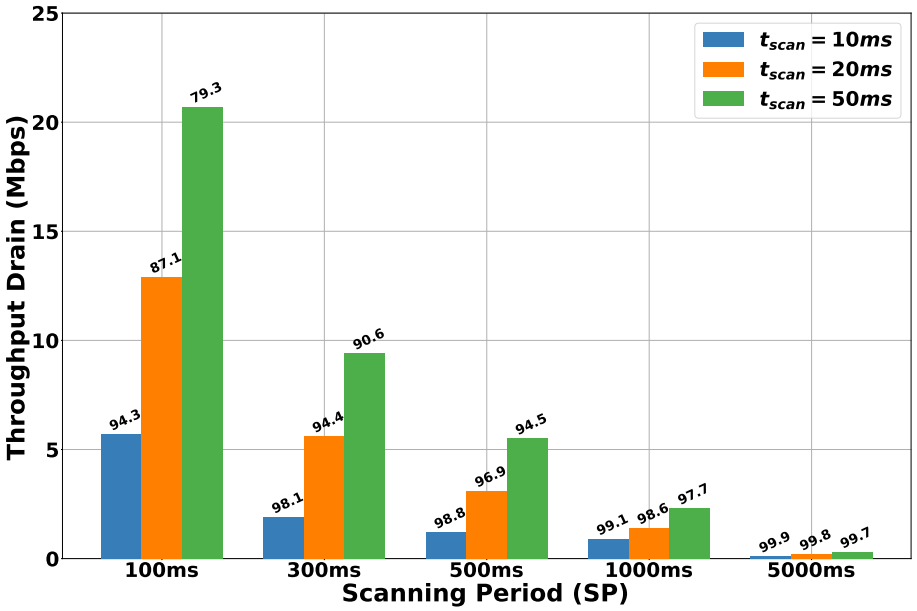


FIGURE 3.3: Performance Drains (Demand 100Mbps UDP)

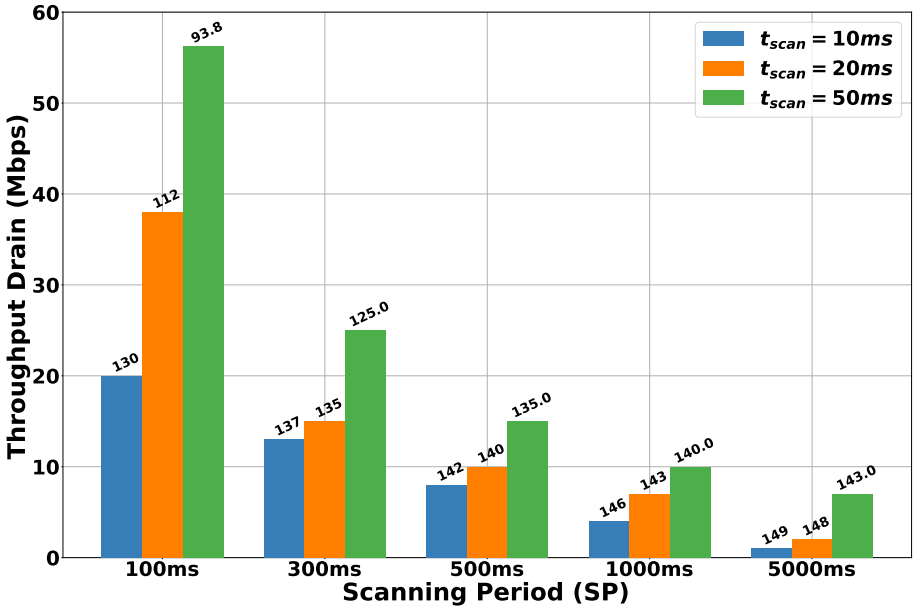


FIGURE 3.4: Performance Drains (Demand 150Mbps UDP)

### 3.4.2 Experimental Setup

At this point, a mobile user (UE) intends to leave the cellular network and has it's traffic demand served through the available Wi-Fi AP candidates. We thoroughly examine how the throughput performance (Mbps) of a UE could vary depending on different AP association decision schemes. Specifically, the default RSSI-based, an approach which is only AP aware and our proposed decision mechanism are compared. The topology under examination is shown in Fig. 3.1.

In this experiment, three IEEE 802.11n 20MHz WLANs of different RSSI levels (high, moderate, low) are used, and act as the alternative point of service for a UE. The RSSI values that were received by the UE are -36dBm, -67dBm, -75dBm for AP1, AP2 and AP3, respectively. We configure these APs at channels 1, 6 and 11 accordingly to eliminate the potential interference among them. Additionally, there exist contending STAs, which are already associated with each AP. Particularly, AP1, AP2 and AP3 has five, three and two connected STAs, respectively. Each STA has a continuous bidirectional UDP traffic demand of 12Mbps from its AP. Finally, a fourth IEEE 802.11n 20MHz WLAN at channel 6 acts as a hidden terminal to AP2, thus none of its transmissions can be decoded and avoided by leveraging the CSMA/CA mechanism. During this experiment, we set a continuous moderate 30Mbps traffic demand at the hidden terminal link.

Table 3.2 summarizes part of the experiment's results. More specifically, the first column is the $\mathcal{DC}$ percentage captured by the UE at channels 1, 6 and 11. Additionally, the second column states the $\mathcal{DC}$ percentage reported to UE from the available APs. It is worth to be noted that the large difference between $\mathcal{DC}_u(\mathcal{F}_c)$ and $\mathcal{DC}_a(\mathcal{F}_c)$ at the second row, indicates the potential presence of hidden terminal at the UE - AP2 link. Since the values of $\mathcal{RSSI}_a$ are known to the UE through beacon frames, the proposed framework estimates the capacity (column capacity $C_{ua}$ (Mbps)). Furthermore, we confirm that the $\mathcal{MCS}_{ua}$ values predicted are the same

with these achieved during experimentation, by using an external wireless monitor. The throughput results (average values of 10 executions) for a UE that applies our proposed WLAN selection framework are depicted in Figure 3.5. The actual throughput ( $C_{ua}^{REAL}$) experienced by the UE when attaching to the respective AP is compared with this estimated from the proposed framework ($C_{ua}$). It is evident that the proposed framework achieves accurate throughput estimation for all the three available WLAN and infers the best candidate AP.

TABLE 3.2: Experimental Results.

| *Scenario* | $\mathcal{DC}_u(\mathcal{F}_c)$ | $\mathcal{DC}_a(\mathcal{F}_c)$ | $\mathcal{DC}_{\max}$ | $\mathcal{MCS}_{ua}$ | $\mathcal{C}_{Th}$(Mbps) | $C_{ua}$(Mbps) |
|---|---|---|---|---|---|---|
| ***High RSSI (AP1)*** | 87.1% | 86.4% | 87.1% | 23 | 195 | 25.155 |
| ***Mod. RSSI (AP2)*** | 89.7% | 21.4% | 89.7% | 21 | 156 | 16.06 |
| ***Low RSSI (AP3)*** | 46.1% | 48.2% | 48.2% | 19 | 78 | 40.4 |

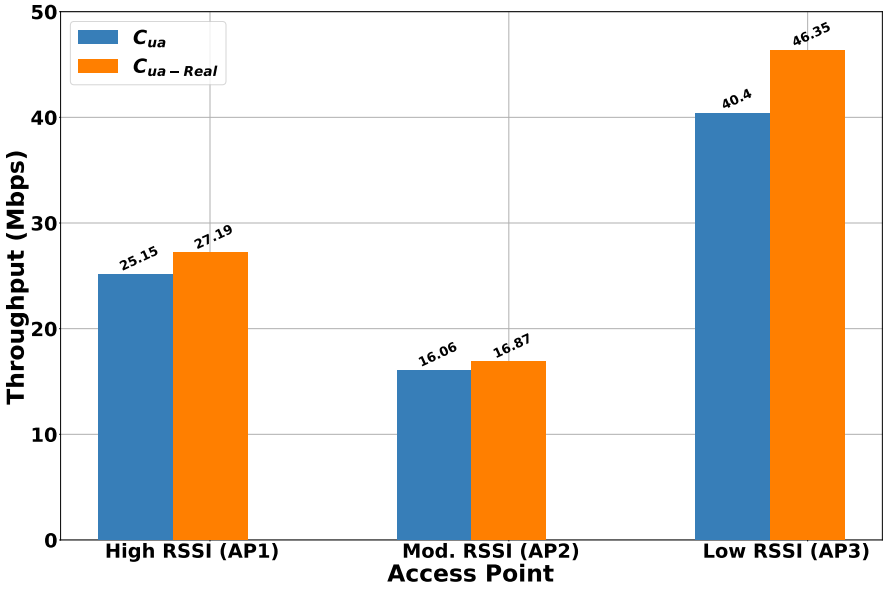


FIGURE 3.5: Achieved Performance per AP

Regarding the part of the association decision: If the default IEEE 802.11 RSSI-based approach was selected, the UE would connect to AP1. In this case the UE would experience relatively low performance as AP1 would have the largest number of contending STAs associated on it and channel conditions would not been considered at all. Furthermore, if the association decision was based exclusively on AP's channel conditions, the AP2 would be chosen from UE. A typical example of such decisioning approach can be found in [69]. Even though this decision seems to be proper at AP's side, the UE's different spectral conditions dramatically affect the performance achieved. Finally, our proposed framework selects the AP3, although it offers the lowest RSSI and has more associated STAs than AP2. However, it turns out to be the best choice as it achieves the largest throughput performance compared with the two aforementioned approaches above.

## 3.5 Conclusions

In this chapter, a novel light-weight UE-driven mechanism for enabling fast roaming decision and WLAN policy selection in 5G networks was introduced. The proposed mechanism is built using commercial hardware and open source software, and offers a ready-to-be deployed solution for future wireless networks. It allows the UEs to thoroughly infer about the performance conditions in the nearby WLANs by incorporating also a fast spectral occupancy assessment on the available Wi-Fi channels. Through extensive testbed experimentation, we demonstrated significant throughput performance gains for the offloaded UE when employing the proposed WLAN decision framework. The utilization of our framework comes with a minimum scanning and processing cost, which is totally compensated by the accurate inference of the wireless conditions, and hence the appropriate selection of the candidate AP/WLAN.

# Chapter 4

# Dynamic Wi-Fi Channel (Re)configuration for DUs

**Contents**



Future wireless infrastructures will have to deal with significantly higher loads of data, produced by applications demanding higher capacity with lower latency for the exchanged information. 5G networks are expected to resolve these problems, by bringing in advanced flexibility of deployment through the Cloud-RAN concept, and new air interfaces. Dense Heterogeneous Networks will also assist in the smooth transition to a holistic approach for managing the wireless network, especially through their integration at the base station level. Nevertheless, networks operating under a very tight spectral environment, with limited spectrum resources, need to be aware of their expected performance in order to optimally decide their operating frequency. In this chapter, we consider a disaggregated heterogeneous base station, complying with the Cloud-RAN concept, and integrate spectral aware non-3GPP access (Wi-Fi) to the base station. We use multi-technology links to serve the end users, through two different paths: an LTE and a Wi-Fi. The Wi-Fi units are able to automatically discover and adjust their operating frequency automatically, ensuring efficient data delivery to the end users. We integrate all our contributions in a framework and deploy it over a real testbed. Our experimental results illustrate enhanced performance for the non-3GPP access of the network, delivering more than 5 times better throughput for high interference scenarios.

## 4.1 Introduction

As the unprecedented demand for continuous wireless connectivity is increasing exponentially, the existing infrastructures are proved inadequate to handle the exchanged data loads efficiently. Recent studies [1] have shown that the request for wireless data will double up in the near future, a burden that the infrastructure providers will have to cope with. Two approaches are considered: 1) the usage of new spectrum bands (e.g. the cm- and mm-Wave bands), and 2) the efficient use of existing sub-6GHz technologies, with advanced spectrum coordination techniques.

The prevailing approach so far, urges the transition from macro cell architectures to the deployment of small and low range base stations that complement the coverage of macro-cells. Therefore, a combination of new-introduced and pre-existing wireless standards, will be used in order to fulfill the increased user demands in modern wireless systems. Additionally, the advent of 5G technologies proposes a novel architecture, through the cloudification of parts of base stations (Cloud-RAN) and the integration of heterogeneous technologies in the cell, as a means to minimize the CAPEX and OPEX costs. In such architecture, all the available heterogeneous radio technologies for serving a client can be aggregated at the cloud, as a means of increasing the overall wireless capacity, needed by novel data-hungry user applications.

Dense Heterogeneous Networks (HetNets) are formed through the integration of smaller scale solutions (e.g. femto- /pico-cells) complementary to the existing macro- and meso- scale base station deployments. These deployments offer efficient data offloading to users within a specific region, and relieve the macro-scale network from the burden of serving the end users at a significantly larger geographical area. The inevitable steer to smaller cells is more than essential in order to ensure a smooth transition to 5G networks, of which they will be an integral characteristic. Nevertheless, the dense deployment of heterogeneous cells, which may operate within the same frequency band, mandate the efficient coordination of the wireless technologies. The harmonic coexistence of several existing wireless protocols mainly operating in sub-6GHz bands (5G-NR, LTE-A, Wi-Fi) is needed for providing increased coverage and capacity for densely populated areas.

Nonetheless, severe performance challenges can be produced through the sharp raise of wireless terminals within densely populated urban environments. More specifically, the unlicensed (ISM) bands can be referred as a typical example of uncoordinated and excessively used spectrum portion, mainly from non-3GPP technologies. Therefore, a large variety of wireless devices including the widely adopted IEEE 802.11 (Wi-Fi), already face degraded performance due to the heavy transmission contention. As expected, these great fluctuations on wireless channel conditions may arise the obvious question:

*"How can such over-congested protocols eliminate the degraded performance and efficiently participate in the 5G heterogeneous architectures?"*

5G networks bring architectural advancements as well, thus creating fertile ground for the efficient coordination of HetNets. Through the introduction of the Cloud-RAN concept, part of the base station can be executed in the cloud, thus allowing several time critical applications for coordination such as eICIC [74] to take place. In this chapter, we consider a heterogeneous technology Cloud-RAN based on the framework proposed in [13], and introduce network driven intelligence for the coordination of the distributed Radio Access Networks (RANs) and the users associated in the formed cells. We consider the disaggregation of the base stations according to the 3GPP Option-2 split [75], between the Packet Data Convergence Protocol (PDCP) and the Radio Link Control (RLC) layer of the base station stack, according to the recent 5G-NR specifications [76]. The two formed units are the Central Unit (CU), incorporating the processes of PDCP and upper layers, as well as the interface with the core network, and the Distributed Unit (DU) incorporating the RLC, MAC and

PHY. The DUs in the 5G architecture may be heterogeneous, as a means to offer expanded capacity to the end-users through legacy technologies (LTE, Wi-Fi).As a matter of fact, Wi-Fi aggregation to the RAN level is expected to be dealt with the NR releases beyond Rel. 17.

In this chapter, we adopt the prototype in [13] and further extend it in order to operate as an autonomic spectral aware base station for the Wi-Fi managed part of the network as follows:

- *Real-time self organized Wi-Fi DUs:* Based on the autonomic channel reconfiguration of each DU, our framework achieves efficient spectrum utilization and load balancing for the over-congested ISM bands. This increases directly the total achieved throughput that can be served from all the DU candidates and any other external interference sources.
- *UE association decisions:* Each UE may associate with a DU in a given region, based on the decisions that it concludes on the expected performance over the network. These decisions are based on information about the wireless spectrum utilization (Chapter 3), contrary to off-the-shelf received signal strength based metrics.
- *Extensive testbed experimentation:* We experiment with the developed solution over a real testbed, and under different external interference settings.

## 4.2 Related

Alongside with the deployment of 5G networks, a rapid increase of smaller and denser networks (DenseNets) is expected. Several research approaches have been proposed in order to deal with the expected disaffects of the dense operation of the networks. Primarily, multiple works propose general architecture designs for ultra dense and small-cell networking [77, 78, 79, 80], either through the formation of similar technology and different scale setups, or using heterogeneous technologies for small cell access. Regarding the former, off-the-shelf solutions exist in the 3GPP specifications, like for example the InterCell Interference Control (ICIC) and enhanced ICIC (eICIC). Through the utilization of Almost Blank Subframes (ABS), the femto-cells are instructed to operate for certain timeslots, without receiving any interference from the macro-cell. Nevertheless, their application in real-world deployments needs low-latency links between the base stations, which is not feasible for monolithic base stations at legacy setups. Regarding the latter, cautious decisions should be taken at all HetNet's tiers for maximizing UE's performance and thus a lot research interest focuses on the coexistence of cellular with non-3GPP technologies (e.g. Wi-Fi). Works [81, 82, 70, 83] are indicative of such setups, primarily focusing on the coexistence of LTE and Wi-Fi within the same region and selecting the technology through which each UE shall be served.

Nevertheless, the advent of 5G technologies brings in new features for increasing the flexibility in network deployment, instantiation, maintenance and operation. The RAN cloudification [12] creates fertile ground for the real world application of operations that formerly where not possible due to stringent latency requirements, like the eICIC [74]. HetNets are expected to play a complementary role to fixed network infrastructure, through their integration in the RAN. Similar efforts existed in the

legacy LTE technology as well, through the introduction of the LTE-WLAN Aggregation Adaptation Protocol (LWAAP) [10]. In such setups, non-3GPP technologies (e.g. Wi-Fi) are integrated and controlled from the operator cell, as a means to access new spectrum towards enhancing the end-user's Quality of Experience (QoE). As such technologies usually access unlicensed spectrum, they suffer from contention and external interference, which leads to performance degradation.

Unlike straightforward resource allocation schemes given in base station centric protocols like LTE, the IEEE 802.11 standard employs a more opportunistic technique based on carrier's sense and multiple access (CSMA-CA). However, uncoordinated existence of densely deployed Access Points (Ext. APs)[1] in the limited overlapping Wi-Fi channels, undoubtedly leads to degraded performance for the network.

In this context, we propose a novel distributed framework in which overall spectral awareness is enabled at both heterogeneous base station deployments and UE's sides. We adopt a disaggregated base station setup, complying with the Cloud-RAN concept, and augment it with non-3GPP technologies as a means to maximize the overall capacity of the network. We disaggregate the base station based on the recent specifications for 5G-NR [76], and create two entities; the Central Unit (CU) and the Distributed Units (DUs)[2]. We integrate the Wi-Fi access in the network as a DU component, controlled through the same CU as it happens for the cellular access case (see Figure 4.1).

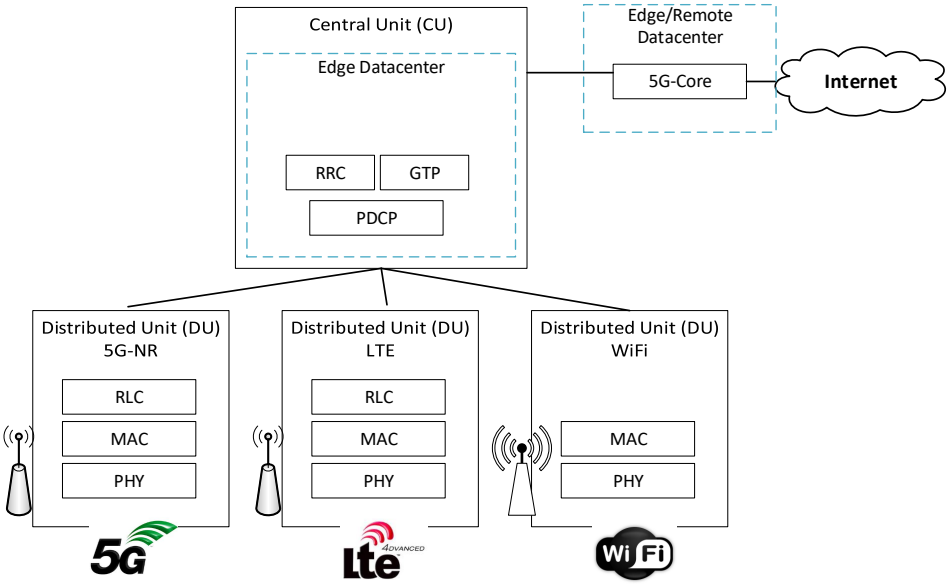


FIGURE 4.1: Disaggregated Heterogeneous Cloud-RAN architecture for 5G: Each component is added to the network as a new DU, suppoting even heterogeneous access technologies, converging at the same CU in the Cloud.

Based on the generic energy detection method and by minimal signaling between the involved entities, our framework is able to dynamically discover and avoid every

[1]These APs are not managed in any way from the CU, thus creating uncoordinated interference at the unlicensed bands. It is noted that thereupon we are also mentioning to the uncoordinated APs as Ext. AP.

[2]In this chapter only IEEE 802.11 DUs are considered. Thus, they are also mentioned as Wi-Fi DUs at System Architecture as well as at the Evaluation sections.

possible source of interference at both Wi-Fi DU and UE sides with minimum overhead. By utilizing commercial Wi-Fi hardware and Software Defined Radio (SDR) components for the cellular network, and after extensive testbed experiments, we prove the system's throughput and spectrum efficiency gains.

## 4.3 Framework

In this section, we initially detail the network architecture, and subsequently provide information on how the wireless network is reconfigured in order to ensure the optimal spectrum allocation.

### 4.3.1 System Architecture

As mentioned above, we employ a disaggregated Cloud-RAN architecture for cellular access, augmented with multiple non-3GPP cells. We target at optimizing the access at the non-3GPP technologies, assisted by the overall cell for the coordination and signalling exchange. According to the defined 5G NR specifications, the base station shall implement the Option 2 3GPP split, between the PDCP and RLC layers. This means that heterogeneous technologies can be integrated to the base station, as new DUs, supporting either cellular access (5G-NR or legacy LTE) or non-3GPP access (Wi-Fi). Each CU may control multiple DUs, and select through which the traffic shall be transmitted for reaching the UE. This process can happen in a per packet basis. From the DU side, each DU can be controlled by only one CU.

In this context, Makris et al. at [13] presented a prototype based on the OpenAir-Interface (OAI) platform [84], which realizes this heterogeneous Cloud-RAN infrastructure. The solution introduces signaling between the PDCP and RLC layers of the cellular stack, and integrates the Wi-Fi Access Point (AP) functionality to the base station level as a DU. In order to accomplish this, a thin software is used at the Wi-Fi DU part in order to handle all the signaling and communication with the PDCP layer located at the DU. The software is aggregating DUs for providing access to a multi-homed UE through different wireless technologies concurrently for the Downlink channel (DL), taking place at the PDCP layer (CU side) and in a per packet and per UE basis. In this chapter, we present an extension to the introduced signaling between the CU and DU as depicted in Figure 4.2.

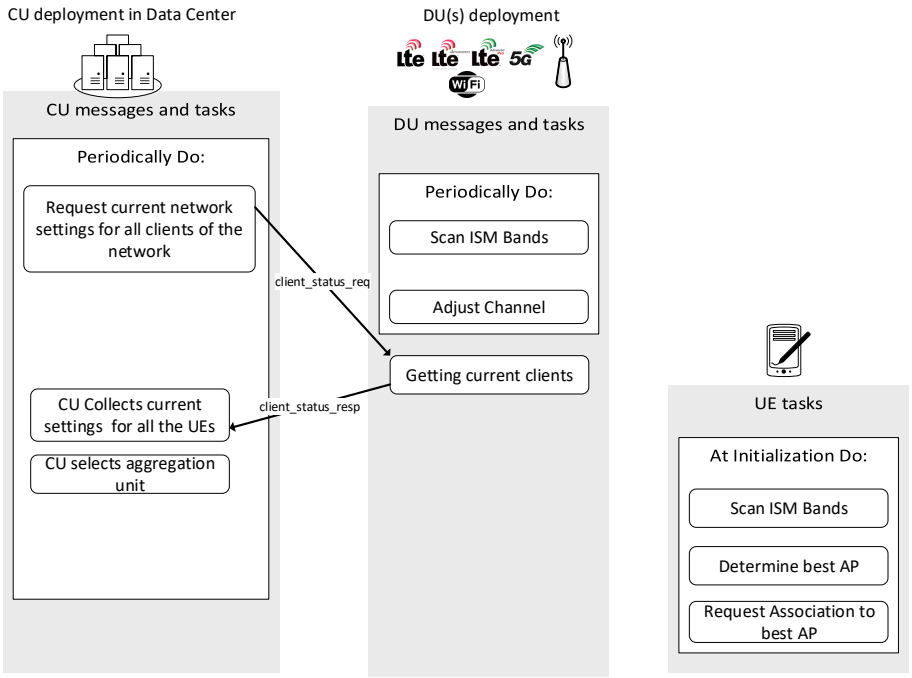


FIGURE 4.2: Signaling and processes developed at each component for this framework: DUs and UEs select their operating frequency based on their perception of the wireless conditions and the information is sent to the CU for selecting which Wi-Fi DU will be aggregated with the LTE part for each specific UE.

The DU parts of the network generate information about the clients that are associated with each DU, and send this information over the network at the CU side of the base station. Based on the information received from all the DUs, the CU concludes on which of the available Wi-Fi DUs will be used as the aggregation unit for the cellular network and for each UE accordingly. Data is flowing over both DUs in order to reach the end user from multiple paths, ensuring that the optimal capacity of the network is ensured. In terms of spectrum management, we introduce a solution running independently at each DU of the network, ensuring that each one will use the spectrum that will provide the most efficient performance over the network. Similarly, the UEs do not use the standard approach of off-the-shelf devices considering the Received Signal Strength, but make their association decisions based on their perspective of the wireless channel. The result is to provide an optimally organized in spectrum DU-UE link, used for aggregating the traffic from the cellular network. More details on the organization of the participating DUs is presented in the subsections below.

### 4.3.2 DU's (Wi-Fi) Channel (Re)configuration

Below, we describe how the DUs select their optimal operating spectrum, the model and the algorithmic implementation. In the proposed **Spectral Aware Channel Selection (SACS)** framework, each Wi-Fi DU autonomously triggers a spectral awareness mechanism for extracting the optimal operating frequency ($targetF_c$). More

specifically, the spectrum sense procedure is periodically enabled for all the available Wi-Fi channels ($F_c$) and thus we are able to discover and avoid interference sources in real time. It is also worth to be noted that the aforementioned mechanism is implemented with using exclusively commercial Wi-Fi adapters (Atheros) and on the top of TP-link routers. Based on Chapter 3, we follow the scan and evaluation procedure in order to calculate the Duty Cycle ($\mathcal{DC}$) for every Wi-Fi channel.

In the context of this framework we trigger the spectrum awareness mechanism every 5 seconds. It has been thoroughly illustrated in [67] and [83], that the spectrum sense procedure adds minimal overhead in the conventional operation of the Wi-Fi adapter. Additionally, we similarly set the wireless adapter to obtain Spectral Samples of 20Mhz / 56 FFT bins. The aforementioned configurations can fluctuate from 20-80 MHz and 56-256 bins depending on the chipset type used.

Finally, after the completion of spectrum sense and $\mathcal{DC}$ extraction for all channels, the Wi-Fi DU (re)configures its operating frequency in that with lowest $\mathcal{DC}$ detected. If a less utilized frequency other than the current is discovered, the the DU carries seamlessly all the associated stations to it, by using the Channel Switch Announcement [85] (CSA) mechanism of IEEE 802.11. Algorithm 1 summarizes the sequence of all necessary operations conducted at DU's side.

**Algorithm 1** Wi-Fi DU Channel (Re)configuration

```
while TRUE do
  senseSpectrum()
  for each F_c in Channels scanned do
    calculateDC(F_c)
    if DC(F_c) < DC(F_{c_operating}) then
      targetF_c = F_c
    end if
  end for
  if F_{c_operating} ≠ targetF_c then
    tuneAP(targetF_c)
  end if
  sleep = 5sec
end while
```

### 4.3.3 UE's Spectral Aware DU Association

Apart from the continuous evaluation and channel reconfiguration applied in the Wi-Fi DUs, we further adopt a spectral aware association approach at UE's side, in order to boost even more the system's performance. Unlike the association scheme proposed from the IEEE 802.11 standard, which considers only the received signal strength from the available APs, we follow the framework described in Chapter 3. There, not only the RSSI but also the exact spectral conditions given at both DU and UE sides are involved in the association decision. Identically, the UE senses and evaluates the spectrum, exactly as described at Section 3.3.2. Thereafter, by combining the $\mathcal{DC}$ values and each link's predicted MCS through RSSI indicators, we are able to precisely calculate and select the DU offering the highest performance (Mbps). For sake of the aforementioned calculations, we transfer the latest $\mathcal{DC}$ values

captured from each DU to the UE, by using the 3GPP DUs of the system. Finally, we apply this association scheme for the UE only once and when she enters the network.

### 4.3.4 Coordination Signalling

In the sections above, we presented our architecture, and the respective algorithms taking place at each DU and UE respectively for determining the best operating channel. In this section, we present our approach in binding all the contributions together in a fully-fledged framework, able to control the flow of data to each UE from the CU side of the network. The differentiation for each UE resides at the PDCP layer of the network CU; the PDCP is used as the aggregation point for all the heterogeneous technologies supported in the base station cell. For the downlink operation, as data flows through the PDCP layer data plane packets (data exchanged between the UEs of the network), a 2-byte long PDCP header is added to the packet. At this point, the differentiation of UEs in the network is taking place through their Radio Network Temporary identifiers (RNTIs). Based on this information, and by assigning identifiers for each new incoming UE, we can select at the output of the PDCP layer to which DU the traffic shall be forwarded. This controller behaviour takes place per-packet and per-user basis, and is the enabler for differentiation between the access technologies used for each UE.

In such a distributed setup, where the UEs are not associated with all the available DUs but only with the one that they conclude will give them the optimal performance, the associations per each DU shall be communicated to the CU side of the network, and provided as argument to the technology selection controller. To this aim, we introduce new signalling between the DUs and the CU, as shown in Figure 4.2 that communicates this information. Periodically, at each non-3GPP Wi-Fi DU of the network, we retrieve the associated clients through off-the-shelf tools (e.g. *hostapd_cli*) and parse this information. This is then encapsulated to an inform message, sent to the CU, which is informed for all the UE identifiers and associations per each DU. In this manner, the CU has a holistic view of the network status and DU associations, and can select the forwarding DU for each UE. As we use the non-3GPP DUs as our aggregation units, the traffic is split for each UE between the cellular and the non-3GPP DUs.

## 4.4 Testbed Experiments

In this section, extensive experiments were conducted in order to prove the proposed system's superiority. We evaluate the framework in the NITOS testbed [52], an open and remotely accessible infrastructure located in University of Thessaly, in Greece. NITOS is offering a wide selection of resources, spanning from commercial LTE to open source Wi-Fi and several Software Defined Radio devices, used to configure our experimentation environment.

### 4.4.1 Experimental Setup

We deploy the disaggregated heterogeneous network setup as follows. One testbed node is used as our Core Network, where the measured traffic is injected, intended

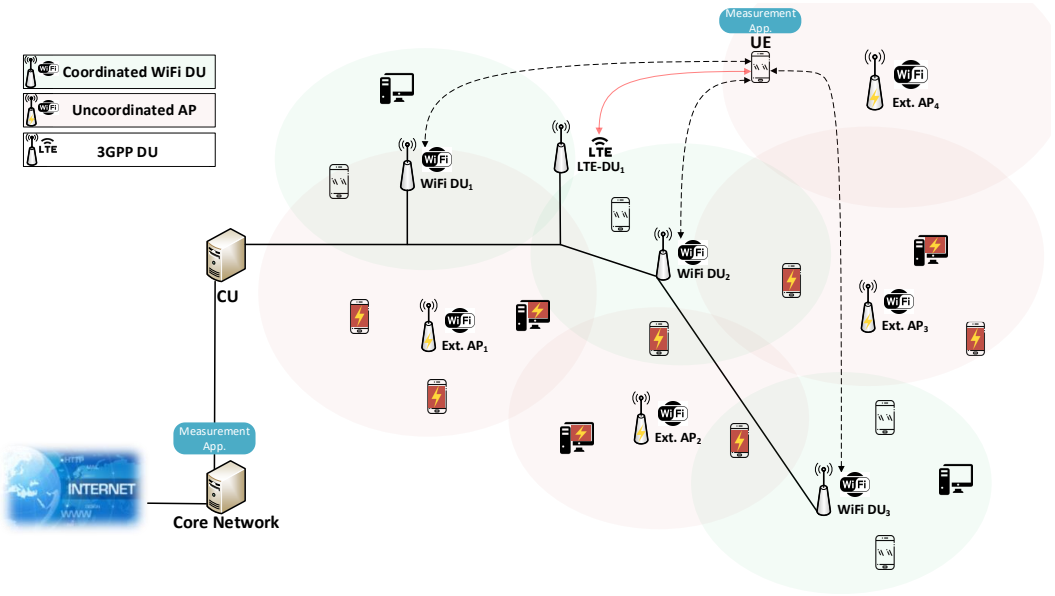


FIGURE 4.3: Experimental Architecture Overview.

to the UE. One node equipped with a Software Defined Radio (SDR) is used as our 3GPP DU component. We use the LTE implementation of OpenAirInterface, with 10MHz channel bandwidth in the 2.6GHz FDD band, using SISO (one antenna). The same node is also hosting the CU implementation. One more node is used as the Wi-Fi DU component, hosting the software for managing it through the CU side of the network, as shown in [13]. One node is playing the role of the UE, equipped with an LTE dongle (Huawei E3372) and a wireless IEEE 802.11 adapter. The nodes of the disaggregated base station network are interconnected using 1Gbps Ethernet links. Finally, we employ 3 pairs of Wi-Fi nodes in total, as our interference generators, set to operate in Channels 1, 6 and 11, creating traffic with different demands for resulting in three scenarios: 1) low, 2) medium and 3) high interference settings. The IEEE 802.11n configuration for these nodes is configured as 3x3 MIMO with 20MHz channel bandwidth. Intentionally, we set channels 1, 6 and 11 to be the operating channels for interfering APs 1, 2 and 3 accordingly, in order to cover the whole band with external interference. Bearing in mind the uneven load distributions are given in typical Wi-Fi networks, we randomly generate traffic demands for each uncoordinated AP during the experiment. More specifically, we randomly adjust the duration and the traffic demand individually for every stream generated. In such way, we maximize the presence of harmful uncoordinated interference in a limited spectrum portion like 2.4GHz ISM band. Table 4.1 shows the average amount of traffic for all interference scenarios that each of the uncoordinated pairs is trying to send over the network. The analytical overview of the examined architecture can also be found in Fig. 4.3.

TABLE 4.1: Throughput Demands (Mbps) per each Uncoordinated AP (Ext. AP) / UE.

| *Scenario* | UE | Ext. AP1 | Ext. AP2 | Ext. AP3 |
|---|---|---|---|---|
| ***High Interference*** | 30 | 263.0 | 261.2 | 295.6 |
| ***Medium Interference*** | | 179.6 | 162.2 | 177.2 |
| ***Low Interference*** | | 23.4 | 24.4 | 26.0 |

### 4.4.2 Evaluation

For the evaluation of the efficiency of our approach, we use different selection schemes for selecting the Wi-Fi DU operating frequency. We measure the downlink (DL) channel operation by injecting UDP traffic at the Core Network side, splitting it over the LTE and Wi-Fi DU and measuring the performance at the receiving multihomed UE. As we did not observe any fluctuations for the LTE link, we ommit plotting the traffic achieved over this network. However, as a reference, the achieved throughput is 34.4Mbps for UDP traffic, when the maximum theoretical is 36.69Mbps based on the hardware configurations.

We follow two approaches for selecting the wireless operating channel at the Wi-Fi coordinated DUs (Wi-Fi DUs). Initially, we employ Linux hostap's Automatic channel selection (ACS) tool [86]. At this case and during the AP's utilization procedure, the wireless adapter executes a survey based algorithm which reveals the less utilized frequency. This approach is based on the channel busy, active and tx times in order to export an interference factor for each frequency, and the channel which holds the lowest interference factor is selected as operating. Contrariwise, the proposed SACS framework is constantly aware of the channel conditions as it is periodically triggered every 5 seconds, as described earlier in this chapter. Additionally, the generic energy detection applied, allows us to discover interference produced by both operating and nearby Wi-Fi channels. Thus, SACS enables the awareness and avoidance of IEEE 802.11 and non interference for all frequencies and in real time.

Figures 4.4, 4.5 and 4.6 depict the results exported for ACS and SACS mechanisms, averaged after 10 experiment runs of 100 seconds in the testbed. We plot the achieved throughput over the Aggregation DU (measured at the UE), and for each of the interfering APs. For the case of low external interference (Figure 4.4), we see that the aggregation DU manages to get roughly 30% better throughput. This is due to the constant changes of the examined link with the CSA mechanism every 5 seconds. The interfering nodes seem to achieve the same performance for the case where we employ SACS on the aggregation DU, although one of the interfering APs seems to achieve less than with the off-the-shelf ACS tool. This is due to the choice of the ACS solution to select a channel from the ones that the interfering links work, in order to content for the medium access instead of selecting a channel where it would create and receive external interference.

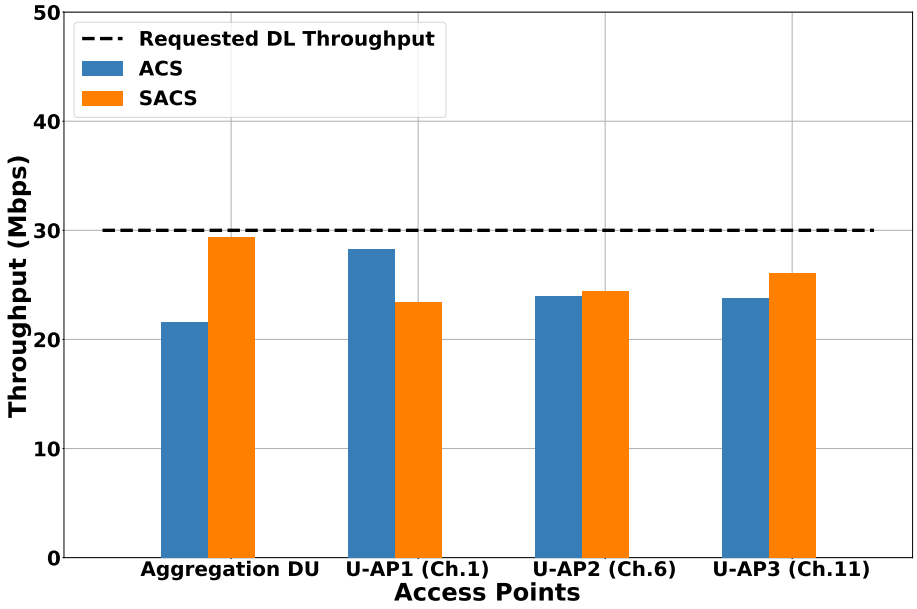


FIGURE 4.4: Evaluation - Low Interference

For the cases of medium (Figure 4.5) and high interference (Figure 4.6) the benefits of our solution are more evident; the throughput achieved through SACS is up to 5 times better, almost achieving the 30Mbps that we inject to the network.

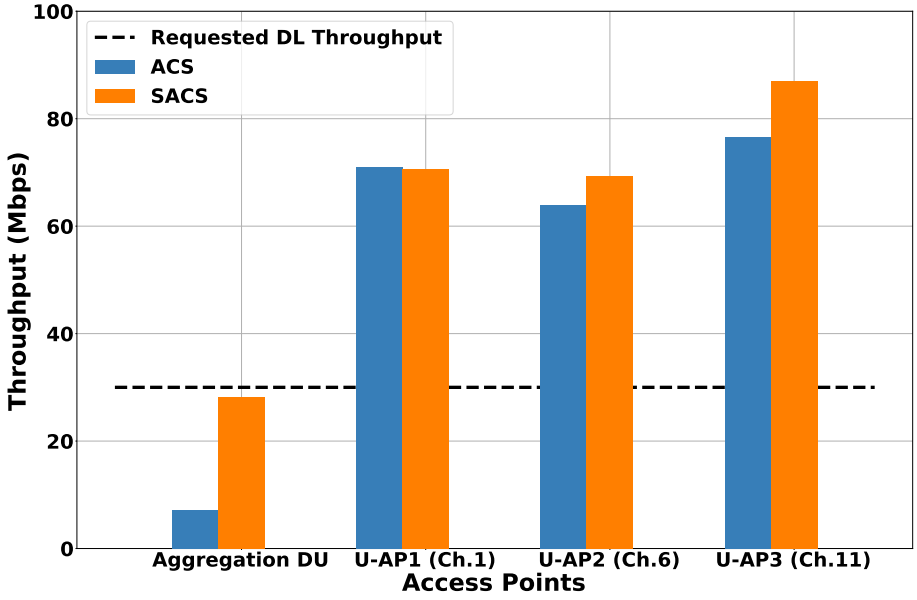


FIGURE 4.5: Evaluation - Medium Interference

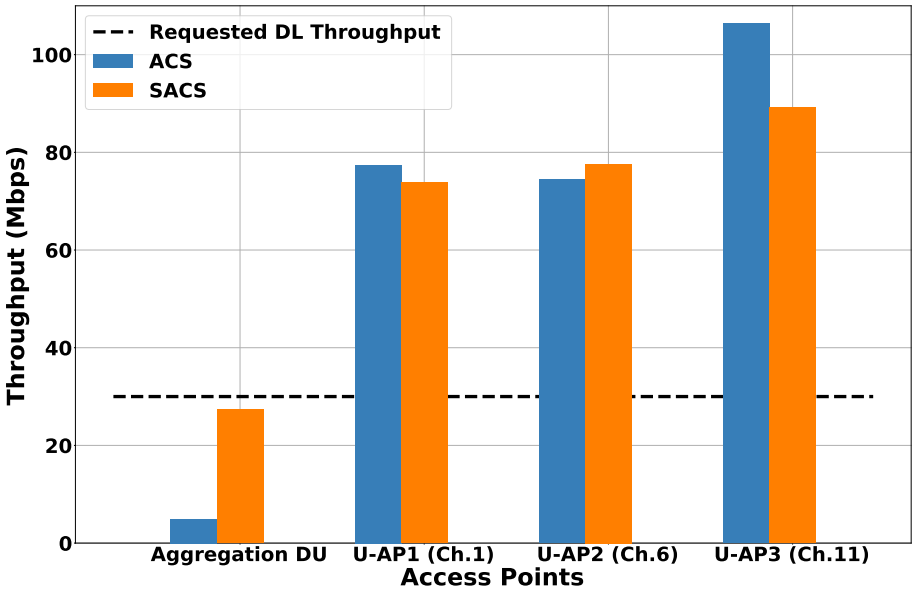


FIGURE 4.6: Evaluation - High Interference

As a conclusion, we note two severe drawbacks detected through our experiments for the off-the-shelf ACS tool. The less utilized channel is only adjusted once and during AP's initialization. This could be characterized as inconsistent with the rapidly fluctuating spectral conditions in today's dense networks, and hence degraded performance is expected at the interfering nodes as well. Furthermore, the channel busy time that is used as a metric to evaluate each channel exclusively takes into account the time in which the wireless adapter tries and fails to initiate a communication at this specific frequency. This entails the omission of possible interference caused by nearby overlapping Wi-Fi channels, which is thoroughly considered in the proposed SACS framework.

## 4.5 Conclusions

In this chapter, we introduced a scheme for creating spectral awareness at non-3GPP DUs in a cloud-RAN infrastructure. Through dedicated signaling between the different participating units and the cloud located part of a base station, we are able to select the most efficient frequency within the operating band. Awareness is also enabled at the UE side of the network, which chooses to associate to the Wi-Fi DU that is considered to be more efficient. By utilizing the Wi-Fi Channel Switch Announcement mechanism, we are able to constantly switch the operating channel, along with the associated UEs. Our testbed experiments illustrate the benefits of our solution, as we are able to transfer up to 5 times more throughput over the network for the cases of heavy external interference.

# Chapter 5

# Interference Prediction and Link Performance Estimation

**Contents**



In this chapter a novel framework for acknowledging future interference levels at IEEE 802.11 networks, is developed and experimentally evaluated. By actively gathering several wireless metrics, the proposed mechanism is able to accurately estimate and predict the performance for any given IEEE 802.11 link at the areas of supervision in real-time, without presupposing any Access Point - Station association. Long-term utilization predictions are exported through Machine Learning, regarding the future (2-hour) utilization at any Wi-Fi channel. Additionally, short-term predictions and accurate throughput calculations are extracted, when the current conditions largely differ from long-term predictions. The proposed framework covers comprehensively the cases of interference created by either 802.11 or non 802.11 devices, which may occur at the target or at any overlapping wireless channel. Finally, extensive testbed experimentation proves the framework's proper functionality and accuracy, under the cases of both Indoor (controlled interference) and Outdoor (uncontrolled massive interference) environments.

## 5.1 Introduction

The ever-increasing demand for continuous wireless connectivity over the past years, drastically formats the landscape of future communication systems. The constantly increasing wireless data demands have gradually rendered the existing infrastructures inadequate to cope with the increasing loads. Furthermore, as the demand for ultra low-latency and Gbps communications is constantly growing with the advent of 5G networks, proper ways for overcoming the spectrum crunch phenomenon are being investigated. Two approaches are considered: 1) the usage of new spectrum bands (e.g. the cm- and mm-Wave bands), and 2) the efficient use of existing sub-6GHz technologies, with advanced spectrum coordination techniques. The prevailing approach so far, urges the transition from macro cell architectures to the deployment of small and low range base stations that complement the coverage of

macro-cells. Therefore, a combination of new-introduced and pre-existing wireless standards, can be used in order to fulfill the increased user demands in modern wireless systems.

Driven by the wide availability of Wi-Fi networks, a significant effort of the current research approaches select IEEE 802.11 (Wi-Fi) cells for dynamically serving large amount of traffic demands in 5G architectures. This can happen with either the densification of the network with heterogeneous technologies, and appropriately steering traffic to them [87], or through the integration of WiFi access in the cellular stack. An example of the latter can be found in the 4G LTE specifications, with the LTE WLAN Aggregation Adaptation Protocol (LWAAP) [10] [9]. Driven by the RAN cloudification in 5G-NR specifications, the integration of heterogeneous access is enabled through heterogeneous Distributed Units (DUs) [76]. Such DUs can support different technologies, e.g. 5G-NR, LTE or non-3GPP like WiFi, and are managed by the same Central Unit (CU). In this chapter, we focus on such architectures, and incorporate sophisticated algorithms and processes for managing the spectrum at the access level, when considering dense deployments of such DUs.

Delving into the different characteristics of each technology, contrary to the frequency and time allocation schemes commonly applied in the licensed spectrum (cellular technologies), most of the protocols/RF devices operating in the ISM bands are designed to transmit opportunistically in a selfish manner. The aforementioned phenomenon combined with both a large number of non-3GPP (Wi-Fi) terminals and external interference sources given nowadays, frequently results to low and unpredictable performance when accessing the ISM spectrum. Consequently, the performance uncertainty for DUs operating at the ISM bands constitutes a real struggle, in the case that they need to provide guaranteed access to the network. Thus, proper ways for predicting the channel quality for these unprotected frequencies are now considered essential. Machine Learning (ML) can play an important role in accurately predicting the expected performance for each network, based on predicting isolated features, the combination of which can reveal the actual offered capacity. The quality prediction problem is usually formulated as a Time-series prediction problem, thus enabling the application of several ML-driven methods for predicting factors and metrics in the network that directly affect the performance over the network.

In this chapter, we adopt the disaggregated multi-technology base station architecture [13] and introduce a novel framework for estimating and predicting the performance of each UE in the unlicensed Wi-Fi bands. More specifically, besides the deployed CU and Wi-Fi DUs, we also introduce the entity of a Monitor DU in the considered network architecture as illustrated in Figure 5.1. The presented framework differentiates from similar efforts in bibliography by predicting the expected Duty Cycle ($\mathcal{DC}$) at each Wi-Fi channel, a metric that can be used alongside with other wireless analytics, to efficiently calculate the estimated capacity of each network. This is, to the best of our knowledge the first apporach that considers the evolution of this metric, towards providing tangible proof [67] about the estimated performance over each wireless link. ML is employed towards predicting such metrics, that are used to estimate the available capacity per each link. The ML models that we use have been selected after multiple experimental evaluations of different Neural Network models, towards increasing the accuracy and lowering the execution time.

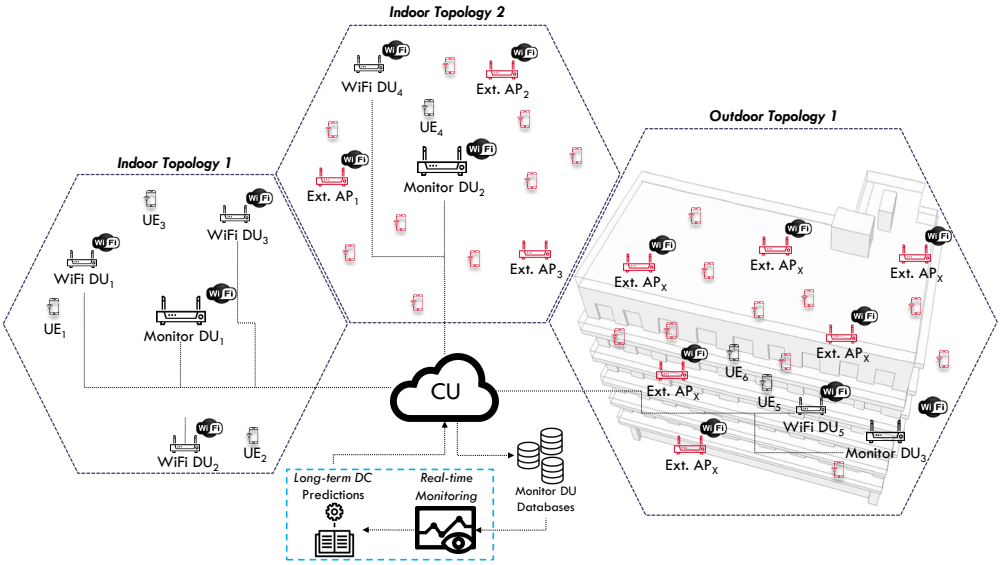


FIGURE 5.1: Under study system architecture: dedicated monitor DUs constantly collect spectrum metrics for their area of supervision, and upload them to the CU running at the network edge. Metrics are extracted, and Machine Learning algorithms are able to predict their evolution in the future, while also estimating the expected performance for each wireless channel through their combination.

The estimation process is running on the operator side of the network, and can assist towards the selection of cells that can serve each client of the network in the most efficient manner. The overall system is experimentally driven and runs on real off-the-shelf devices, deployed in an outdoor dense urban area with entirely uncontrolled external interference settings. Contrary to our approach, prior works are mainly focusing on predictions at the client side, based on the received signal strength. The key contributions of this chapter can be summarized as follows:

- To dynamically estimate and predict the delivered performance ( *network capacity*) that a user shall get over a target non-3GPP DU. Through the employment of advanced wireless analytics, we are able to make long and short-term accurate predictions on the utilization of each network. This is, to the best of our knowledge, the first approach in which the estimation is taking place before the user association with the DU.
- To export performance estimation calculations and predictions for all Wi-Fi channels by taking into consideration analytically the interference occurred by (1) Wi-Fi terminals from overlapping channels, (2) WiFi terminals at the same channel and (3) non-IEEE 802.11 interference.
- To experimentally evaluate and showcase the gains in a real ultra-dense network setups, for several different controlled and uncontrolled interference scenarios.

## 5.2 Related Work

Performance estimation approaches for either wired or wireless networks has fostered efforts in several research works in relevant literature. As the network deployments become denser and rich in the offered technologies, their efficient coordination, planning and placement in operating spectrum is of primary importance for providing high quality connectivity services to end users. The ability to accurately calculate and predict the expected performance, may constitute a crucial factor for the proper and efficient network design and planning. Three different types for performance predictions can be extracted from the proposed research approaches [88]: 1) formula-based (e.g. [89]), 2) history-based (e.g. [90]) and 3) based on the application of machine learning (ML) (e.g. [91]). We organize the relevant works in two subsections: (1) on performance estimation, based on either formulas/historical data, and (2) based on the application of ML models.

### 5.2.1 Performance Estimation

This category covers works which develop mathematical formulas for modeling TCP or UDP behaviour, based on several link characteristics (rate, jitter, packet loss, round trip time etc). For history-based approaches, the estimation is calculated based on previous performance measurements (e.g. throughput calculation during a specific time period). The future throughput predictions are based on the moving averages for past values. As the wireless network can have wide fluctuations in the quality, affecting the client performance, link estimation is of crucial importance for the efficient operation of the network. Authors in [88] estimate the cellular network performance, by employing 7 different algorithms. They introduce the theory of differential entropy to estimate the lower bound on throughput predictions, and use actual celluar data for efficiently preddicting the TCP throughput In the case of non-3GPP access, estimations are harder to be made efficiently, due to the opportunistic access of the spectrum. Therefore, performance estimation is usually backed by an interference detection/estimation scheme. Authors in [92], propose a network planning scheme for Wi-Fi networks deployed in ultra dense scenarios. Their work is based on interference alignment, with their cells being separated into smaller subregions, and using the same channel allocation. The proper size of the subregions as well as the selected channel is extracted by maximizing the Degree of Freedom (DoF). However, in practical ultra dense networks and in the case of the unlicensed frequencies, there can be no assurance for the absence of external not coordinated Wi-Fi APs.

Similarly, in [93] a Dynamic Channel Selection (DCS) algorithm for sectorized WiFi cells is proposed. More specifically, the authors share the coordinated APs between the three "non" overlapping (1,6 and 11) channels. Under the use of RSSI and RF utilization metrics, they periodically create an interference map which drives the DCS. Although the mechanism measures the Wi-Fi interference created from both coordinated and uncoordinated APs, the interference occured from channels besides 1,6 and 11 is not considered. Authors in [94] delve into interference mitigation techniques, towards enhancing the quality of the offered wireless services. Works [95, 96, 97] present different analytical models which focus on Wi-Fi related parameters like A-MPDU aggregation, Block ACKs and packet retransmissions. Indicatively, Nayak et al. [95] introduce the Virtual Speed Test (VST), an AP analysis tool for

estimating the performance in both downlink and uplink TCP traffic scenarios. By passively collecting statistics for all the active TCP connections, they calculate the time needed for transmitting and acknowledging each packet. The aforementioned approach assumes that all the examined stations are connected and actively transmit large amounts of data, in order to be identified and successfully measured.

### 5.2.2 ML based estimation

ML techniques that have been very popular lately have transformed as the prevailing approach for performance prediction especially for wireless networks. For such networks, the sophisticated pattern recognition may provide accurate predictions, driven by historical data, while adapting the estimations based on a different variables and features that might impact performance.

Their adoption is also reflected in the current efforts under the Open RAN (O-RAN) alliance [98], through the integration of ML analysis for channel quality measurements driving resource allocation in the RAN. In [99], authors describe how a data-driven architecture of a wireless network can benefit from the application of online learning, such as in the cases of load balancing, etc. In [100], authors argue about the opportunities in the cellular network for applying ML towards optimizing its behavior. Authors in [101], present an analytical survey on models and concepts based on ML that can be used for managing and organizing cellular 5G networks. In [102], authors use an edge-controller-based architecture for cellular networks and describe how the controllers can be used to run ML algorithms to predict the number of users in each base station. Finally, a use case in which these predictions are exploited by a higher-layer application to route vehicular traffic according to network Key Performance Indicators (KPIs).

Specifically to non-3GPP access, authors in [103] develop an unsupervised Neural Network to filter the detected transmission collision probability in the unlicensed spectrum. Their solution is trained online, and can precisely rectify the measurement error and estimate the number of active WiFi users from the user side. In [104], a reinforcement learning algorithm is introduced, aiming at the problem of opportunistic coexistence of unlicensed LTE and WiFi. The proposed approach in particular is based on Q-Learning, which provides a robust and model-free decision-making framework. Authors in [105], design and formulate a function for autonomous APs that estimates throughput and delay of its clients in 2.4GHz WiFi channels. The target AP can estimate throughput and delay of its clients without actually switching to each channel, but only monitoring MAC level information sent over the network. Authors in [106, 107], exploit ML for predicting wireless channel quality. In [106], a deep learning scheme is applied to predict wireless interference, showcasing gains in Signal to Noise Ratio (SNR) monitored at the network's clients. Struye et. al in [107] propose a Neural Network-based Interference prediction scheme. More specifically, the authors try to deal with the unexpected presence of interference existing at city environments. They employ a Gated Recurrent Neural Network (RNN) towards forecasting the RSSI values for each deployed AP at different times of the day.

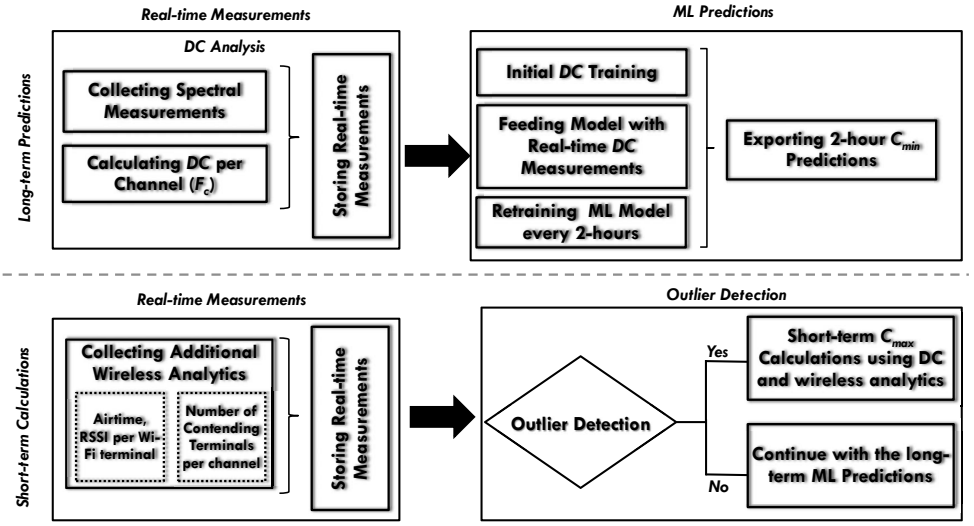


FIGURE 5.2: Process flow for the proposed framework

Process flow for the proposed framework; the framework is able to predict accurately for the long-term, by performing DC analysis and using our ML model. The long-term predictions are validated through extended analytics, and if found invalid are corrected with the short-term predictions.

### 5.2.3 Contribution with respect to State-of-the-Art

In this chapter, we develop an analytical framework for estimating the network capacity of non-3GPP Wi-Fi networks, using a wide set of wireless analytics. We differentiate from the previous works by focusing on the prediction of the Duty Cycle ($\mathcal{DC}$) metric, contrary to prior approaches focusing on common values such as the RSSI, which in turn can be used to efficiently estimate the available network capacity that can be used by each network client. The $\mathcal{DC}$ metric can generalize to other types of networks as well, showing the measured energy values in defined chunks of spectrum. Thus, it can be applied to networks using other access mechanisms and different physical access schemes other than the ones used in Wi-Fi (CSMA/CA and OFDM/OFDMA). We apply the scheme in a novel disaggregated 5G Cloud-RAN, based on our prior contributions in [108]. The ML approach is based on a Gated Recurrent Unit (GRU) Neural Network, which has been selected over other approaches after extended testing and evaluation of the training time needed and achieved prediction accuracy. In the following section we detail the proposed framework and ML model that we use.

## 5.3 Framework

In this chapter we design, develop and experimentally evaluate a hybrid novel framework for estimating, predicting and calculating channel performance for each client operating at the unlicensed Wi-Fi bands and in real-time. More specifically, by actively gathering several wireless metrics which are obtained from commercial off-the-shelf (COTS) devices, the proposed framework predicts the transmission opportunities per channel for the next 2-hours, with a minute-based resolution through

ML. When the ongoing spectral conditions largely differ from the long-term predicted, an additional history-based short-term mechanism is activated and calculates the exact performance which can be currently achieved. Both mechanisms run in parallel for collecting metrics, and make conclusions only when the framework decides that they should run. Figure 5.2 shows how the different components interact with each other. In the subsections below, we detail how each of the components works. It is worth to be noted that the proposed mechanism does not require in any case Wi-Fi DU - UE associations. The next sections describe how the framework is organized: Sections 5.3.1 and 5.3.2 show the internals of the long term prediction model, while sections 5.3.3 and 5.3.4 describe how we employ additional analytics and make short-term estimations on throughput.

### 5.3.1 Motivation and Data Set Description

In the context of this chapter, we use part of a data set which uninterruptedly stores measurements since 2016. Similarly with [107], we take advantage of the spectral measurements which can be revealed through the application of Energy Detection on commercial Wi-Fi chipsets. Indicatively, we have deployed a Monitor DU on the top of an office building (3rd floor) in the densely populated city center of Volos, Greece. In particular, the TP-link WR2543ND V1 [109] router is engaged to run as a spectrum analyzer, monitoring of all the sub-6GHz IEEE 802.11(a/ac/b/g/n) wireless standards.


FIGURE 5.3: Monitor DU Device

In contrast with prior works, in which the Received Signal Strength Indicator (RSSI) is used as a key metric, we extract the Duty Cycle ($\mathcal{DC}$) of each scanned channel based on the spectral measurements. For each Wi-Fi channel ($\mathcal{F}_c$), we collect multiple spectral samples ($\mathcal{N}_S$) and export the $\mathcal{DC}$ percentage utilization as follows:

$$\mathcal{DC}_{\mathcal{F}_c} = \frac{1}{\mathcal{N}_S} \sum_{S=1}^{\mathcal{N}_S} on(\mathcal{P}(\mathcal{S}, \mathcal{F}_c), \mathcal{P}_{TH}), \tag{5.1}$$

More specifically, we use $\mathcal{P}(\mathcal{S}, \mathcal{F}_c)$ to denote the power of each Spectral Sample ($\mathcal{S}$) that has been collected on the central frequency $\mathcal{F}_c$. Thereupon, each Spectral Sample's power is compared with a power threshold ($\mathcal{P}_{TH}$) and consider it "on" if found higher than that. In order to set the $\mathcal{P}_{TH}$, the proposed framework uses the Energy Detection (ED) and Clear Channel Assessment (CCA) thresholds, as defined per each IEEE 802.11 standard version. Additionally, we collect 200 $\mathcal{N}_S$ per $\mathcal{F}_c$ for increasing the precision of the detection process. It is worth to be noted that the spectral samples are captured in 20MHz width and with 56-FFT bin resolution. There are multiple spectral sample configurations which are supported from the wireless adapters (up to 80MHz with 256 bins). However, we employ this configuration at the lowest channel settings, as it may be multiplied for higher channel widths without any information losses. Through the proper adjustment of the CCA/ED thresholds, the $\mathcal{DC}$ information is calculated for the primary and secondary(ies) channels, and useful utilization and performance information for 20-160MHz wide channels can be retrieved. Based on the applied configurations, the spectral scan for all channels in both 2.4GHz and 5GHz is calculated within ∼240ms. The detection accuracy of the aforementioned approach has been proven analytically in [67]. Furthermore, we trigger each monitor DU to obtain spectral measurements and calculate the $\mathcal{DC}$ utilization values for all 20MHz Wi-Fi channels every 10 seconds. While the aforementioned procedure is uninterruptedly executed from May 2016 until today, we now hold a data set of ∼16 million $\mathcal{DC}$ values for each frequency.

As the $\mathcal{DC}$ notion is solely based on Energy Detection measurements, some interesting facts can be summarized as follows. Primarily, both the amount of interference occurred from IEEE 802.11, as well as for non-IEEE 802.11 devices (e.g. microwave ovens, baby monitors, Bluetooth devices, wireless cameras etc) are included in the $\mathcal{DC}$ metric. Furthermore, medium and frequency access schemes (e.g. CSMA/CA, OFDM, OFDMA), do not affect $\mathcal{DC}$ calculation, as it is extracted by raw energy of spectral samples which are taken over time.

By taking into account equation 5.1 and all the remarks stated above, the $\mathcal{DC}$ metric may also represent the minimum free transmission opportunities, which are given at each $\mathcal{F}_c$:

$$\mathcal{C}_{min} = (1 - \mathcal{DC}_{\mathcal{F}_c}) * \mathcal{T}_{\mathcal{MCS}}, \tag{5.2}$$

where $\mathcal{T}_{\mathcal{MCS}}$ is the theoretical throughput corresponding to each case Modulation and Coding Scheme (MCS), for either UDP or TCP traffic streams [110]. Finally, by gathering additional wireless metrics as described in the following Sections, this framework tackles the problem of the performance estimation uncertainty for IEEE 802.11 systems and export the maximum transmission opportunities ($\mathcal{C}_{max}$) which can be achieved for each channel.

### 5.3.2 Machine Learning $\mathcal{DC}$ Training and Prediction

In the context of this chapter, we additionally develop Machine Learning (ML) models to make long-term (2-hour) predictions of the $\mathcal{DC}$ utilization for all Wi-Fi channels. Specifically, we make a prediction for the $\mathcal{DC}$ utilization every minute into the

future, based on historic measurements. Thus, a detailed analysis for the expected $\mathcal{C}_{min}$ of every Wi-Fi terminal is outputted, by jointly taking into account, the frequently updated RSSI values in the central database. Since the problem we tackle is a time series prediction, we use Recurrent Neural Networks (RNNs). This type of networks have been proven to be appropriate for modeling sequence data [111, 112], due to the fact that they can recognize temporal patterns by remembering aspects of past inputs in their internal memory.

In particular, we have tested Gated Recurrent Unit (GRU)[113] and Long short-term memory (LSTM) [114] models, which are implementations of the RNN concept. Both deployed models contain two stacked GRU/LSTM layers of 500 units each, followed by a fully connected layer which reduces the outputs to a single value. Additionally, they are trained for 100 epochs and by using the adam optimizer [115]. Furthermore, early stopping with patience argument [116] was used, in order to make model training procedure even faster. In such way, when the monitored metric stops improving, the training process is being terminated and based on the defined patience given.

As input, we feed the models with a part of the $\mathcal{DC}$ dataset described in Section 5.3.1. There, an uninterrupted monitoring of the spectrum conditions, is taking place from May 2016 and until today. As it is analytically described, through the appropriate use of equation 5.1, we are able to calculate the $\mathcal{DC}$ utilization for each Wi-Fi channel every 10sec. In the proposed approach, we use the most recent $\mathcal{DC}$ measurements which are from January until October 2020. The input data are split in 70-30 ratio for training and validating the models accordingly. Furthermore, the measurements are normalized between 0 and 1. Since the target prediction is for two hours in the future, the model is retrained every two hours to keep up with the real-time collected $\mathcal{DC}$ measurements. The machine used for (re)training our models is using an Intel Core i7-8700 CPU at 3.20GHz with 16GB RAM. The initial training process lasts approximately 20 minutes for GRU and 45 minutes for LSTM. Due to the fact that we use an early stopping with patience of 25, while monitoring the validation loss, the GRU model stops training at 43 epochs, compared to LSTM which terminates training at 100 epochs. It is also noted that the retraining procedure lasts less than a minute for both models. Additionally, smaller patience for the LSTM model could be given, which may lead to faster training. However, it was deemed correct to compare these models under exact same configurations. Several configurations (layer units, epochs, patience etc) were extensively tested for the developed ML models. However, the aforementioned configurations were selected as they efficiently fulfill the dynamic requirements of the proposed framework, with the minimal overhead.

However, in real world uncontrolled spectrum environments, the channel utilization and in consequence the $\mathcal{DC}$ values per second may contain great variations. This is due to the frequent arrival and departure of Wi-Fi stations, as well as in the various traffic demand profiles of each device. For this reason, the prediction of the $\mathcal{DC}$ value in a decimal place precision, would be both hard and unnecessary. In such way, for evaluating the final results, we create three classes: "class2", "class5" and "class10". These numbers represent the class size in percentages of the $\mathcal{DC}$ value. Therefore, for example in class10 we have batches of $\mathcal{DC}$ values between 0-10, 10-20 and so on until 90-100%. In the proposed model, we classify the predicted values and the actual values into these three classes and measure the accuracy of each class for both GRU and LSTM, as depicted in Figures 5.4 and 5.5 .

In order to evaluate the model, we feed it with the $\mathcal{DC}$ data from January through

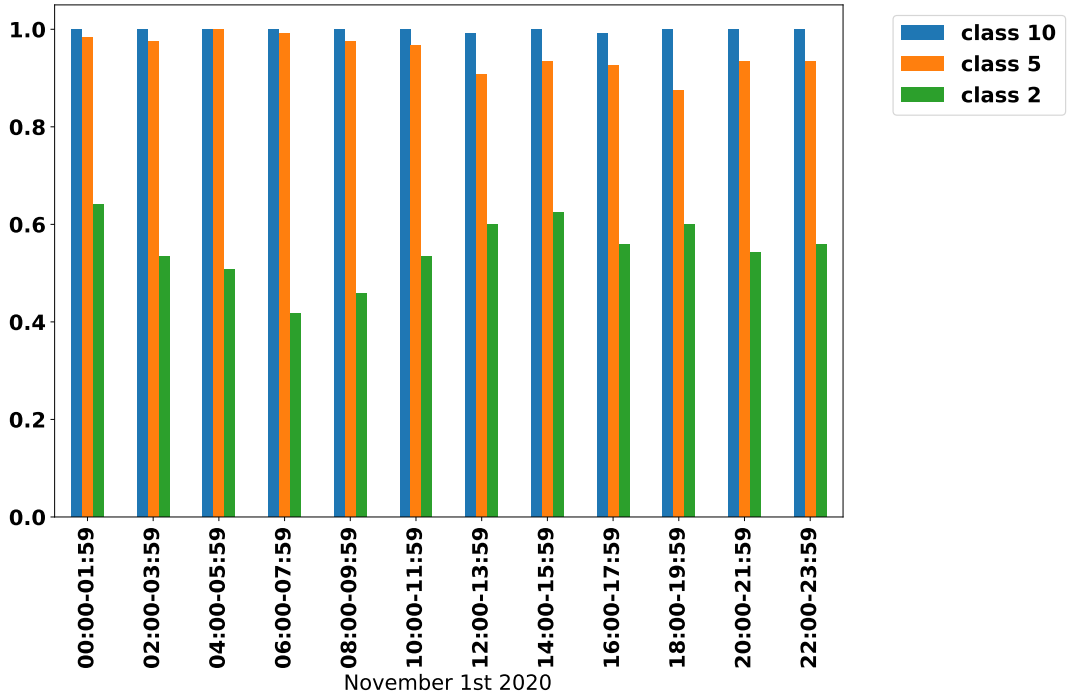


FIGURE 5.4: DC Class Prediction Accuracy (per-minute).

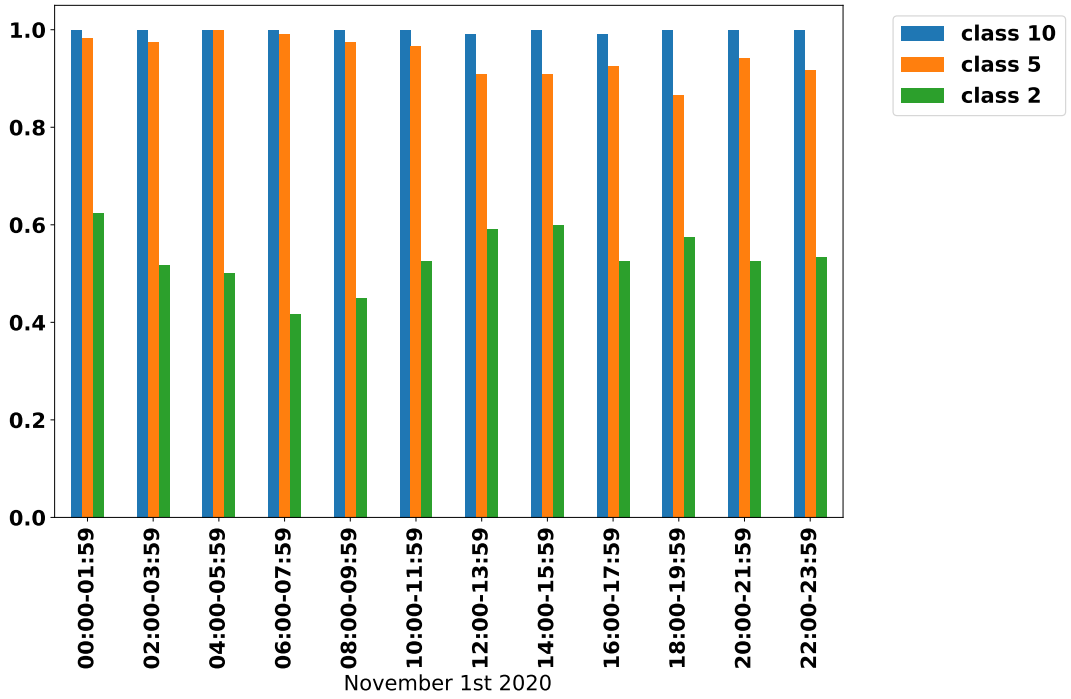


FIGURE 5.5: DC Class Prediction Accuracy (per-minute).

October 2020 and we indicatively forecast the first day of November. Within the 2-hour intervals, the GRU model achieves accuracy which ranges between 41-64%, 87-99%, 99-100% for classes 2, 5 and 10 respectively (Figure 5.4). Respectively, for the same class sizes, LSTM achives prediction accuracy of 40-62%, 86-98% and 99-100% (Figure 5.5) and thus, the model selected for this framework is the GRU which is slightly better. Thus, it is confirmed that great $\mathcal{DC}$ utilization variations are given at

those uncoordinated outdoor environments. In such way, lower $\mathcal{DC}$ detection accuracy is observed for classes 2 and 5. This is happening due to the dynamics of the wireless conditions that we test our framework, as it is a dense outdoor environment with high uncontrolled external interference. This in turn causes the $\mathcal{DC}$ metric to greatly variate in smaller examined batches causing lower accuracy for the lower classes. As we consider higher classes, the variations in the $\mathcal{DC}$ diminish. Based on our findings, the class size 10 is selected for performing the $\mathcal{DC}$ predictions, as it offers the highest accuracy. More specifically, we keep the mean value of each predicted class for performing the long-term $\mathcal{C}_{min}$ calculations. Therefore, an error up to $\pm$5% may arise at the predicted $\mathcal{C}_{min}$ value per each minute.

### 5.3.3 Estimated Throughput Calculation

As stated in Section 5.3.1, the calculation of the $\mathcal{DC}$ metric can export useful information for the utilization of each Wi-Fi channel. However, this utilization percentage may contain both IEEE 802.11 and non-802.11 interference, which practically means that the estimated performance can not be characterized solely from it. A typical example could be that if an $\mathcal{F}_c$ is considered fully utilized from IEEE 802.11 stations ($\sim$100% $\mathcal{DC}$), this will not result to zero transmission opportunities if a new Wi-Fi terminal would try to transmit in the same frequency. As a rule, the occupied utilization at a Wi-Fi channel can be distinctly separated in:

$$\mathcal{DC}_{\mathcal{F}_c} = \mathcal{I}nt_{(Wi-Fi)} + \mathcal{I}nt_{(Ext)} \tag{5.3}$$

where $\mathcal{I}nt_{(Wi-Fi)}$ defines the sum of the airtime utilization for all the Wi-Fi terminals ($\mathcal{N}_{Terms}$), which transmit at the examined $\mathcal{F}_c$

$$\mathcal{I}nt_{(Wi-Fi)} = \sum_{i=1}^{N_{Terms}} (air_{i_{(\%)}}) \tag{5.4}$$

and $\mathcal{I}nt_{(Ext)}$ is the external interference occurred either from non-IEEE 802.11 devices, or from Wi-Fi terminals which transmit at the neighboring overlapping channels. The latter is a phenomenon happening by the design of the Wi-Fi protocol, as transmissions from neighbouring channels can be captured in a terminal but in most cases cannot be fully decoded.

$$\mathcal{I}nt_{(Ext)} = \mathcal{DC}_{\mathcal{F}_c} - \mathcal{I}nt_{(Wi-Fi)} \tag{5.5}$$

The substantial difference between $\mathcal{I}nt_{(Wi-Fi)}$ and $\mathcal{I}nt_{(Ext)}$ is that in the former, conventional mechanisms of the IEEE 802.11 standard as CSMA/CA, are activated and some transmission opportunities become available. In the latter, the presence of such interference exceeding the ED threshold, directly leads to failed / backed-off transmissions. For this reason it is essential to measure the amount of interference ($\mathcal{DC}$) at each $\mathcal{F}_c$, and perceive what causes it. In this manner, we can conclude on the maximum supported capacity of a cell at a given time. Similarly with [67], we follow all the pre-defined ED/CCA standard thresholds, in order to characterize an captured signal as harmful interference, thus including it in $\mathcal{N}_{Terms}$, $\mathcal{I}nt_{(Wi-Fi)}$, $\mathcal{I}nt_{(Ext)}$ and in

| type | mac_address | associated_to_mac | ssid | channel | rssi | airtime | dateandtime ▲ 1 |
|---|---|---|---|---|---|---|---|
| AP | C8:B3:73:21:DD | - | | 1 | -47 | 2.16801 | 2020-10-30 15:18:51 |
| STA | 38:BA:F8:58:08: | C8:B3:73:21:DD | | 1 | -52 | 0.766859 | 2020-10-30 15:18:52 |
| AP | B0:AC:D2:7A:AF | - | | 1 | -39 | 2.34183 | 2020-10-30 15:18:52 |
| STA | D4:76:EA:26:73: | (not associated) | | 1 | -63 | 0 | 2020-10-30 15:18:52 |
| AP | 96:B5:88:A8:F6: | - | | 1 | -65 | 0.192728 | 2020-10-30 15:18:52 |

FIGURE 5.6: Additional Wireless Analytics Instance

Additional Wireless Analytics developed and used for increasing the accuracy of our predictions; associations per each station, RSSI and airtime percentages for each Wi-Fi device are constantly monitored and logged in a central database, enabling the creation of a rich "spectral" map for the monitored area.

the airtime metric. All the calculations concerning the airtime percentages include the transmissions, re-transmissions as well as the control and management frames of each Wi-Fi device.

As the detection of $\mathcal{DC}$ metric takes ∼240ms and the procedure is executed periodically every 10 seconds, we take advantage of the idle time to capture several additional useful channel analytics. The collected analytics and metrics are further discussed in this section. The overall algorithm is summarized as follows: (1) Initially, the DC analysis from spectral scan is extracted. The process is blocking meaning that the wireless devices cannot be used during this interval (∼240ms) for any transmission/reception of data. (2) The mode of the wireless device is switched to a *monitor* mode, allowing the collection of the different metrics. The metrics collected under this mode assist in the identification of possible external and IEEE 802.11 interference, from adjacent/overlapping channels. This process is lasting for 10 secs - 240 ms. In this manner, the entire analysis of the channel conditions is restricted to 10 seconds in total, ensuring that enough spectral data covering a rich number of different cases are collected. (3) From the data collected within the second interval, we calculate the maximum capacity per each channel, as further defined in this section. This process is repeated per each minute, and runs completely at the Monitor DU entity of the network.

Regarding the collected metrics, when the wireless adapter is switched to the *monitor* mode, it acts as a packet sniffer by utilizing *airodump* [117], *tcpdump* [118] and *tshark* [119] Linux tools. By serially scanning all the Wi-Fi channels with airodump, we are able to create every minute an additional useful spectrum map, which contains all the present AP-STA associations per channel and the RSSI for each terminal. Furthermore, the exact airtime for each Wi-Fi terminal is calculated through the use of tcpdump and tshark tools. A python script was developed in order to orchestrate the above procedure and similarly with $\mathcal{DC}$, store all the results in a database as shown in Figure 5.6. In such way, the exact $\mathcal{C}_{max}$ performance which can be achieved at each $\mathcal{F}_c$, can be indicated under the proper combination of $\mathcal{DC}$ with the number of terminals and the occupied airtime. Based on IEEE's 802.11 Distributed Coordination Function (DCF), the medium should be equally distributed in all users, thus achieving service fairness [120] at each wireless channel. As $\mathcal{I}nt_{(Ext)}$ unavoidably leads to failed / backed-off transmissions, we need to further break down $\mathcal{I}nt_{(Wi-Fi)}$ percentage for exploiting the contendable transmission opportunities. In a given $\mathcal{F}_c$, the users ($\mathcal{N}_{ContTerms}$) who will be affected in terms of performance, upon the arrival of a new user will be those of whom:

$$air_{(\%)} > (1 - \mathcal{I}nt_{(Ext)}) / (\mathcal{N}_{Terms} + 1) \tag{5.6}$$

and thus, the total percentage of the occupied contendable airtime in a channel can be calculated as follows:

$$\mathcal{C}ont_{(air)} = \sum_{j=1}^{N_{ContTerms}} (air_{j_{(\%)}}) \tag{5.7}$$

If we combine all equations introduced so far and by covering every possible case of fully utilized or not channels, the estimated throughput for a Wi-Fi terminal after associating at a specific $\mathcal{F}_c$ can be defined as:

$$\mathcal{C}_{max} = \frac{1 - \mathcal{DC}_{\mathcal{F}_c} + \mathcal{C}ont_{(air)}}{\mathcal{N}_{ContTerms} + 1} * T_{\mathcal{MCS}} \tag{5.8}$$

Despite the fact that the calculation at equation 5.8 reports the estimated throughput in a primary 20MHz channel, the appropriate reconfiguration of the CCA/ED thresholds, extracts the results for secondary channels, in the cases of 40-160MHz bandwidths.

### 5.3.4 Real-time Outlier Detection

As described at Section 5.3.2, accurate long-term (2-hours in a minute basis) utilization predictions can be provided, under the proper use of $\mathcal{DC}$ metric through ML. However, based on the dynamic demand profiles of the wireless users and the fluctuating dynamics of the wireless medium, several severe short-term variations may occur. These variations are considered as outliers and it is practically impossible to be predicted efficiently through ML in long-term periods [121].

In this way, we need to shield our system by dynamically detecting these short-term non periodic events. Thus, an additional rapid real-time prediction mechanism is developed and enabled when the current performance largely differs from the values which were predicted with the contributions described in Section 5.3.2. Let us consider the topology of "Outdoor Topology 1", as illustrated in Figure 5.1. Alongside with the Monitor $DU_3$, the Wi-Fi $DU_5$ is deployed and can be orchestrated from the CU. In order to successfully recognize the potential outliers, which may cause performance impairments in the short-term, we make use of the most recent $\mathcal{DC}$ measurements and the additional wireless analytics reported from Monitor $DU_3$. As described in the previous sections, we are able to accurately detect and calculate the impact of both IEEE 802.11 and non-802.11 interference, regardless whether this occurs in the target $\mathcal{F}_c$, or at overlapping channels.

Initially, it is very important to clarify if any abnormal spectrum behaviour is caused from the under consideration coordinated Wi-Fi DU and its associated UE(s) ($\mathcal{N}_{CoordTerms}$), or by external interference sources. In the proposed framework, the mechanism retrieves new $\mathcal{DC}$ measurements every 10 seconds (Section 5.3.1) and we define the current utilization $\overline{\mathcal{DC}}_{\mathcal{F}_c}(t_0)$, as the weighted moving average [122] of the last 6 measurements, which were obtained during the previous minute.

$$\overline{\mathcal{DC}}_{\mathcal{F}_c}(t_0) = \sum_{n=-1}^{-6} \mathcal{DC}_{\mathcal{F}_c}(t_n) * \mathcal{W}_{|n|} \tag{5.9}$$

Under the use of the weight vector $\mathcal{W}_n = [\,0.2857 \quad 0.2381 \quad 0.1905 \quad 0.1429 \quad 0.0952 \quad 0.0476\,]$, slightly greater emphasis is given on the most recent $\mathcal{DC}$ measurements. Furthermore, the proposed framework (Section 5.3.3) stores the additional wireless analytics one time every minute. In such way, we capitalize on the latest measurements for calculating the current airtime generated by the target coordinated devices:

$$\mathcal{C}oord_{(air)}(t_0) = \sum_{k=1}^{N_{CoordTerms}} (air_{k_{(\%)}}) \tag{5.10}$$

and subtract it from $\overline{\mathcal{DC}}_{\mathcal{F}_c}(t_0)$. The subtraction result is compared with the predicted class mean value of the current minute, as extracted from the ML long-term model. If the difference is greater than 10%, we consider that there is an active outlier, besides the coordinated terminals, which largely affects the $\mathcal{F}_c$. In such a case, the short-term $\hat{\mathcal{C}}_{max}$ calculation is enabled. In any other case, the proposed framework continues to calculate the $\mathcal{C}_{min}$, based on the ML prediction model described in Section 5.3.2. Additionally, the latest values of the wireless analytics database participate in the calculation for $\mathcal{N}_{ContTerms}(t_0)$ and $\mathcal{C}ont_{(air)}(t_0)$. Alongside with $\mathcal{C}oord_{(air)}(t_0)$ and under the use of equation 5.8, the next minute's short-term $\hat{\mathcal{C}}_{max}$ prediction is calculated. This procedure is executed every minute and effectively protects the proposed system from short-term outliers as proved in Section 5.4.

## 5.4 Evaluation

In this section, the evaluation of the proposed solution and the analysis of the collected results are described. It is worth to be noted that our framework is designed, developed and evaluated by exclusively using commercial off-the-shelf (COTS) hardware in a real testbed environment, under controlled and uncontrolled external interference settings. More specifically, the indoor and outdoor testbeds of NITOS, located in the premises of University of Thessaly in Greece are used [52]. In this manner, we are able to prove the functionality and benefits of the framework, in both interference controlled (indoor) and fully uncontrolled (outdoor) spectrum environments. In the context of this chapter, we evaluate the proposed framework for different channel widths (20-40MHz) in the 2.4GHz ISM band. In this band, given the country restrictions for the operation of devices the phenomenon of overcongestion and interference presence is more intense, contrary to the 5GHz band. More specifically, the overlapping channels in parallel with the signal interference created by non-IEEE 802.11 devices, highly increase the $\mathcal{I}nt_{(Ext)}$ factor. In contrary, such a case is very unusual in the 5GHz Wi-Fi frequencies due to the orthogonal channel allocation within the band. Of course, the proposed solution is applicable for both 2.4 and 5GHz Wi-Fi bands and with channel widths 20-160MHz. However, we opt to evaluate our framework under the most dense settings, in a disadvantageous and hostile spectrum environment.

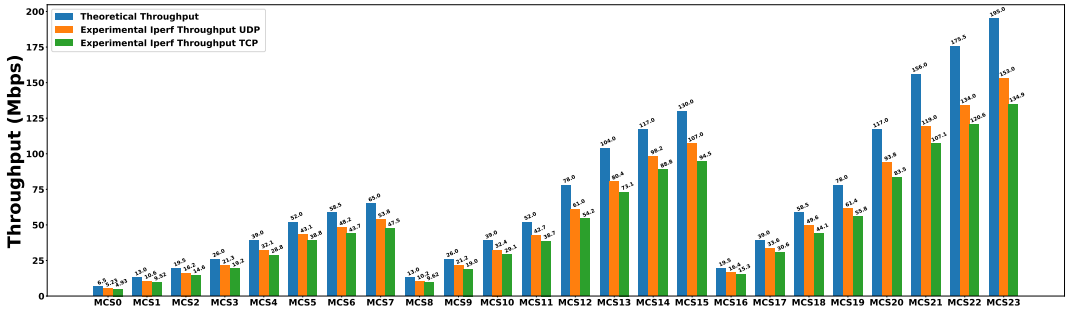


(a) 20MHz - Long GI

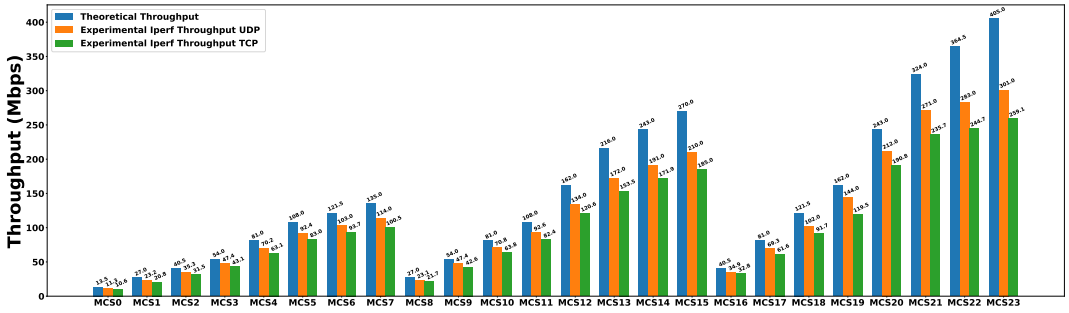


(b) 40MHz - Long GI

FIGURE 5.7: (Indoor Topology 1) - Application Layer Goodput.

### 5.4.1 Real-World Considerations

Initially, the maximum theoretical throughput ($\mathcal{T}_{\mathcal{MCS}}$) is considered (eq: 5.2, 5.8), for predicting the estimated link's capacity. In the context of this chapter, we evaluate the proposed system under both TCP and UDP traffic requests. Thus, it is useful to compare how the experimentally achieved throughput ($\mathcal{A}_{thr}$), converges to the theoretical for each available MCS. More specifically, the proposed framework calculates the estimated capacity $\mathcal{C}_{min}$ and $\mathcal{C}_{max}$, as reported by a traffic generator tool (*iperf* [123]). In this manner, the estimated throughput reflects the results based on the goodput received at the application layer. Of course, lower values than the theoretical limits are expected, as the throughput at this layer does not contain overheads like IEEE 802.11 headers, IP headers which are removed from lower OSI layers. Furthermore, it is very important to execute the experiments in completely isolated and unutilized frequencies. The deployed topology of this scenario corresponds to "Indoor Topology 1" in Figure 5.1. Specifically, we deploy a strong signal link (-23dbm), between a Wi-Fi DU and a station, which are equipped with at least one of the Qualcomm Atheros (QCA) 93xx/986x/988x 802.11a/b/g/n/ac wireless network adapters. We carefully select the deployed links to perform as optimal as possible. All the examined links continuously achieved greater than 99.4% probability of successful transmissions during the experiments, at the highest MCS 23 for both 20 and 40MHz channels. We configure the Wi-Fi DU to operate at primary channel 6 with HT40- capabilities and long Guard Intervals (GI). Serially, we configure all the available MCS profiles for the IEEE 802.11n standard and measure for 60 seconds the performance of each link, by creating saturated downlink TCP and UDP traffic streams with *iperf*. The averaged results after ten executions at each MCS, for both 20 and 40MHz channel widths and 1-3 spatial streams (SS), are depicted in Figure 5.7.

Furthermore, two similar strong signal links with different wireless adapters were identically instantiated and tested, in order to validate the results obtained from the first deployed link. It is worth to be noted that no significant deviations were observed between these three different examined links.

Additionally, the proposed model states the exploitable capacity of each channel to be "1". Practically, this means that an IEEE 802.11 device with no contention or external interference would be able to utilize 100% of the channel's airtime. However, based on the IEEE 802.11 standard, DCF Interframe Spaces (DIFS), Short Interframe Spaces (SIFS), Network Allocation Vectors (NAV), Contention Windows (CW) and other time depended parameters, some inevitable unexploited transmission slots exist in the Wi-Fi operation. In such way, it would be useful to experimentally measure these lost transmission opportunities and calculate the actual feasible channel airtime. During the calculation of $\mathcal{A}_{thr}$ as described in the previous scenario, we also examine the $\mathcal{DC}$ measurements for both primary and secondary operating channels per each MCS. In this manner, we observe the actually achieved channel utilization percentage to range from 90.91% to 96.17%. As this scenario involves the use of only two Wi-Fi devices, it is interesting to study if the participation of additional Wi-Fi DUs - STAs at the architecture, affects the aforementioned results. For this reason, we deploy additional links either at a random partially/fully overlapping channel with the primary one, which also transmit saturated traffic from the Wi-Fi DUs to STA(s). By altering the number of deployed Wi-Fi DUs from 1-5 and the associated STAs per each DU to 1-4, we observe that the $\mathcal{DC}$ values at the primary channel fluctuate from 90.58% to 96.70%. Finally, after averaging all the scenarios mentioned above, we calculate the total feasible channel utilization ($\mathcal{A}_{cc}$) to be 95.65%. Thereafter, we replace "1" with $\mathcal{A}_{cc}$ and $\mathcal{T}_{\mathcal{MCS}}$ with $\mathcal{A}_{thr}$ at the proposed model for remaining of our experiments.

### 5.4.2 Estimated Throughput Model Evaluation

In this experimental scenario, the proper function for the model proposed in Section 5.3.3 is extensively evaluated. More specifically, we assess the accuracy of the estimated throughput calculation in a target operating Wi-Fi channel. Likewise with the previous subsection, we obtain and evaluate the experimental results under the presence of controlled interference. In this context, we deploy a testbed node to act as the Monitor $DU_2$ and report the $\mathcal{DC}$ utilization values of the target channel, as well as the additional wireless analytics in real-time. These values alongside with those calculated in Section 5.4.1, are used to feed the proposed model and extract the estimated throughput as proposed at Section 5.3.3. The deployed under consideration "Indoor Topology 2", is analytically depicted in Figure 5.1. For all illustrated cases hereunder, we configure the devices to use channel 6 (2437MHz) with 20MHz width acting as the the target operating $\mathcal{F}_c$ for the Wi-Fi $DU_4$ (**S**ystem **U**nder **T**est - SUT). It is worth to be noted that we select the aforementioned channel intentionally, as it can be considered the most vulnerable one, by receiving interference from both two sides of the channel, i.e. channels 2-5 and 7-10.

**Non-Overlapping Interference**

In this case, the interference resulting between two seemingly non-overlapping channels in the 2.4GHz band is analyzed and experimentally evaluated. Initially, we deploy the external interference link (Ext. $AP_3$) to operate in channel 1 and create medium UDP traffic of 25Mbps using MCS15. As the theoretical operating frequencies of channels 1 (2402-2422MHz) and 6 (2427-2447MHz) do not overlap, no interference impact is expected in the under test link. However, Monitor $DU_2$ reports the $\mathcal{DC}_{\mathcal{F}_c}$ to be 14.1% for channel 6, which is considered directly as $\mathcal{I}nt_{(Ext)}$ with no contention opportunities. Based on the proposed model, the $\mathcal{C}_{max}$ is calculated to be 109,2 Mbps for MCS 22 used from Wi-Fi $DU_4$. In fact, the under-test link achieves 107.1Mbps as depicted in Figure 5.8(a), which is actually 15.7% lower than the $\mathcal{A}_{cc}$, as calculated in Section 5.4.1. For this scenario, the existence of interference as well as its impact, even for theoretically non-overlapping channels is highlighted. For this reason, the applicability of the proposed framework can also be considered essential for the 5GHz Wi-Fi band, in which the channels are orthogonal and therefore non-overlapping.

**Saturated External Interference**

In this scenario, we examine how accurate the proposed model can be, under the existence of heavy $\mathcal{I}nt_{(Ext)}$. More specifically, we set Ext. $AP_2$ and Ext. $AP_3$ to operate at channels 8 and 3 accordingly. Furthermore, saturated UDP traffic is generated from Ext. APs to their connected stations. The Monitor $DU_2$ reports the $\mathcal{DC}_{\mathcal{F}_c}$ to be 90.6% and $\mathcal{C}_{max}$ is calculated to be 6,76 Mbps. Veritably, the average throughput achieved at Wi-Fi $DU_4$ link is 6.68 Mbps and the experimental results are analytically shown in Figure 5.8(b). It is obvious that the Ext. APs deplete any transmission opportunities for the Wi-Fi $DU_4$, by generating a high amount of interference at the target $\mathcal{F}_c$. As the proposed framework can distinctly separate $\mathcal{I}nt_{(Ext)}$ from $\mathcal{I}nt_{(Wi-Fi)}$, the actual transmission opportunities at each channel can be retrieved. Thus, based on the same experimental setup, the $\mathcal{C}_{max}$ is calculated to be 51.2 Mbps for channel 8 and 53.8Mbps for channel 3. It is evident that if the proposed framework was utilized for channel selection schemes, it would lead to significantly higher performance for the SUT link.

**Saturated Contention**

For this case, the accuracy of $\mathcal{C}_{max}$ calculation is examined, when high contention exists in the same channel. More specifically, we deploy Ext. $AP_1$ to transmit saturated traffic in channel 6, towards generating channel contention with Wi-Fi $DU_4$. The $\mathcal{C}_{max}$ is calculated to 64.07 Mbps for the Wi-Fi $DU_4$ while in practice the link achieves 63.3Mbps. Figure 5.8(c) illustrates that the two links share equally the medium as expected in the scenario of IEEE 802.11 and CSMA/CA contention. Almost identical performance can be observed, 63.3 Mbps for the Wi-Fi $DU_4$ and 66.5 Mbps for the Ext. $AP_1$, while both links operate using MCS 22.

**Mixed Interference**

Finally, three different scenarios with combined $\mathcal{I}nt_{(Ext)}$ and $\mathcal{I}nt_{(Wi-Fi)}$ are presented, for concluding the model's evaluation. Similarly with the previous, we keep Ext. $AP_1$ operating in channel 6 in order to create $\mathcal{I}nt_{(Wi-Fi)}$ to the SUT. Additionally, the Ext. $AP_2$ operates in channel 8 and the Ext. $AP_3$ in channel 3, thus generating various amounts of $\mathcal{I}nt_{(Ext)}$ to the Wi-Fi $DU_4$. As illustrated in Figures 5.8(d), 5.8(e) and 5.8(f), three scenarios with low, medium and high amount of mixed interference are demonstrated.

Initially, we configure the Ext. $AP_1$ to transmit 10 Mbps of UDP traffic, in order to create $\mathcal{I}nt_{(Wi-Fi)}$ to the SUT's $\mathcal{F}_c$. Moreover, the Ext. $AP_2$ and Ext. $AP_3$ create 10 and 15 Mbps of UDP traffic respectively. In this manner, 53.2% of $\mathcal{DC}_{\mathcal{F}_c}$ is reported by the Monitor $DU_2$ with $\mathcal{C}_{max}$ estimated to be 56.88 Mbps. It is worth to be noted that, even though there is presence of $\mathcal{I}nt_{(Wi-Fi)}$ in this case, Ext. $AP_1$ can not be included in $\mathcal{N}_{ContTerms}$, since its total airtime (13.7%) does not conform with equation (5.6). Therefore, the achieved performance of Ext. $AP_1$ will not be affected from the saturated transmissions of the under-test link, which is indeed depicted in Figure 5.8(d). In practice, the SUT achieved 55.3 Mbps during the experiment.

Following this, we increase the traffic demands for Ext. $AP_1$, Ext. $AP_2$ and Ext. $AP_3$ to 45, 20 and 25Mbps accordingly. In this case, the Monitor $DU_2$ calculates the $\mathcal{DC}_{\mathcal{F}_c}$ to be 78.8% and the increased demands of Ext. $AP_1$ characterize now this terminal as $\mathcal{N}_{ContTerms}$. Thus, the SUT and Ext. $AP_1$ will equally compete for the available transmission opportunities in channel 6, with respect to the interference $\mathcal{I}nt_{(Ext)}$ caused by Ext. $AP_2$ and Ext. $AP_3$. This is also evident in Figure 5.8(e), where the under-test link is shown to achieve achieve 26.4 Mbps, while the Ext. $AP_1$ gets 27.1 Mbps. Based on the proposed model, the $\mathcal{C}_{max}$ for the SUT is calculated to 27.47 Mbps.

Finally, we further increase the demands of Ext. APs to 55, 30 and 35 Mbps. Similarly with the previous case, the under-test link will contend for channel 6, while lower performance is anticipated based on the increased demands. Figure 5.8(f) illustrates that the experiment's results validate the expectations and the under-test link achieves 14.8 Mbps compared with the 15.17 calculated from the proposed model. Additionally, during this case, the competitive Ext. $AP_1$ achieved 19.2 Mbps.

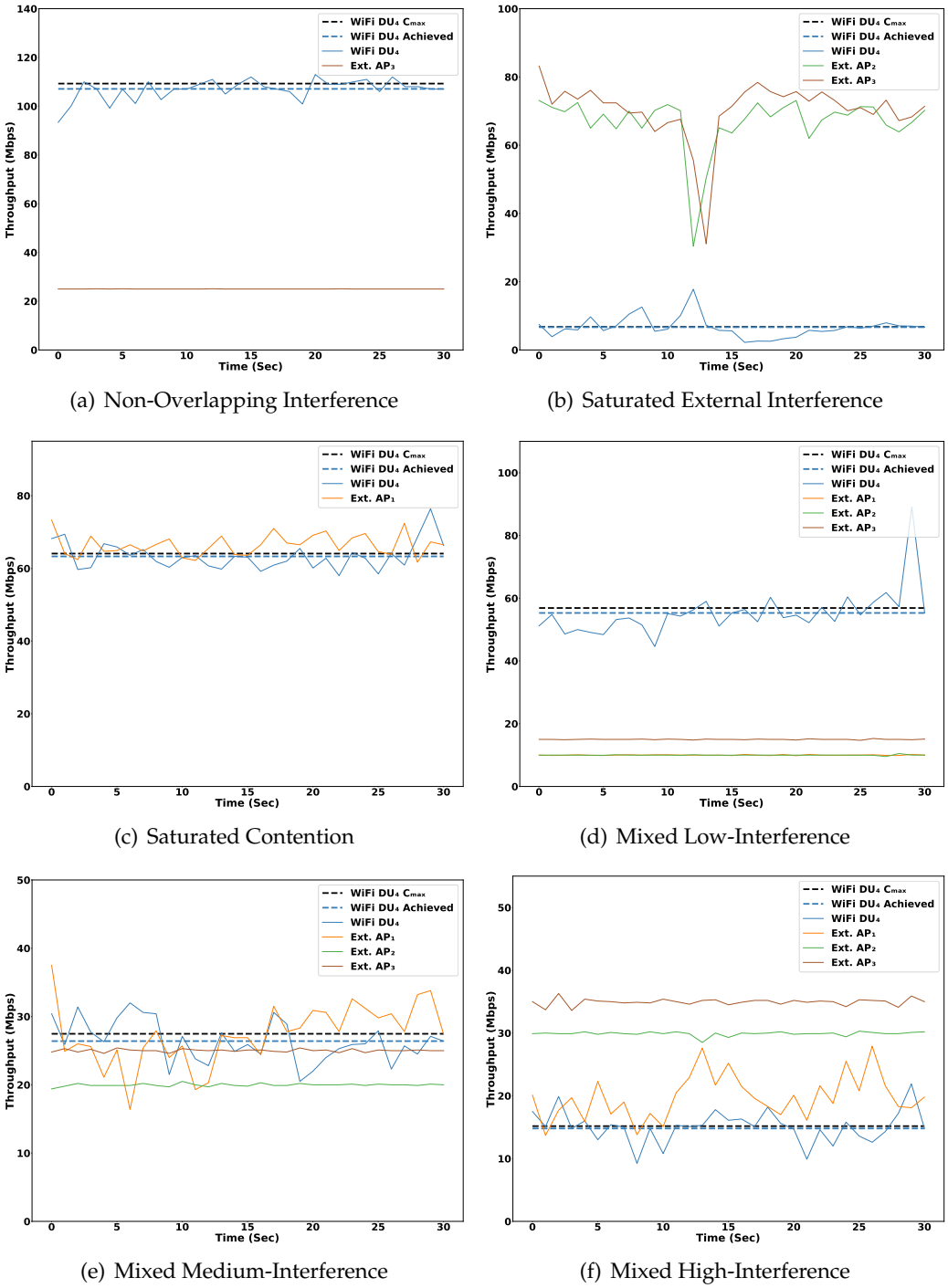


(a) Non-Overlapping Interference

(b) Saturated External Interference

(c) Saturated Contention

(d) Mixed Low-Interference

(e) Mixed Medium-Interference

(f) Mixed High-Interference

FIGURE 5.8: (Indoor Topology 2) - Estimated Throughput Evaluation.

In this subsection, several testbed scenarios were executed, in order to prove the proper functionality of the $\mathcal{C}_{max}$ throughput estimation model, introduced in Section 5.3.3. Specifically, the estimation error varies from 1.19% to 3.9% across the scenarios, with a mean value of 2.24%. Therefore, it is verified that the proposed model is able to make accurate throughput estimations, under several challenging interference scenarios, which include the combination of $\mathcal{I}nt_{(Ext)}$ (from both overlapping and non channels) and $\mathcal{I}nt_{(Wi-Fi)}$.

### 5.4.3 Performance Evaluation Outdoor Topology

The following subsection aims to highlight the proper joint operation, of the performance estimation and prediction models, under entirely uncontrolled spectrum conditions. In this context, we design, develop and evaluate the examined scenario in the NITOS Outdoor Testbed, as shown in ("Outdoor Scenario 1") Figure 5.1. Two stations were employed ($UE_5$ and $UE_6$), which are in close proximity with the Wi-Fi $DU_5$, thus achieving high rate transmissions. Specifically, $UE_5$ achieves MCS23 with the use of 3 antennas, while $UE_6$ MCS14 with 2 antennas. Of course, the number and placement of the depicted Ext. APs / Ext. UEs are completely unknown for the specific scenario and it is provided for the completeness of representation. Furthermore, the depicted Monitor $DU_3$ refers to the hardware which generates the spectral datasets, as described at the previous Sections.

#### General Observations

Initially, it is worth to state some observations, in order to fully comprehend the challenging spectral conditions given in the examined area. During the collection of the spectral measurements ($\mathcal{DC}$ + wireless analytics) at each execution, the Monitor $DU_3$ senses on average 114 present uncoordinated APs. 49 of these APs are categorized as potentially harmful, since they exceed the CCA threshold. Furthermore, on average 27 STAs are associated in the vicinity, 12 of which may potentially be active interferers. The above statistics describe the entire number of Wi-Fi terminals given at all available channels (1-11) of the 2.4GHz ISM band. It is also observed that 72% and 57% of the sensed APs and STAs, are operating in channels 1, 6 and 11. In such way, it is showcased that these three commonly used channels, can be largely affected from external interference. The Monitor $DU_3$ is deployed in the 3rd floor of a building, in which the wider area is mainly composed of stores, offices and coffee shops. Thus, similar differences on the spectrum utilization were observed between weekdays and weekends, as well as between working and non hours. Finally, significant reduction at the $\mathcal{DC}$ utilization appeared at all channels, during the lockdown periods of the COVID-19 pandemic.

#### Long-Term $\mathcal{DC}$ Predictions Evaluation

The following experiments aim to showcase that the mechanism proposed in Section 5.3.2 is suitable for making accurate long-term utilization predictions, when severe short-term outliers are not present. More specifically, as long as the long-term predictions match the ongoing $\mathcal{DC}$ values, there is no need for activating the "Real-time Outlier Detection". Through the use of the RSSI value for each Wi-Fi DU / UE, which is available and updated every minute in the wireless analytics central database, we are able to calculate the $\mathcal{C}_{min}$ based on the long-term predicted $\mathcal{DC}$ values. In this case, the equation 5.2 is used, by replacing the $\mathcal{T}_{\mathcal{MCS}}$ with $\mathcal{A}_{thr}$, as described in Section 5.4.1.

Initially, we consider the link Wi-Fi $DU_5$ - $UE_5$ and the time period between 00:00 - 01:59am for November 6th 2020. In order to get the reported values, saturated TCP traffic was generated during this experiment. The link was able to constantly achieve MCS23 and all the predicted $\mathcal{DC}$ values ranged between 2-9% for class 0-10.

As described in Section 5.3.2, we keep the mean $\mathcal{DC}$ value of the target predicted class, which in this case is equal to 5 for the entire duration of the experiment. Additionally, the use of the mean value can add an error at the $\mathcal{C}_{min}$ prediction, which corresponds up to ±5%. In Figure 5.9, it can be observed that the predicted values of the $\mathcal{C}_{min}$ fully match with the actually achieved throughput during the 2-hour execution of the experiment. Based on the mean predicted $\mathcal{DC}$ value, the $\mathcal{C}_{min}$ is calculated to be 128.15 Mbps. In practice, the link achieved in average 124.8 Mbps, with all values ranging within the admissible limits of $\mathcal{C}_{min}$ ±5% (± 6.40 Mbps).

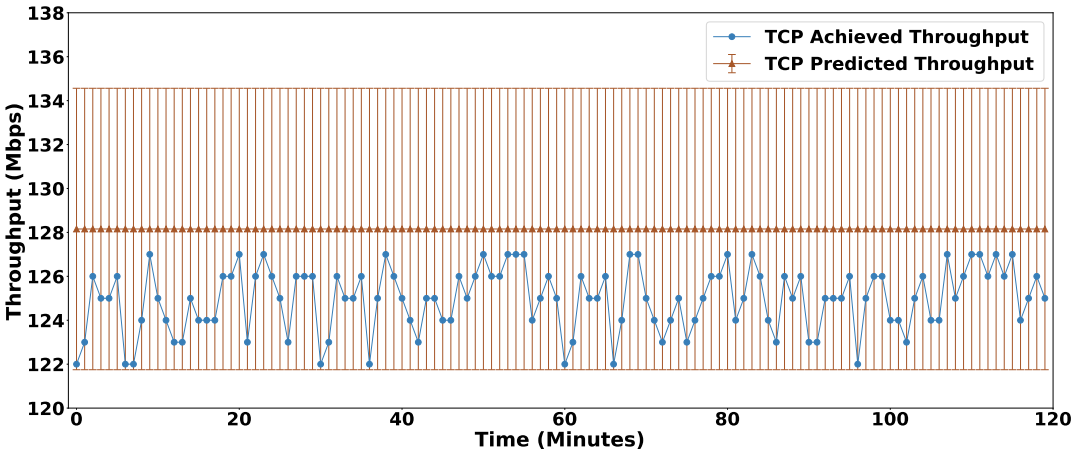


FIGURE 5.9: Long-Term Predictions - 06-Nov. 00:00 - 01:59 am

Thereafter, we also examine the Wi-Fi $DU_5$ - $UE_6$ link under saturated TCP traffic (MCS14) and between 13:00 - 14:59 pm of November 6th 2020. In this case, the deviation of the predicted $\mathcal{DC}$ values was between 3-16%, resulting in two different predicted classes (0-10) and (10-20). More specifically, from 0 - 45 minutes, the model predicts a mean $\mathcal{DC}$ value 15 ($\mathcal{C}_{min}$ = 75.47 Mbps) and then reduces this utilization prediction to 5 ($\mathcal{C}_{min}$ = 84.36 Mbps). In Figure 5.10, it is shown that during the two hour experiment only one missed detection from the proposed framework was identified. However, the deviation was not greater than "10%", which has been defined as the threshold for activating the "Real-time Outlier Detector", as discussed in Section 5.3.4.

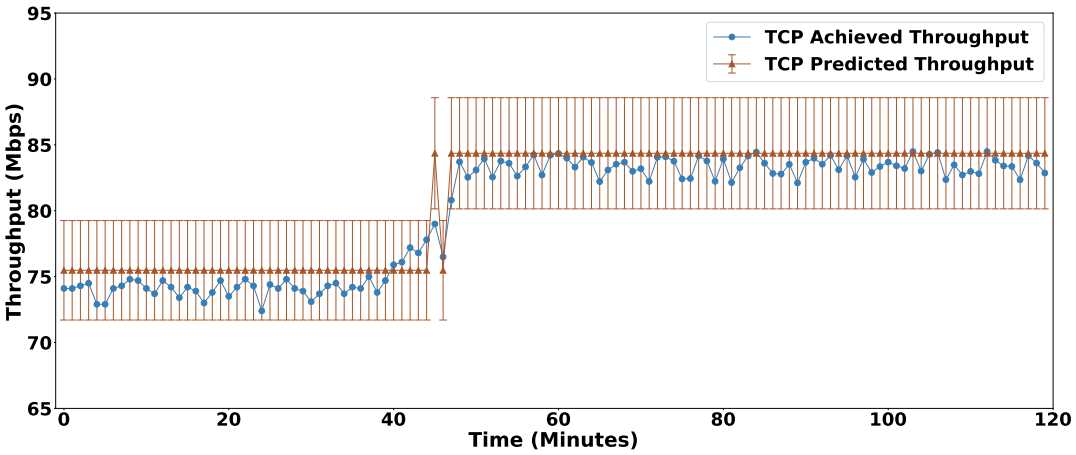


FIGURE 5.10: Long-Term Predictions - 06-Nov. 13:00 - 14:59 pm

**Outlier Detector Evaluation**

Finally, the experimental results below showcase the proposed framework's operation under the presence of several short-term outliers. More specifically, the link Wi-Fi $DU_5$ - $UE_6$ is considered between 10:00 - 11:59 am, on December 23th 2020. The predicted values from the long-term ML model ranged between 23-29%, resulting in one predicted class (20-30). Thus the mean value of 25, was set for the entire experiment's duration. In order to evaluate the target link, saturated UDP traffic under the achieved MCS 14 was generated. Therefore, the predicted $\mathcal{C}_{min}$ is calculated to 73.65 Mbps with $\pm$ 3.68Mbps error margin. The analytical results of the 2-hour experiment are summarized in Figure 5.11. As it can be observed, 4 severe interferers of varied intensity and duration appeared during the experiment. For these cases, the proposed short-term mechanism was activated immediately and the $\hat{\mathcal{C}}_{max}$ values were extracted accurately. More specifically, the $\hat{\mathcal{C}}_{max}$ calculation mean error compared with the actual throughput achieved is 4.81%. As described in Section 5.3.4, the current $\overline{\mathcal{DC}}_{\mathcal{F}_c}(t_0)$ is calculated through the $\mathcal{W}_n$ weight vector. An exponential weight vector could be applicable as well, by giving even greater emphasis on the most recent values. Hence, reduction of the $\hat{\mathcal{C}}_{max}$ mean error could be achieved. However, this could also result to short-term mechanism misuse when sharp peaks of $\mathcal{DC}$ appear. We consider the confrontation of this trade-off as future work.

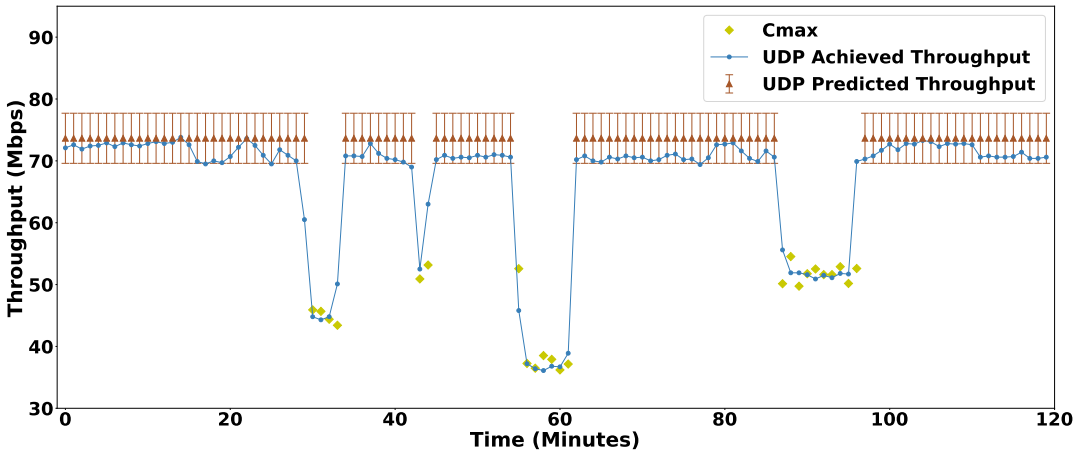


FIGURE 5.11: (Outdoor Topology 1) - Short-term Outlier Detection

## 5.5 Considerations

In this chapter, all the provided results under the examined experimental scenarios, represent the spectrum conditions from each Monitor DU's perspective. Concluding on the results, the proposed framework is able to export all the performance estimations and predictions. As the whole framework is based on Energy Detection methods, differences might occur between Monitor DUs and each Wi-Fi DU spectrum conditions. Of course, this is directly associated with the distance between the deployed Monitor DU and each Wi-Fi DU. In the examined scenarios, all the WiFi-DUs were in close proximity (1-7m) with the Monitor DUs, thus eliminating the above phenomenon. However, the low cost and the plug & play installation can assist in the wide application of the proposed framework. More specifically, every

Wi-Fi DU can be easily converted to Monitor DU by deploying an additional wireless adapter. The cost for the involved Atheros chipsets starts at ∼15$ and can be installed at any conventional host machine through PCI or USB ports. In terms of software, the framework utilizes exclusively open source wireless drivers [48, 50] and open source software such as airodump, tcpdump and tshark. Therefore, the proposed framework can directly plug in any existing deployment. For denser and larger deployments, the proposed Monitor DU framework can be extended with more entities, each supervising a smaller region and providing accurate predictions in a common database environment. Such data can be used for forming radio interference maps, including predicted long-term values, allowing the configuration of each device in the most efficient manner. As the execution and the decisions made from the proposed mechanism are running on the operator side of the network, they do not require any software or hardware specific requirements on the STA side. Some interesting aspects which emerge in such architectures may contain the proper placement and channel selection for Wi-Fi / Monitor DUs, UE cell steering, as well as load balancing and social welfare maximization for devices operating in the unlicensed ISM bands. Recent research approaches can be found in literature, regarding channel selection and interference mitigation schemes [92, 93, 108, 124], which can be compared with the proposed framework. Finally, greater emphasis at spectrum anomalies like capture effect and hidden terminals, can be given. There are already compatible mechanisms with our approach, such as the work in[125], which aims in detecting such anomalies through the use of ML.

## 5.6 Conclusions

In this chapter, a novel framework for estimating and predicting future interference levels at IEEE 802.11, was presented and experimentally evaluated. Analytical formulas for accurately calculating the available channel capacity $\mathcal{C}_{min}$ and $\mathcal{C}_{max}$ were developed and presented. By taking advantage of a ML approach, long-term $\mathcal{C}_{min}$ predictions can be extracted for the next 2-hours and with one minute accuracy. Additionally, a history-based short-term mechanism was developed, in order to shield our mechanism and when the ongoing spectrum conditions largely differ from the long-term predicted. These results are driven through the close monitoring of several wireless metrics, which are actively gathered from Monitor devices in our architecture and stored in central databases. Finally, extensive experiments at both Indoor and Outdoor network setups, showcased the accurate prediction and calculation for both $\mathcal{C}_{min}$ and $\mathcal{C}_{max}$, as well as the gains which can be obtained from the proposed framework. In the future, we foresee to extend this framework towards increasing the accuracy of the ML predictions for shorter-term periods, by considering changes in the ML model and predicting further metrics, stemming from the wireless analytics that we employ for channel capacity estimation.

# Chapter 6

# Dynamic Resource Pricing and Leasing for 5G Networks

**Contents**



In this chapter, a novel framework for enabling dynamic Policy and Charging Rules in modern 5G multi-tenancy environments is designed and presented. More specifically, adaptive pricing schemes are utilized by MNOs for instantiating tailored slices, when the resources of a Mobile Network Operator (MNO) are insufficient to serve the connected users. A scheme where an MNO seeks and leases additional resources from an Infrastructure Provider (InP) is examined in this chapter. Their negotiation is modeled as a Service Level Agreement (SLA) and the dynamic charging rules are implemented as an extension of the 5G Policy Charging Function (PCF). The analytical structure of the proposed architecture as well as all the methods and signals developed for MNO and InP collaboration, are described in the context of this chapter. Finally, extensive testbed experimentation proves proper functioning of the proposed framework, under both UDP and TCP additional traffic demands.

## 6.1 Introduction

Over the last years, we are witnessing an indisputable rise on the users' demand for consuming multimedia data traffic. This situation exerts pressure on network operators for fulfilling the end users requirements. Currently, the infrastructure-centric approach of the past network architectures is proved inadequate to handle the increasing traffic volume and impacts negatively the operational expenditures of the operators. As a result, telecommunications service providers and mobile network operators have been seeking for alternative non-costly and performance-efficient solutions that would be able to accommodate the ever-increasing users' demand.

Unavoidably, the transition from large scale base stations to small remote radio heads supporting disagreggation of the protocol stack to enable agile deployments, is essential to reconsider the cellular network architecture. Agile network deployments supporting low latency and higher throughput communications with lower

maintenance and operational costs are currently required for enabling ultra reliable and ubiquitous communication services. Towards this pace, 5G is anticipated to change drastically the way that the information is being used, processed and handled, supporting smarter and higher performing flexible networks.

Recent technological advances like Network Functions Virtualization (NFV) [17, 126, 127] and Software Defined Networks (SDN) [128, 129, 130] as well as ongoing standardization efforts [131, 132] render the new 5G architecture highly attractive by encompassing NFV, SDN and cloud technologies, which offer diversified capabilities regarding the programmability of the network functionalities. Those technologies have introduced the following principles on the network architecture design. Namely,:

- *Disaggregation:* It is the procedure of the vertical and distinct separation of integrated systems into independent components being equipped with open interfaces. The adoption of network function disaggregation principles, enables network operators to select the best combination among several individual hardware and software components while eliminating integrated systems and protocols lock. All the networking software needed to enable networking functionality is broken down and thus can be operated more efficiently, which leads to improved physical resources utilization.
- *Virtualization:* It provides the ability to instantiate, run and operate multiple independent copies/replicas of the network functionalities on a common hardware platform. From a network perspective, the concept of slicing [17] has been recently introduced in 5G architecture to enable the partitioning of the underlying network infrastructure in independent logical networks and guarantee the isolation among network tenants.
- *Commodification:* of information data and data transactions combined with the provision of inexpensive and high performance infrastructure (both virtual and physical) and spectrum availability. It is the ability of elastic scaling on the virtual network components across commodity hardware bricks as workload and networking requirements dictate.

To this end, the rise of 5G technology is expected to create new collaboration opportunities among operators and enable new Business to Business (B2B) models [14, 15, 16]. Existing stakeholders that used to consume data and infrastructure services will update their role and will share their resources acting as potential infrastructure providers (InPs) in the upcoming 5G network models and under the introduction of network slicing. Thus, there is an immediate need for deploying proper resource brokering mechanisms to the slice providers, as significant economic benefits can occur. Additionally, several challenges on how the slice providers will economically interact with verticals and resource providers are being emerged in 5G networks.

## 6.2 Contributions

In this chapter, we design a novel framework for virtual MNOs[1] which enables dynamic allocation of resources to expand their network's capacity through resource

[1]With the term MNO, we refer also to mobile network operators that offer their services virtually.

leasing and by negotiating an SLA agreement with the InP. Thus, MNOs in need of additional resources, due to a possible temporal or constant capacity crunch can request on demand from other MNOs or InPs resources to fulfill their needs and provide sufficient services to users guaranteeing performance. We conduct extensive testbed experimentation to thoroughly assess our design. Relying on our recent theoretical work [27] that models the interactions among users, MNOs and infrastructure providers in a 5G network context, and utilizing the designated optimal policies for pricing and leasing of resources, we design the blueprints for a Policy and Charging Control (PCC) core network entity that it can dynamically coordinate pricing and leasing decisions. The key contributions of this chapter can be summarized as follows:

- ***Dynamic PCC Rules:*** We design a novel framework that allows dynamic leasing and pricing of networking resources. Our solution monitors the users demands and assist operators to apply optimal pricing strategies. Besides, in the case of network capacity depletion, virtual MNOs are assisted by our solution to acquire the appropriate amount of additional resources through leasing from the InP in order to accommodate the extra demand.
- ***Extensive evaluation:*** We assess the proposed solution using real testbed experimentation utilizing OpenAirInterface [133] and FlexRAN [134] software. Leveraging our theoretical pricing and leasing framework[27], we demonstrate the applicability of our framework in real 5G systems. Extensive performance testing has been conducted in order to validate and assess the proposed framework's proper functionality.

The rest of this chapter is organized as follows: In Section 6.3 the related work is presented. Furthermore, in Section 6.4 the architecture of the proposed framework is described analytically. Section 6.5 presents the evaluation scenarios as well as the collected experimental results. Finally, Section 6.6 concludes the chapter and presents possible extensions.

## 6.3 Related

**Standardization Efforts:** Three different Specification Groups (SG) were formed by 3GPP, the Radio Access Network (TSG-RAN), the Services & System Aspects (TSG-SA) and the Core Network & Terminals (TSG-CT). These groups are responsible for creating holistic architectural designs for the upcoming network generations. Huge emphasis is being lately given to the softwarization and virtualization according to which, all the software needed for the base stations is ported on the cloud. The new network architecture leverages Virtual Network Functions (VNFs) to compose the core network entities, as a way of implementing modern architectures under a more accessible, distributed and flexible way. Consequently, the symmetrical use of common physical infrastructures for more than one competitive MNOs/InPs and under the use of Service Based Architectures (SBAs), are now in the spotlight of the research approaches. However, the simultaneous use of common physical resources raises several challenges as well. Distinct separation as well as proper orchestration and resource management, are now essential for achieving smooth operation at 5G networks. Network slicing offers huge opportunities for efficient utilization of the

limited network resources. The 3GPP (TSG-SA) working group is responsible to capture in detail, how network slices will be integrated at 5G core architectures. More specifically, the Technical Specifications (TS) 23.501[131], 23.502[132] and 23.503[135] contain all the information regarding System Architecture, 5G System and PCF aspects accordingly.

**Research Efforts:** With emphasis at some of the most vital details for networks slices, a high-level view can be defined as follows. Network slice is an independent end-to-end logical network which runs on a shared physical infrastructure and is capable of providing an agreed quality of service. This type of agreement is established between two entities (e.g. InP and MNO) and it is referred as an SLA. As the core network will be implemented in a cloud and generally all architectures are now software oriented, multiple approaches for network slicing are given in the literature so far [17]. Moreover, Oladejo et al. in [136] describe practical considerations for how multi-tenancy network slicing, can affect the overall network capacity. Specifically, they examine how the number of users in a slice, the total number of slices and the transmit power affect the capacity of an V-MNO. In addition to the tailored performance, each slice will have the flexibility to operate either under unified or separate set of NFs, as shown in Fig.6.1. In such way, the ability for discriminated pricing at each slice, will be enabled at 5G networks. Appropriate techniques for dynamic pricing of the leased resources are being investigated and tested in the context of 5G networks [137, 138].

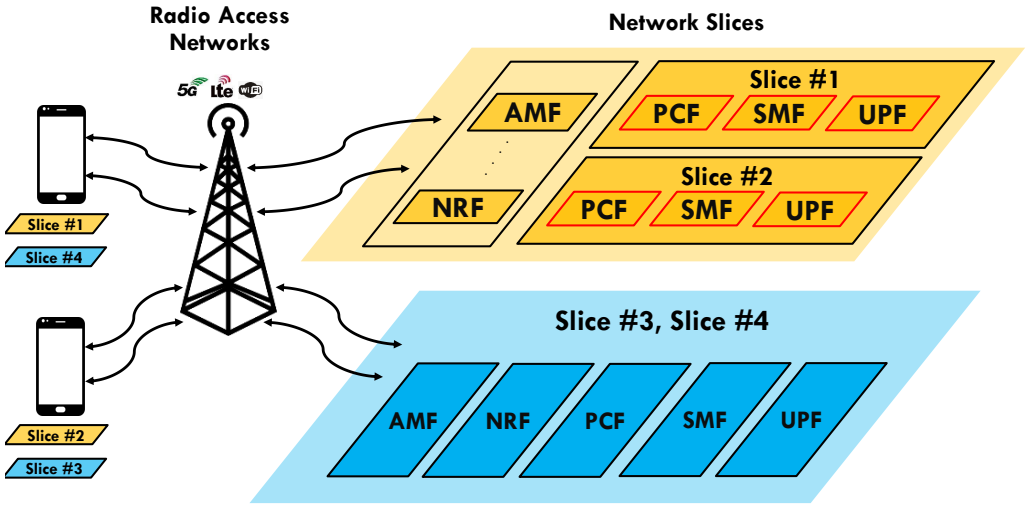


FIGURE 6.1: Unified / Separate Network Function Slices.

Extensive functionality for policy based control of traffic and user services, is now essential for the upcoming network architectures. By replacing the former 4G Policy Control and Charging Rules function (PCRF), the PCF will undertake this critical role. Therefore, transparent control for monitoring the consumption of network resources (slices) will be provided through PCF. Both online (OCS) and offline (OFCS) charging are now implemented as an entity called Convergent Charging System (CCS) and enclosed in 5G Charging Function (CHF). Based on the 3GPP PCF [135], the Policy and Charging control (PCC) rules incorporate all the information for enabling the user plane detection of the policy control and proper charging for a service

data flow. Additionally, the tight coordination of PCF with different fundamental 5G Network Functions (NFs) like UDR, AMF, SMF and CHF, enables additional policy control functionalities besides charging. Indicatively, rules for how the users and data sessions are controlled in terms of Quality of Service (QoS), Geographical Restrictions and available RAN selection are some of the extended PCF responsibilities.

## 6.4 Framework

In this chapter, we design and present a framework which extends the standard operation of the PCF function. During real-time service delivery, PCF is in charge to coordinate and enforce control and user plane rules. The intellectual merit of this framework develops a charging and pricing solution that helps MNOs that face capacity shortcomings and their service capability does not suffice due to the increased users' demand. The proposed design is used to monitor the control and data plane traffic and apply specific rules that assist MNOs to acquire additional resources through leasing from the InP or from nearby MNOs when the MNO faces service insufficiency as well as to apply optimal pricing to its users. Therefore, the MNO in need and the InP interact with each other and transact for leasing resources. The requested resources after being purchased by the MNO, are attached to its network slice, thus extending its service capability with extra capacity to serve its users. The analytical call flow for the proposed architecture as well as the interactions between the MNO and the InP are illustrated in Fig. 6.2.

### 6.4.1 Overview of the Leasing Interaction

In the context of this chapter, we leverage on our theoretical framework [27], which considers the problem for MNOs of leasing resources, servicing and pricing mobile users. Through a three-stage Stackelberg game solved by backward induction, the optimal pricing decisions when MNO's supplying capacity suffices users' demand, as well as when supplying capacity is deficient are calculated. In the latter case, when MNOs supplying capacity doesn't suffice, the MNO requests through leasing the proper amount of additional resources from the InP that not only resolves its deficiency but also incurs the maximum benefit given the leasing cost by the InP. The interactions among the UEs, the MNO and the InP can be summarized as follows: The operation of the proposed solution is performed in real-time.

The MNO, firstly assesses the total demand that is requested by the associated users and depending on that, MNO checks his capacity availability and determines the amount of resources that needs (or not) to purchase from the infrastructure provider in order to satisfy this demand. In sequence, the MNO determines the optimal pricing that increases its profits. Thus, the MNO announces that price to the users and then, the users by taking into consideration the price that the MNO had already announced, demand on their side the corresponding rate that maximizes their own benefit, as this is expressed by their *payoff* function. For more details, on the modeling of the game among the users, the MNO and the InP, the interested reader is refered to [27].

### 6.4.2 Call Flow

Fig. 6.2 shows an illustration of the call flow that is initiated when the MNOs network controller detects service performance insufficiency and specifies the need for the MNO to acquire additional resources. All the modules and signaling that is being communicated in the proposed framework are described below. The implementation of the proposed framework was developed by using Python programming language. Furthermore, the communication among the network entities (e.g. UEs, MNO and InP) is performed through socket messaging and by utilizing the corresponding Python library.

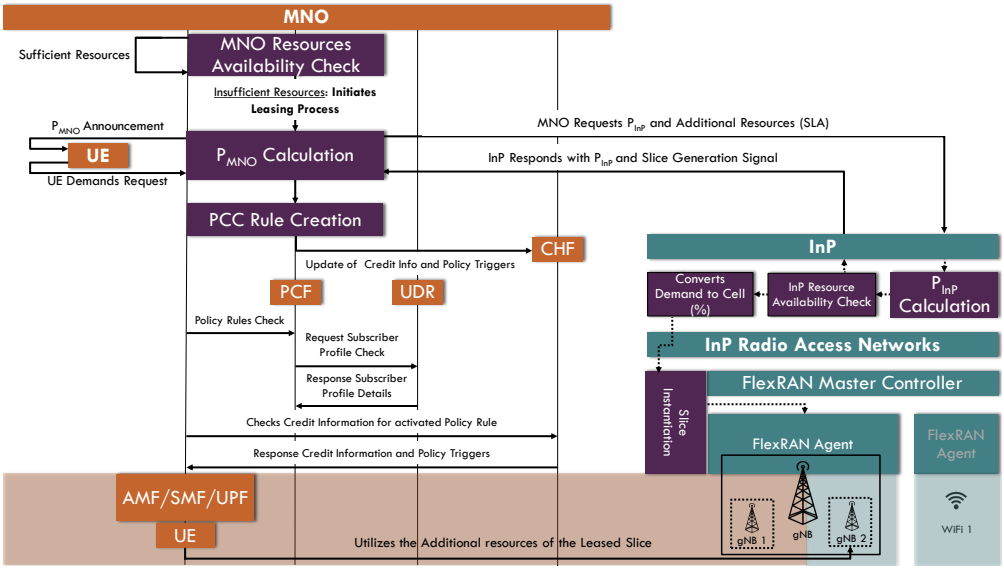


FIGURE 6.2: Pricing and Leasing of Network Resources - Proposed Framework Call Flow.

- ***MNO Resource Availability Check:*** This module is used by the MNO to assess the capacity of its network resources (*"gNB1"*) whether they are capable for providing sufficient services to its connected UEs. If the resources of MNO do not suffice, a signal is used for requesting additional capacity given the leasing cost price $P_{\mathsf{InP}}$ that the InP imposes to the MNO.

- $P_{\mathsf{MNO}}$ ***Calculation:*** This module receives all the necessary inputs for determining the optimal price $P_{\mathsf{MNO}}$, that the MNO announces to its users.

- $P_{\mathsf{MNO}}$ ***Announcement:*** This signal is sent between the MNO and UEs and it refers to the announcement to the UEs for the price $P_{\mathsf{MNO}}$.

- ***UE Demands Request:*** In response to the pricing $P_{\mathsf{MNO}}$ Announcement signal, this signal is used to communicate to the MNO the respective UE demand.

- ***Request for Additional Resources-Capacity given the leasing cost*** $P_{\mathsf{InP}}$***:*** This signal is used by the MNO to get notified for the leasing cost $P_{\mathsf{InP}}$ set by the InP and to request the amount of capacity that wishes to lease from the InP given the cost $P_{\mathsf{InP}}$.

- $P_{\mathsf{InP}}$ ***Calculation:*** This module is used by the InP to determine the leasing cost $P_{\mathsf{InP}}$ to be announced to the MNO.

- ***InP Resource Availability Check:*** Similarly with MNO, the InP should assess its resource availability. The provisioned resources could be either cellular (e.g. from the slice that corresponds to the "$gNB_2$" cell) or Wi-Fi network resources. Part of those resources can be attached to the MNO's slice (e.g "$gNB_1$") upon request to serve the increased users' demand.

- ***Normalization of the demand volume to a percentage of utilized resources:*** In this module and after successfully accepting the capacity request from the MNO, the InP instantiates the procedure to provide the MNO with the requested amount of capacity that corresponds to the virtual resources to be attached to the MNO's slice. It should be noted that the slice reconfiguration with the additional amount of resources is achieved through FlexRAN [134], a programmable platform for managing real-time and dynamically the physical resources of a 5G network. More specifically, leveraging OpenAirInterface [133] Core Network and Radio Access Network (OAI-CN/OAI-RAN), FlexRAN can provide flexible re-configuration and scalability of network slices in radio access networks (RANs). Furthermore, the description and the transmission of the requests/responses between the Master Controller and the RAN Agents is performed through the FlexRAN API that utilizes *curl* command and *json* files. However in the slice creation, FlexRAN takes as an input the percentage that the new slice will occupy in the overall's cell capacity. Based on that, we convert the requested demand from the MNO (Mbps) to cell percentage. An analytical description for the cell percentage calculation, is given in Section 6.5.

- ***Slice Instantiation/Re-configuration:*** Finally, after retrieving the downlink/uplink percentages from the Demand Conversion function, we communicate through the appropriate *json* descriptions to the target gNB's FlexRAN Agent[2] in order to instantiate or re-configure the new slice.

- ***Response with $P_{\mathsf{InP}}$ and Slice Status:*** This signal is responsible either to inform the MNO for the $P_{\mathsf{InP}}$ or to report the status for a requested slice.

- ***PCC Rule Creation:*** In this module and after being informed for the cost $P_{\mathsf{InP}}$, the MNO undertakes to create a custom PCC rule for the UE which requested additional resources (leased slice).

  As mentioned in a prior section, a PCC rule [135] is a set of information which enables the detection of a service data flow and provides parameters for proper policy and/or charging controls. Each PCC rule functions under a set of operations in the 5G networks. Indicatively, the PCF function can activate, modify and deactivate a PCC rule at any time. The PCC rules are divided into two types, the predefined and the dynamic. The former are predefined rules which are configured into SMF and only referenced by the PCF, while the latter can be dynamically provisioned by the PCF to the SMF. It is worth to be noted that modifications are applicable only to dynamic PCC rules. Additionally, the session management related policy control functionality of the PCF in combination with the PCC rules, enable the functions for dynamic policy and charging control as well as event reporting for service data flows in 5G systems. In the context of this chapter and through the use of dynamic PCC rules, the credit info updated dynamically for each UE in a per slice basis and based on the

[2]The FlexRAN version that we used in our framework, supported fully the LTE 4G cellular technology while the 5G is under development process.

announced price cost $P_{\text{InP}}$. More specifically, proper PCF decisions are taken and provided to the SMF for each leased slice. These decisions consist of both PCC rules as well as with the appropriate customized PDU session related attributes.

## 6.5 Evaluation

In this Section, we evaluate the performance of the proposed framework and we analyze the collected results. We conducted extensive experimentation using real hardware equipment in the NITOS Testbed (University of Thessaly, Greece.) [52]. There, a wide variety of software and hardware supporting heterogeneous communication technologies are available to the experimenter 24/7.

### 6.5.1 Topology and Configurations

For the experimentation scenarios under consideration, we used 6 testbed nodes in the network topology shown in Fig. 6.3.

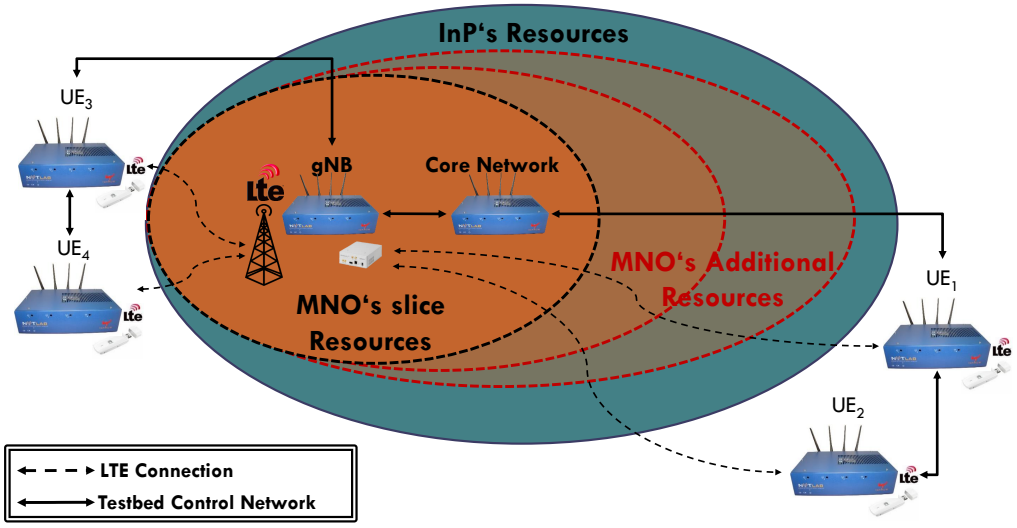


FIGURE 6.3: Testbed Experimentation Network Topology.

Specifically, 4 of the nodes equipped with Huawei's E-392 [139] LTE usb sticks were instantiated as user equipments (UEs). Moreover, we used one node to act as host for the core network for which we utilised the OpenAirInterface framework [133] (OAI-CN) to instantiate it. For the radio access network we used the OAI-RAN and the USRP B210 [53] Software Defined Radio equipment. The gNB is configured with a 20 MHz channel bandwidth, 64 QAM modulation, single input - single output (SISO) antenna and employs a Frequency Division Duplexing (FDD) channel access scheme. To properly configure the capacity of the MNO's RAN slice we used the FlexRAN framework which takes as an input configuration parameter the percentage of the network capacity that will be allocated to the slice. Relying on

a pre-assessment of the total provisioned capacity of the radio infrastructure, we measured the maximum capacity (throughput rate in bps) to be 72.2 Mbps for UDP traffic and 47.5 Mbps for TCP respectively, while the theoretical maximum rate is 75 Mbps (according to the base station RF configuration).

### 6.5.2 Experimental Scenarios

#### UDP Traffic Evaluation

The aim of this scenario is to showcase the adaptability of the proposed framework to the network changes. The MNO has been allocated a slice of resources (part of the gNB's capacity) that are initially owned by the InP. The slice settings can be re-configured on-the-fly and on demand according to the MNO's needs to service its users by using the FlexRAN API. Initially, the MNO's slice is configured with a pre-defined bandwidth budget that corresponds to the 16 % of the gNB's 72.25 Mbps maximum capacity. (Therefore the MNO's initial capacity is approximately 12 Mbps). We used 4 testbed nodes to act as UEs and we initiated multiple UDP traffic flows (5 per UE) requesting download services using the *iperf* command. Figure 6.4 shows the respective collected measurements. In the first 30 seconds of the experiment, the MNO's supplying capacity (12 Mbps) is less than the users' demand $r = 13$ Mbps and users receive a total service of around 12 Mbps. Therefore, there is an insufficiency gap for servicing the full rate of users demand. Afterwards, between $31 - 60$ secs, the MNO announces the pricing to its users $p = 0.47\$$ and respectively the users respond by requesting an extra demand based on that price[3]. As a result the total user demand increases and exceeds the initial MNO's servicing capability. Immediately, to mitigate this incident, the MNO determines its deficit and seeks to acquire additional resources from the InP. The InP leases the additional resources and the MNO purchases them at a cost $P_{\mathsf{InP}} = 0.4\$$. In this period the MNO's slice is reconfigured accordingly using FlexRAN to support this demand. Next, between $61 - 90$ secs, arrivals of new users occur and the total demand increases. The proposed framework monitors the increase in this demand and the MNO's slice is reconfigured accordingly.

[3]The interested user should refer to [27] for an analytical presentation of the theoretical game.

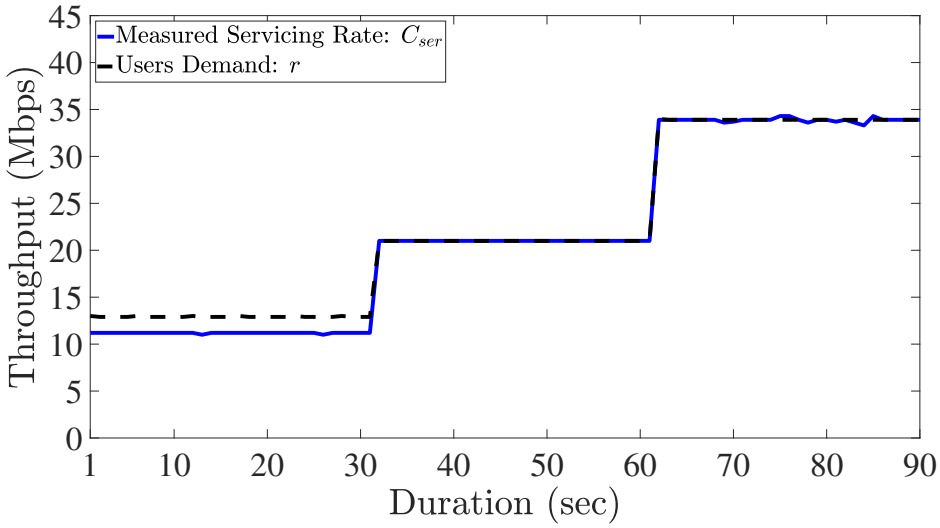


FIGURE 6.4: Scenario: UDP Traffic.

**MPEG-DASH Video Streaming**

In this scenario, we assess the performance of the proposed framework under Dynamic Adaptive Streaming over HTTP (MPEG-DASH) [140]. An APACHE HTTP web server [141] was placed in the host node of the core network to serve the requested video streams from the UEs. Each DASH formatted video stream, consists of chunked videos with multiple available stream-qualities per chunk. These video parts are also called segments, which in the examined case have a time duration of 1 *sec*. Before servicing a video segment to the client, the MPEG-DASH algorithm selects the appropriate video quality that can be supported based on some specific metrics. The key metric that we utilized in our setup refers to the experienced rate. Therefore, the MPEG-DASH selects the maximum quality that can be achieved for each segment given the link's capacity. The minimum segment quality of the tested video corresponds to an achieved rate of 0.13 Mbps while the maximum is 4.72 Mbps. Additionally, between the minimum and the maximum rates, 18 segment rates are available for usage offering quality differentiation, thus ensuring the best fit at each segment served. In the UE's side, we use VLC 3.0.3 Vetinari [142] for retrieving the DASH video streams. Similarly with the UDP scenario presented, the experiment's duration is 90s. At $t_0 = 0$ we simultaneously initiate 7 VLC DASH streams from the UE4, which is connected to the gNB. We trigger the proposed framework every 30s and follow the exact same supplying capacity configurations as the UDP scenario. Finally, we alternate the adaptive buffer size in the DASH protocol and run the experimental scenario for two different values. The former adaptive buffer size is configured to 0s, which practically means that there will be no future segment buffering, while the latter configuration is set to 5s.

The collected results for each adaptive buffer configuration are depicted in Fig. 6.5. There, we observe that the 7 VLC DASH streams initiated from the UEs, utilize almost all the capacity leased from the InP. Furthermore, we see that 3-5s are needed after the cell re-configurations for the MPEG-DASH to calibrate the best fitting rate.

It is worth to be noted that, we don't observe full cell's utilization between 60-90s because even if all the 7 streams are served at the highest available rate of 4.72 Mbps, 33,08 Mbps are needed in total. Finally, it can be observed from Fig. 6.5 that the streams of 5s buffer size are served in a slightly lower quality. This is absolutely rational, as in the same experiment's duration, 90 video segments are retrieved when we have 0s buffer size compared to 105 for 5s.

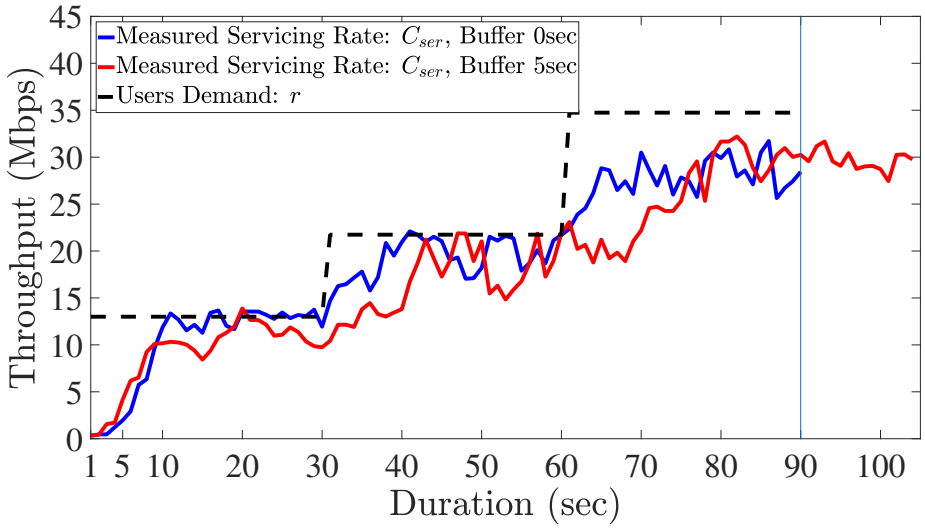


FIGURE 6.5: Scenario: MPEG-DASH.

## 6.6 Conclusions

In this chapter, a novel framework for supporting dynamic charging rules was developed and presented. The proposed scheme extends the conventional PCF functioning and provides dynamic pricing when additional resources (slices) in case of capacity depletion should be leased by an InP. Through extensive experimentation, we assessed the performance of the proposed framework for both UDP and TCP additional traffic demands. We relied on the stable release of the FlexRAN implementation that currently supports the LTE-A 4G protocol stack to implement our framework. Though it is being evolved to the next 5G protocol stack, the new releases are still under development. However, due to FlexRAN's elasticity, the agents/master controller can be extended in order to support additional protocols. As a future extension, we examine the integration of Wi-Fi, since the widely deployed IEEE 802.11 networks are anticipated to play an important role in the 5G network architectures.

# Chapter 7

# Conclusions and Future Work

In this dissertation, several models / mechanisms for utilizing the limited available spectrum resources efficiently, are developed, presented and thoroughly evaluated. Under the exclusive use of open-source software and commercial hardware, all the proposed schemes are implemented at NITOS indoor and outdoor testbed infrastructures. Through extensive experimentation, significant performance gains are noted at end users, when applying the proposed solutions.

Motivated by the dubious and fluid spectrum conditions given at the ISM bands, this thesis initially focuses on the widely deployed IEEE 802.11 standard. As the integration of Wi-Fi is strongly appeared in 5G architectures, proactive mechanisms which guard and boost the end users performance are now investigated.

Therefore, a novel spectral analysis mechanism, which is based exclusively on commercial IEEE 802.11 chipsets is proposed in Chapter 2. Through the extraction of Duty Cycle metric, the developed mechanism is able to perceive and quantify the interference levels for the Wi-Fi bands in real time. Several experimental scenarios, prove that accurate detection of both Wi-Fi and non interference, as well as the disclosure of spectrum anomalies like hidden terminals, are achieved with the proposed framework. By additionally taking into consideration, its seamless applicability and the minimal overhead added, we hold the aforementioned mechanism as the basis for Chapters 3, 4 and 5.

Subsequently and in the context of 5G networks, a UE-driven scheme for optimal non-3GPP (Wi-Fi) association is introduced in Chapter 3. Each UE is able to discover the trusted AP which offers the highest normalized capacity ($C_{ua}$), based on RSSI and current spectrum conditions at both AP/UE sides. The proposed scheme is extensively validated through testbed experiments, and significantly prevails over association approaches which are given at the literature so far.

Afterwards, the efforts of this thesis focus on centralized spectrum utilization and coordination techniques in 5G Cloud-RAN architectures. Specifically, in contrast with static channel selection approaches, a scheme for self-organized non-3GPP DUs (Wi-Fi) is proposed at Chapter 4. Through continuous spectral analysis, each DU is able to dynamically discover and select the least utilized channel at its perspective. The proposed framework presents significant performance gains, compared to static channel allocation schemes and under different interference scenarios.

By taking Cloud-RAN concept a step further, the novel entity of Monitor DU is introduced and thoroughly evaluated in Chapter 5. Through the active collection and storage of several wireless metrics (DC, airtime, number of active terminals),

Monitor DUs undertake to predict the future interference levels in their areas of supervision, as well as to estimate each link's performance. More specifically, under the use of large Duty Cycle datasets, accurate long-term (2-hour) utilization predictions can be exported for all Wi-Fi channels and through Machine Learning. Thus, if combined with the RSSI of each available Wi-Fi link, the minimum transmission opportunities ($\mathcal{C}_{min}$) can be calculated. Furthermore, short-term predictions and accurate performance estimations ($\mathcal{C}_{max}$) are exported, when the current conditions are largely differentiated from the long-term predictions. The proper functioning for this comprehensive framework, is analytically proved through several Indoor and Outdoor experimental scenarios.

As analytically described above, this thesis initially focuses on the efficient spectrum utilization for Wi-Fi bands and through spectral analysis techniques. In addition to that, a novel framework for enabling dynamic Policy and Charging Rules at modern 5G multi-tenancy environments, is designed and presented in Chapter 6. By taking into consideration the symmetrical use of heterogeneous radio resources which takes place in 5G architectures, the proposed solution establishes tailored network slices under Service Level Agreements. More specifically, the OpenAirInterface and FlexRAN software were used for developing the proposed solution. Finally, several experimental UDP and TCP traffic scenarios, were performed for evaluating the proposed framework.

In the future, we foresee to extend the dynamic leasing and pricing scheme proposed in Chapter 6, for Wi-Fi radio resources. However, as extensively proved in this doctoral thesis, no guarantee for the achieved performance can be provided, at the unlicensed Wi-Fi bands. Thus, pricing and leasing could be extremely complex topic and for which a solution is sought in 5G architectures. In such way, we aim to propose novel spectrum aware pricing and leasing schemes, which can be exported from interference predictions and performance estimations (Chapter 5). Additionally, except from the Monopoly economical model which is used in Chapter 6, auction models could be an interesting alternative approach for the future as well.

# Bibliography


[1] CISCO. *Visual Networking Index: Global Mobile Data Traffic Forecast, 2018-2023*. Last accessed 30 April 2021. 2020. URL: https://www.cisco.com/c/en/us/solutions/collateral/executive-perspectives/annual-internet-report/white-paper-c11-741490.html.

[2] J. Navarro-Ortiz, P. Romero-Diaz, S. Sendra, P. Ameigeiras, J. J. Ramos-Munoz, and J. M. Lopez-Soler. "A Survey on 5G Usage Scenarios and Traffic Models". In: *IEEE Communications Surveys Tutorials* 22.2 (2020), pp. 905–929. DOI: 10.1109/COMST.2020.2971781.

[3] S. Zhang, Y. Wang, and W. Zhou. "Towards secure 5G networks: A Survey". In: *Computer Networks* 162 (2019), p. 106871. ISSN: 1389-1286. DOI: https://doi.org/10.1016/j.comnet.2019.106871. URL: https://www.sciencedirect.com/science/article/pii/S138912861830817X.

[4] G. A. Akpakwu, B. J. Silva, G. P. Hancke, and A. M. Abu-Mahfouz. "A Survey on 5G Networks for the Internet of Things: Communication Technologies and Challenges". In: *IEEE Access* 6 (2018), pp. 3619–3647. DOI: 10.1109/ACCESS.2017.2779844.

[5] G. Hampel, C. Li, and J. Li. "5G Ultra-Reliable Low-Latency Communications in Factory Automation Leveraging Licensed and Unlicensed Bands". In: *IEEE Communications Magazine* 57.5 (2019), pp. 117–123. DOI: 10.1109/MCOM.2019.1601220.

[6] S. Lien, S. Shieh, Y. Huang, B. Su, Y. Hsu, and H. Wei. "5G New Radio: Waveform, Frame Structure, Multiple Access, and Initial Access". In: *IEEE Communications Magazine* 55.6 (2017), pp. 64–71. DOI: 10.1109/MCOM.2017.1601107.

[7] X. Lin, J. Li, R. Baldemair, J. T. Cheng, S. Parkvall, et al. "5G New Radio: Unveiling the Essentials of the Next Generation Wireless Access Technology". In: *IEEE Communications Standards Magazine* 3.3 (2019), pp. 30–37. DOI: 10.1109/MCOMSTD.001.1800036.

[8] A. Pyattaev, K. Johnsson, S. Andreev, and Y. Koucheryavy. "3GPP LTE traffic offloading onto WiFi direct". In: *2013 IEEE Wireless Communications and Networking Conference Workshops (WCNCW)*. IEEE. 2013, pp. 135–140.

[9] 3GPP. *TS 23.402 V14.7.0 (2018-03), 3rd Generation Partnership Project; Technical Specification Group Services and System Aspects; Architecture enhancements for non-3GPP accesses (Release 14)*. Last accessed 30 April 2021. 2017. URL: https://www.3gpp.org/ftp//Specs/archive/23_series/23.402/23402-e70.zip.

[10] 3GPP. *TS 36.360 V14.0.0 (2017-03), 3rd Generation Partnership Project; Technical Specification Group Radio Access Network; Evolved Universal Terrestrial Radio Access (E-UTRA); LTE-WLAN Aggregation Adaptation Protocol (LWAAP) specification (Release 14)*. Last accessed 30 April 2021. 2017. URL: https://www.3gpp.org/ftp//Specs/archive/36_series/36.360/36360-e00.zip.

[11] 3GPP. *Release 17*. Last accessed 30 April 2021. 2020. URL: https://www.3gpp.org/release-17.

[12] N. Nikaein, R. Knopp, L. Gauthier, E. Schiller, T. Braun, et al. "Closer to Cloud-RAN: RAN as a Service". In: *Proceedings of the 21st Annual International Conference on Mobile Computing and Networking*. ACM. 2015, pp. 193–195.

[13] N. Makris, C. Zarafetas, P. Basaras, T. Korakis, N. Nikaein, and L. Tassiulas. "Cloud-based convergence of heterogeneous RANs in 5G disaggregated architectures". In: *2018 IEEE International Conference on Communications (ICC)*. IEEE. 2018, pp. 1–6.

[14] B. Khodapanah, A. Awada, I. Viering, D. Oehmann, M. Simsek, and G. P. Fettweis. "Fulfillment of Service Level Agreements via Slice-Aware Radio Resource Management in 5G Networks". In: *2018 IEEE 87th Vehicular Technology Conference (VTC Spring)*. 2018, pp. 1–6.

[15] V. Sciancalepore, X. Costa-Perez, and A. Banchs. "RL-NSB: Reinforcement Learning-Based 5G Network Slice Broker". In: *IEEE/ACM Transactions on Networking* 27.4 (2019), pp. 1543–1557.

[16] N. C. Luong, P. Wang, D. Niyato, Y. Liang, Z. Han, and F. Hou. "Applications of Economic and Pricing Models for Resource Management in 5G Wireless Networks: A Survey". In: *IEEE Communications Surveys Tutorials* 21.4 (Sept. 2019), pp. 3298–3339. ISSN: 2373-745X. DOI: 10.1109/COMST.2018.2870996.

[17] J. Ordonez-Lucena, P. Ameigeiras, D. Lopez, J. J. Ramos-Munoz, J. Lorca, and J. Folgueira. "Network Slicing for 5G with SDN/NFV: Concepts, Architectures, and Challenges". In: *IEEE Communications Magazine* 55.5 (2017), pp. 80–87.

[18] G. Caso, M. Le, L. De Nardis, and M.G. Di Benedetto. "Non-Cooperative and Cooperative Spectrum Sensing in 5G Cognitive Networks". In: May 2017, pp. 1–21. ISBN: 978-981-10-1389-8. DOI: 10.1007/978-981-10-1389-8_7-1.

[19] G. Caso, L. De Nardis, and M. Di Benedetto. "Toward Context-Aware Dynamic Spectrum Management for 5G". In: *IEEE Wireless Communications* 24.5 (2017), pp. 38–43. DOI: 10.1109/MWC.2017.1700090.

[20] F. Hu, B. Chen, and K. Zhu. "Full Spectrum Sharing in Cognitive Radio Networks Toward 5G: A Survey". In: *IEEE Access* 6 (2018), pp. 15754–15776. DOI: 10.1109/ACCESS.2018.2802450.

[21] A. A. Esswie and K. I. Pedersen. "On the Ultra-Reliable and Low-Latency Communications in Flexible TDD/FDD 5G Networks". In: *2020 IEEE 17th Annual Consumer Communications Networking Conference (CCNC)*. 2020, pp. 1–6. DOI: 10.1109/CCNC46108.2020.9045657.

[22] A. Yonis, M. Abdullah, and M. Ghanim. "LTE-FDD and LTE-TDD for cellular communications". In: *Progress in Electromagnetics Research Symposium* (Jan. 2012).

[23] S. Chen, S. Sun, Y. Wang, G. Xiao, and R. Tamrakar. "A comprehensive survey of TDD-based mobile communication systems from TD-SCDMA 3G to TD-LTE(A) 4G and 5G directions". In: *China Communications* 12.2 (2015), pp. 40–60. DOI: 10.1109/CC.2015.7084401.

[24] C. She, R. Dong, W. Hardjawana, Y. Li, and B. Vucetic. "Optimizing Resource Allocation for 5G Services with Diverse Quality-of-Service Requirements". In: *2019 IEEE Global Communications Conference (GLOBECOM)*. 2019, pp. 1–6. DOI: 10.1109/GLOBECOM38437.2019.9014271.

[25] M. Alasti, B. Neekzad, J. Hui, and R. Vannithamby. "Quality of service in WiMAX and LTE networks [Topics in Wireless Communications]". In: *IEEE Communications Magazine* 48.5 (2010), pp. 104–111. DOI: 10.1109/MCOM.2010.5458370.

[26] K. Zheng, X. Zhang, Q. Zheng, W. Xiang, and L. Hanzo. "Quality-of-experience assessment and its application to video services in lte networks". In: *IEEE Wireless Communications* 22.1 (2015), pp. 70–78. DOI: 10.1109/MWC.2015.7054721.

[27] A. Apostolaras, K. Chounos, L. Tassiulas, and T. Korakis. "Servicing Inelasticity, Leasing Resources and Pricing in 5G Networks". In: *2020 18th International Symposium on Modeling and Optimization in Mobile, Ad Hoc, and Wireless Networks (WiOPT)*. 2020, pp. 1–8.

[28] S. Rayanchu, A. Patro, and S. Banerjee. "Airshark: Detecting non-WiFi RF Devices Using Commodity WiFi Hardware". In: *Proceedings of IMC*. 2011.

[29] S. Gollakota, F. Adib, D. Katabi, and S. Seshan. "Clearing the RF Smog: Making 802.11N Robust to Cross-technology Interference". In: *Proceedings of SIGCOMM*. 2011.

[30] Qualcomm. "Extending the Benefits of LTE to Unlicensed Spectrum". In: *LTE in Unlicensed Spectrum workshop, Paris, France*. 2014.

[31] IEEE. *Evolution of LTE in Release 13*. Last accessed 30 April 2021. 2015. URL: http://www.3gpp.org/news-events/3gpp-news/1628-rel13.

[32] IEEE. "IEEE Standard for Information technology– Local and metropolitan area networks– Specific requirements– Part 11: Wireless LAN Medium Access Control (MAC)and Physical Layer (PHY) Specifications Amendment 5: Enhancements for Higher Throughput". In: *IEEE Std 802.11n-2009 (Amendment to IEEE Std 802.11-2007 as amended by IEEE Std 802.11k-2008, IEEE Std 802.11r-2008, IEEE Std 802.11y-2008, and IEEE Std 802.11w-2009)* (2009), pp. 1–565. DOI: 10.1109/IEEESTD.2009.5307322.

[33] IEEE. "IEEE Standard for Information technology– Telecommunications and information exchange between systemsLocal and metropolitan area networks–Specific requirements–Part 11: Wireless LAN Medium Access Control (MAC) and Physical Layer (PHY) Specifications–Amendment 4: Enhancements for Very High Throughput for Operation in Bands below 6 GHz." In: *IEEE Std 802.11ac-2013 (Amendment to IEEE Std 802.11-2012, as amended by IEEE Std 802.11ae-2012, IEEE Std 802.11aa-2012, and IEEE Std 802.11ad-2012)* (2013), pp. 1–425. DOI: 10.1109/IEEESTD.2013.6687187.

[34] E. Khorov, A. Kiryanov, A. Lyakhov, and G. Bianchi. "A Tutorial on IEEE 802.11ax High Efficiency WLANs". In: *IEEE Communications Surveys Tutorials* 21.1 (2019), pp. 197–216. DOI: 10.1109/COMST.2018.2871099.

[35] S. Rayanchu, V. Shrivastava, S. Banerjee, and R. Chandra. "FLUID: Improving Throughputs in Enterprise Wireless Lans Through Flexible Channelization". In: *Proceedings of MOBICOM*. 2011.

[36] Y. Zeng, P. H. Pathak, and P. Mohapatra. "A first look at 802.11ac in action: Energy efficiency and interference characterization". In: *Proceedings of IFIP*. 2014.

[37] M. D. Dianu, J. Riihijärvi, and M. Petrova. "Measurement-Based Study of the Performance of IEEE 802.11ac in an Indoor Environment". In: *Proceedings of ICC*. 2014.

[38] M. López-Benítez and F. Casadevall. "Spectrum Occupancy in Realistic Scenarios and Duty Cycle Model for Cognitive Radio". In: *Advances in Electronics and Telecommunications* 1.1 (Apr. 2010).

[39] M. Cardenas-Juarez, M. A. Diaz-Ibarra, U. Pineda-Rico, A. Arce, and E. Stevens-Navarro. "On spectrum occupancy measurements at 2.4 GHz ISM band for cognitive radio applications". In: *Proceedings of CONIELECOMP*. Feb. 2016, pp. 25–31. DOI: 10.1109/CONIELECOMP.2016.7438547.

[40] J. Bajaj, W. Kim, S. Y. Oh, and M. Gerla. "Cognitive radio implementation in ISM bands with Microsoft SORA". In: *Proceedings of PIMRC*. Sept. 2011, pp. 531–535. DOI: 10.1109/PIMRC.2011.6140018.

[41] V. Shrivastava, N. Ahmed, S. Rayanchu, S. Banerjee, S. Keshav, et al. "CENTAUR: Realizing the Full Potential of Centralized Wlans Through a Hybrid Data Path". In: *Proceedings of Mobicom*. 2009.

[42] Ubiquiti. *Air View*. Last accessed 30 April 2021. 2017. URL: https://help.ubnt.com/hc/en-us/articles/204950584-airMAX-How-to-use-airView-to-find-the-best-channel.

[43] netAlly. *Air Magnet Spectrum XT*. Last accessed 30 April 2021. 2017. URL: https://www.netally.com/products/airmagnet-spectrum-xt/.

[44] CISCO. *Meraki*. Last accessed 30 April 2021. 2017. URL: https://meraki.cisco.com/.

[45] IEEE. "IEEE Standard for Information Technology - Telecommunications and Information Exchange Between Systems - Local and Metropolitan Area Networks - Specific Requirements - Part 11: Wireless LAN Medium Access Control (MAC) and Physical Layer (PHY) Specifications". In: *IEEE Std 802.11-2007 (Revision of IEEE Std 802.11-1999)* (2007), pp. 1–1076. DOI: 10.1109/IEEESTD.2007.373646.

[46] G. Bianchi. "Performance analysis of the IEEE 802.11 distributed coordination function". In: *Selected Areas in Communications, IEEE Journal on* 18.3 (Mar. 2000), pp. 535–547.

[47] T.H. Meng, B. McFarland, D. Su, and J. Thomson. "Design and implementation of an all-CMOS 802.11a wireless LAN chipset". In: *Communications Magazine, IEEE* 41.8 (Aug. 2003), pp. 160–168.

[48] Openwrt. *About Ath9k backports*. Last accessed 30 April 2021. 2017. URL: https://wireless.wiki.kernel.org/en/users/drivers/ath9k.

[49] Intel. *Iwlwifi - Intel Driver 802.11n*. Last accessed 30 April 2021. 2017. URL: https://wiki.debian.org/iwlwifi.

[50] Openwrt. *Ath10k backports Releases*. Last accessed 30 April 2021. 2017. URL: https://wireless.wiki.kernel.org/en/users/drivers/ath10k/backports.

[51] Qualcomm. *AR9380 Chipset*. Last accessed 30 April 2021. 2017. URL: https://www.ath-drivers.eu/qualcomm-atheros-datasheets-for-AR9380.html.

[52] NITlab. *NITOS testbed*. Last accessed 30 April 2021. 2021. URL: https://nitlab.inf.uth.gr/NITlab/.

[53] ETTUS. *USRP B210 board*. Last accessed 30 April 2021. 2017. URL: https://www.ettus.com/all-products/ub210-kit/.

[54] SRS. *srsLTE - open-source LTE library*. Last accessed 30 April 2021. 2017. URL: https://github.com/srsLTE/srsLTE.

[55] Microsoft. *Skype Bandwidth Requirements*. Last accessed 30 April 2021. 2017. URL: https://support.skype.com/en/faq/FA1417/how-much-bandwidth-does-skype-need.

[56] NETFLIX. *Internet connection speed recommendations*. Last accessed 30 April 2021. 2017. URL: https://help.netflix.com/en/node/306.

[57] 3GPP. *TS 23.402 V15.3.0 (2018-03), 3rd Generation Partnership Project; Technical Specification Group Services and System Aspects; Architecture enhancements for non-3GPP accesses (Release 15)*. Last accessed 30 April 2021. 2018. URL: https://www.3gpp.org/ftp//Specs/archive/23_series/23.402/23402-f30.zip.

[58] 3GPP. *TS24302 3rd Generation Partnership Project; Technical Specification Group Core Network and Terminals; Access to the 3GPP Evolved Packet Core (EPC) via non-3GPP access networks; Stage 3 (Release 15)*. Last accessed 30 April 2021. 2018. URL: https://portal.3gpp.org/desktopmodules/Specifications/SpecificationDetails.aspx?specificationId=1073.

[59] K. Lee, J. Lee, Y. Yi, I. Rhee, and S. Chong. "Mobile Data Offloading: How Much Can WiFi Deliver?" In: *IEEE/ACM Trans. Netw.* 21.2 (Apr. 2013), pp. 536–550. ISSN: 1063-6692. DOI: 10.1109/TNET.2012.2218122. URL: http://dx.doi.org/10.1109/TNET.2012.2218122.

[60] 3GPP. *TS24312 3rd Generation Partnership Project; Technical Specification Group Core Network and Terminals; (ANDSF) and (MO) (Release 14)*. Last accessed 30 April 2021. 2017. URL: https://portal.3gpp.org/desktopmodules/Specifications/SpecificationDetails.aspx?specificationId=1077.

[61] S. Keranidis, T. Korakis, I. Koutsopoulos, and L. Tassiulas. "Contention and traffic load-aware association in IEEE 802.11 WLANs: Algorithms and implementation". In: *2011 International Symposium of Modeling and Optimization of Mobile, Ad Hoc, and Wireless Networks*. May 2011, pp. 334–341. DOI: 10.1109/WIOPT.2011.5930036.

[62] H. Sangtae, S. Soumya, J.W. Carlee, I. Youngbin, and C. Mung. "Tube: Time-dependent pricing for mobile data". English (US). In: *Proceedings of the ACM SIGCOMM 2012 and Best Papers of the Co-located Workshops*. Vol. 42. Dec. 2012, pp. 247–258. ISBN: 9781450314190. DOI: 10.1145/2377677.2377723.

[63] F. Mehmeti and T. Spyropoulos. "Is it worth to be patient? Analysis and optimization of delayed mobile data offloading". In: *IEEE INFOCOM 2014 - IEEE Conference on Computer Communications*. Apr. 2014, pp. 2364–2372. DOI: 10.1109/INFOCOM.2014.6848181.

[64] J. Lee, Y. Yi, S. Chong, and Y. Jin. "Economics of WiFi offloading: Trading delay for cellular capacity". In: *2013 Proceedings IEEE INFOCOM*. Apr. 2013, pp. 3309–3314. DOI: 10.1109/INFCOM.2013.6567156.

[65] E. Almeida, A. M. Cavalcante, R. C. D. Paiva, F. S. Chaves, F. M. Abinader, et al. "Enabling LTE/WiFi coexistence by LTE blank subframe allocation". In: *ICC 2013*. June 2013, pp. 5083–5088. DOI: 10.1109/ICC.2013.6655388.

[66] K. Shuaib, M. Boulmalf, F. Sallabi, and A. Lakas. "Co-existence of Zigbee and WLAN, A Performance Study". In: *2006 Wireless Telecommunications Symposium*. Apr. 2006, pp. 1–6. DOI: 10.1109/WTS.2006.334532.

[67] K. Chounos, S. Keranidis, T. Korakis, and L. Tassiulas. "Characterizing the impact of interference through spectral analysis on commercial 802.11 devices". In: *2017 IEEE International Conference on Communications (ICC)*. 2017, pp. 1–6.

[68] S. Wiethölter, M. Emmelmann, R. Andersson, and A. Wolisz. "Performance evaluation of selection schemes for offloading traffic to IEEE 802.11 hotspots". In: *ICC 2012*. June 2012, pp. 5423–5428. DOI: 10.1109/ICC.2012.6363943.

[69] N. Nguyen and T. Sato. "A Proposal for Dynamic WLAN Selection for Mobile Data Offloading in Heterogeneous Network". In: *2014 IEEE 79th Vehicular Technology Conference (VTC Spring)*. May 2014, pp. 1–5. DOI: 10.1109/VTCSpring.2014.7022792.

[70] M. H. Cheung, R. Southwell, and J. Huang. "Congestion-aware Network Selection and Data Offloading". In: *2014 48th Annual Conference on Information Sciences and Systems (CISS)*. Mar. 2014, pp. 1–6. DOI: 10.1109/CISS.2014.6814132.

[71] A. Apostolaras, G. Iosifidis, K. Chounos, T. Korakis, and L. Tassiulas. "A Mechanism for Mobile Data Offloading to Wireless Mesh Networks". In: *IEEE Transactions on Wireless Communications* 15.9 (Sept. 2016), pp. 5984–5997. ISSN: 1536-1276. DOI: 10.1109/TWC.2016.2574862.

[72] V. Passas, K. Chounos, S. Keranidis, W. Liu, L. Hollevoet, et al. "Online Evaluation of Sensing Characteristics for Radio Platforms in the CREW Federated Testbed". In: MobiCom '13. 2013.

[73] S. Keranidis, V. Passas, K. Chounos, W. Liu, T. Korakis, et al. "Online Assessment of Sensing Performance in Experimental Spectrum Sensing Platforms". In: WiNTECH '14. 2014.

[74] D. Lopez-Perez, I. Guvenc, G. de la Roche, M. Kountouris, T. Q. S. Quek, and J. Zhang. "Enhanced Intercell Interference coordination challenges in Heterogeneous Networks". In: *IEEE Wireless Communications* 18.3 (June 2011), pp. 22–30.

[75] 3GPP. *TR 38.806 V15.0.0 (2017-12), 3rd Generation Partnership Project; Technical Specification Group Radio Access Network; Study of separation of NR Control Plane (CP) and User Plane (UP) for split option 2; (Release 15)*. Last accessed 30 April 2021. 2017. URL: https://portal.3gpp.org/desktopmodules/Specifications/SpecificationDetails.aspx?specificationId=3307.

[76] 3GPP. *TS 38.470 V0.3.0 (2017-09), 3rd Generation Partnership Project; Technical Specification Group Radio Access Network; NG-RAN; F1 general aspects and principles (Release 15)*. Last accessed 30 April 2021. 2017. URL: https://portal.3gpp.org/desktopmodules/Specifications/SpecificationDetails.aspx?specificationId=3257.

[77] M. Agiwal, A. Roy, and N. Saxena. "Next Generation 5G Wireless Networks: A Comprehensive Survey". In: *IEEE Communications Surveys Tutorials* 18.3 (Sept. 2016), pp. 1617–1655. ISSN: 1553-877X. DOI: 10.1109/COMST.2016.2532458.

[78] A. Gupta and R. K. Jha. "A Survey of 5G Network: Architecture and Emerging Technologies". In: *IEEE Access* 3 (2015), pp. 1206–1232. ISSN: 2169-3536. DOI: 10.1109/ACCESS.2015.2461602.

[79] M. Kamel, W. Hamouda, and A. Youssef. "Ultra-Dense Networks: A Survey". In: *IEEE Communications Surveys Tutorials* 18.4 (Sept. 2016), pp. 2522–2545. ISSN: 1553-877X. DOI: 10.1109/COMST.2016.2571730.

[80] X. Ge, S. Tu, G. Mao, C. Wang, and T. Han. "5G Ultra-Dense Cellular Networks". In: *IEEE Wireless Communications* 23.1 (Feb. 2016), pp. 72–79. ISSN: 1536-1284. DOI: 10.1109/MWC.2016.7422408.

[81] H. Ramazanali, A. Mesodiakaki, A. Vinel, and C. Verikoukis. "Survey of user association in 5G HetNets". In: *2016 8th IEEE Latin-American Conference on Communications (LATINCOM)*. Nov. 2016, pp. 1–6. DOI: 10.1109/LATINCOM.2016.7811565.

[82] L. Wang, W. Chen, and J. Li. "Congestion aware dynamic user association in Heterogeneous cellular network: A stochastic decision approach". In: *2014 IEEE International Conference on Communications (ICC)*. June 2014, pp. 2636–2640. DOI: 10.1109/ICC.2014.6883721.

[83] K. Chounos, S. Keranidis, A. Apostolaras, and T. Korakis. "Fast Spectral Assessment for Handover Decisions in 5G Networks". In: *2019 16th IEEE Annual Consumer Communications Networking Conference (CCNC)*. 2019, pp. 1–6. DOI: 10.1109/CCNC.2019.8651673.

[84] N. Nikaein, M. Marina, S. Manickam, A. Dawson, R. Knopp, and C. Bonnet. "OpenAirInterface: A flexible platform for 5G research". In: *ACM SIGCOMM Computer Communication Review* 44.5 (2014), pp. 33–38.

[85] IEEE. *Extended Channel Switch Announcement*. Last accessed 30 April 2021. 2017. URL: https://tinyurl.com/8wzmurzk.

[86] *ACS (Automatic Channel Selection)*. Last accessed 30 April 2021. 2019. URL: https://wireless.wiki.kernel.org/en/users/documentation/acs.

[87] A. Pyattaev, K. Johnsson, S. Andreev, and Y. Koucheryavy. "3GPP LTE traffic offloading onto WiFi Direct". In: *2013 IEEE Wireless Communications and Networking Conference Workshops (WCNCW)*. 2013, pp. 135–140. DOI: 10.1109/WCNCW.2013.6533328.

[88] Y. Liu and J. Y. B. Lee. "An Empirical Study of Throughput Prediction in Mobile Data Networks". In: *2015 IEEE Global Communications Conference (GLOBECOM)*. 2015, pp. 1–6. DOI: 10.1109/GLOCOM.2015.7417858.

[89] J. Padhye, V. Firoiu, D. Towsley, and J. Kurose. "Modeling TCP throughput: A simple model and its empirical validation". In: *Proceedings of the ACM SIGCOMM'98 conference on Applications, technologies, architectures, and protocols for computer communication*. 1998, pp. 303–314.

[90] Q. He, C. Dovrolis, and M. Ammar. "On the predictability of large transfer TCP throughput". In: *ACM SIGCOMM Computer Communication Review* 35.4 (2005), pp. 145–156.

[91] C. Wang, M. Di Renzo, S. Stanczak, S. Wang, and E. G Larsson. "Artificial Intelligence Enabled Wireless Networking for 5G and Beyond: Recent Advances and Future Challenges". In: *IEEE Wireless Communications* 27.1 (2020), pp. 16–23.

[92] M. Peng, C. Kai, X. Cheng, and Q. F. Zhou. "Network Planning Based on Interference Alignment in Density WLANs". In: *IEEE Access* 7 (2019), pp. 70525–70534. DOI: 10.1109/ACCESS.2019.2919646.

[93] J. Mack, S. Gazor, A. Ghasemi, and J. Sydor. "Dynamic Channel Selection in cognitive radio WiFi networks: An experimental evaluation". In: *2014 IEEE International Conference on Communications Workshops (ICC)*. 2014, pp. 261–267.

[94] F. Maturi, F. Gringoli, and R. Lo Cigno. "A dynamic and autonomous channel selection strategy for interference avoidance in 802.11". In: *2017 13th Annual Conference on Wireless On-demand Network Systems and Services (WONS)*. 2017, pp. 1–8. DOI: 10.1109/WONS.2017.7888756.

[95] P. Nayak, S. Pandey, and E. W. Knightly. "Virtual Speed Test: an AP Tool for Passive Analysis of Wireless LANs". In: *IEEE INFOCOM 2019 - IEEE Conference on Computer Communications*. 2019, pp. 2305–2313. DOI: 10.1109/INFOCOM.2019.8737598.

[96] T. Y. Arif and R. F. Sari. "Throughput Estimates for A-MPDU and Block ACK Schemes Using HT-PHY Layer." In: (2014).

[97] K. Mansour, I. Jabri, and T. Ezzedine. "Revisiting the IEEE 802.11n A-MPDU Retransmission Scheme". In: *IEEE Communications Letters* 23.6 (2019), pp. 1097–1100. DOI: 10.1109/LCOMM.2019.2911834.

[98] H. Lee, J. Cha, D. Kwon, M. Jeong, and I. Park. "Hosting AI/ML Workflows on O-RAN RIC Platform". In: *2020 IEEE Globecom Workshops (GC Wkshps*. IEEE. 2020, pp. 1–6.

[99] T. Wang, S. Wang, and Z. H. Zhou. "Machine learning for 5G and beyond: From model-based to data-driven mobile wireless networks". In: *China Communications* 16.1 (2019), pp. 165–175. DOI: 10.12676/j.cc.2019.01.015.

[100] H. Fourati, R. Maaloul, and L. Chaari. "A survey of 5G network systems: challenges and machine learning approaches". In: *International Journal of Machine Learning and Cybernetics* 12.2 (2021), pp. 385–431.

[101] J. Moysen and L. Giupponi. "From 4G to 5G: Self-organized network management meets machine learning". In: *Computer Communications* 129 (2018), pp. 248–268.

[102] M. Polese, R. Jana, V. Kounev, K. Zhang, S. Deb, and M. Zorzi. "Machine Learning at the Edge: A Data-Driven Architecture with Applications to 5G Cellular Networks". In: *IEEE Transactions on Mobile Computing* (2020), pp. 1–1. DOI: 10.1109/TMC.2020.2999852.

[103] R. YIN, Z. ZOU, C. WU, J. YUAN, X. CHEN, and G. YU. "Learning-Based WiFi Traffic Load Estimation in NR-U Systems". In: *IEICE Transactions on Fundamentals of Electronics Communications and Computer Sciences* 104.2 (Feb. 2021), pp. 542–549. DOI: 10.1587/transfun.2020EAP1063. arXiv: 2102.04346 [cs.IT].

[104] N. Rastegardoost and B. Jabbari. "A Machine Learning Algorithm for Unlicensed LTE and WiFi Spectrum Sharing". In: *2018 IEEE International Symposium on Dynamic Spectrum Access Networks (DySPAN)*. 2018, pp. 1–6. DOI: 10.1109/DySPAN.2018.8610489.

[105] S. Kajita, H. Yamaguchi, T. Higashino, H. Urayama, M. Yamada, and M. Takai. "Throughput and Delay Estimator for 2.4GHz WiFi APs: A Machine Learning-Based Approach". In: *2015 8th IFIP Wireless and Mobile Networking Conference (WMNC)*. 2015, pp. 223–226. DOI: 10.1109/WMNC.2015.30.

[106] S. Chinchali and S. Tandon. "Deep Learning for Wireless Interference Segmentation and Prediction". In: 2012.

[107] J. Struye, B. Braem, S. Latré, and J. Marquez-Barja. "The CityLab testbed — Large-scale multi-technology wireless experimentation in a city environment: Neural network-based interference prediction in a smart city". In: *IEEE INFOCOM 2018 - IEEE Conference on Computer Communications Workshops (INFOCOM WKSHPS)*. 2018, pp. 529–534. DOI: 10.1109/INFCOMW.2018.8407018.

[108] N. Makris, P. Karamichailidis, C. Zarafetas, and T. Korakis. "Spectrum Coordination for Disaggregated Ultra Dense Heterogeneous 5G Networks". In: *2019 European Conference on Networks and Communications (EuCNC)*. IEEE. 2019, pp. 512–517.

[109] TP-LINK. *WR2543ND V1*. Last accessed 30 April 2021. 2020. URL: https://www.tp-link.com/us/support/download/tl-wr2543nd/.

[110] CISCO. *IEEE 802.11ac MCS rates*. Last accessed 30 April 2021. 2018. URL: https://community.cisco.com/t5/wireless-mobility-documents/802-11ac-mcs-rates/ta-p/3155920.

[111] H. Hewamalage, C. Bergmeir, and K. Bandara. "Recurrent Neural Networks for Time Series Forecasting: Current status and future directions". In: *International Journal of Forecasting* 37.1 (2021), pp. 388–427. ISSN: 0169-2070. DOI: https://doi.org/10.1016/j.ijforecast.2020.06.008. URL: https://www.sciencedirect.com/science/article/pii/S0169207020300996.

[112] R. Fu, Z. Zhang, and L. Li. "Using LSTM and GRU neural network methods for traffic flow prediction". In: *2016 31st Youth Academic Annual Conference of Chinese Association of Automation (YAC)*. 2016, pp. 324–328. DOI: 10.1109/YAC.2016.7804912.

[113] R. Dey and F. M. Salem. "Gate-variants of Gated Recurrent Unit (GRU) neural networks". In: *2017 IEEE 60th International Midwest Symposium on Circuits and Systems (MWSCAS)*. 2017, pp. 1597–1600. DOI: 10.1109/MWSCAS.2017.8053243.

[114] F. A. Gers, J. Schmidhuber, and F. Cummins. "Learning to forget: continual prediction with LSTM". In: *1999 Ninth International Conference on Artificial Neural Networks ICANN 99. (Conf. Publ. No. 470)*. Vol. 2. 1999, 850–855 vol.2.

[115] D. Kingma and J. Ba. "Adam: A Method for Stochastic Optimization". In: *International Conference on Learning Representations* (Dec. 2014).

[116] Keras. *Machine Learning: Early Stopping*. Last accessed 30 April 2021. 2021. URL: https://keras.io/api/callbacks/early_stopping/.

[117] *Airodump-ng*. Last accessed 30 April 2021. 2020. URL: https://www.aircrack-ng.org/doku.php?id=airodump-ng.

[118] F. Fuentes and D. Kar. "Ethereal vs. Tcpdump: a comparative study on packet sniffing tools for educational purpose". In: *Journal of Computing Sciences in Colleges* 20.4 (2005), pp. 169–176.

[119] Wireshark. *tshark - Dump and analyze network traffic*. Last accessed 30 April 2021. 2020. URL: https://www.wireshark.org/docs/man-pages/tshark.html.

[120] M. Bredel and M. Fidler. "Understanding Fairness and its Impact on Quality of Service in IEEE 802.11". In: *IEEE INFOCOM 2009*. 2009, pp. 1098–1106.

[121] H. J. Escalante. "A comparison of outlier detection algorithms for machine learning". In: *Proceedings of the International Conference on Communications in Computing*. 2005, pp. 228–237.

[122] R. Sparks. "Weighted moving averages: An efficient plan for monitoring specific location shifts". In: *International Journal of Production Research* 42 (June 2004). DOI: 10.1080/0020754042000197720.

[123] *Iperf Speed Test Tool*. Last accessed 30 April 2021. 2021. URL: https://iperf.fr/.

[124] K. Chounos, N. Makris, and T. Korakis. "Enabling Distributed Spectral Awareness for Disaggregated 5G Ultra-Dense HetNets". In: *2019 IEEE 2nd 5G World Forum (5GWF)*. 2019, pp. 304–309. DOI: 10.1109/5GWF.2019.8911661.

[125] I. Syrigos, N. Sakellariou, S. Keranidis, and T. Korakis. "On the Employment of Machine Learning Techniques for Troubleshooting WiFi Networks". In: *2019 16th IEEE Annual Consumer Communications Networking Conference (CCNC)*. 2019, pp. 1–6. DOI: 10.1109/CCNC.2019.8651823.

[126] F. Z. Yousaf, M. Bredel, S. Schaller, and F. Schneider. "NFV and SDN—Key Technology Enablers for 5G Networks". In: *IEEE Journal on Selected Areas in Communications* 35.11 (2017), pp. 2468–2478.

[127] C. Bouras, A. Kollia, and A. Papazois. "SDN NFV in 5G: Advancements and challenges". In: *2017 20th Conference on Innovations in Clouds, Internet and Networks (ICIN)*. 2017, pp. 107–111.

[128] S. Matoussi, I. Fajjari, N. Aitsaadi, R. Langar, and S. Costanzo. "Joint Functional Split and Resource Allocation in 5G Cloud-RAN". In: *IEEE International Conference on Communications (ICC)*. 2019.

[129] A. Maeder, M. Lalam, A. De Domenico, E. Pateromichelakis, D. Wübben, et al. "Towards a flexible functional split for cloud-RAN networks". In: *2014 European Conference on Networks and Communications (EuCNC)*. 2014, pp. 1–5.

[130] D. Wubben, P. Rost, J. S. Bartelt, M. Lalam, V. Savin, et al. "Benefits and Impact of Cloud Computing on 5G Signal Processing: Flexible centralization through cloud-RAN". In: *IEEE Signal Processing Magazine* 31.6 (2014), pp. 35–44.

[131] 3GPP. *TS 23.501 System architecture for the 5G System (5GS)*. Last accessed 30 April 2021. 2020. URL: https://portal.3gpp.org/desktopmodules/Specifications/SpecificationDetails.aspx?specificationId=3144.

[132] 3GPP. *TS 23.502 3GPP Procedures for the 5G System (5GS)*. Last accessed 30 April 2021. 2020. URL: https://tinyurl.com/yp4m5756.

[133] *Open Air Interface*. Last accessed 30 April 2021. 2021. URL: https://www.openairinterface.org/.

[134] X. Foukas, N. Nikaein, M. M. Kassem, M. K. Marina, and K. Kontovasilis. "FlexRAN: A Flexible and Programmable Platform for Software-Defined Radio Access Networks". In: *Proceedings of*. CoNEXT. 2016.

[135] 3GPP. *TS 23.503 Policy and charging control framework for the 5G System (5GS)*. Last accessed 30 April 2021. 2020. URL: https://tinyurl.com/76fp3bnk.

[136] S. O. Oladejo and O. E. Falowo. "5G network slicing: A multi-tenancy scenario". In: *2017 Global Wireless Summit (GWS)*. 2017, pp. 88–92.

[137] G. Iosifidis, L. Gao, J. Huang, and L. Tassiulas. "A Double-Auction Mechanism for Mobile Data-Offloading Markets". In: *IEEE/ACM Transactions on Networking* 23.5 (2015), pp. 1634–1647.

[138] M. Mira, C. Tijani, C. Lin, E. Jocelyne, and M. Fabio. "A two-level auction for resource allocation in multi-tenant C-RAN". In: *Comput. Networks* 135 (2018), pp. 240–252. DOI: 10.1016/j.comnet.2018.02.005. URL: https://doi.org/10.1016/j.comnet.2018.02.005.

[139] HUAWEI. *E392 LTE Dongle*. Last accessed 30 April 2021. 2020. URL: https://routerunlock.com/huawei-e392-modem-features-specifications/.

[140] I. Sodagar. "The MPEG-DASH Standard for Multimedia Streaming Over the Internet". In: *IEEE MultiMedia* 18.4 (2011), pp. 62–67.

[141] APACHE. *HTTP Server*. Last accessed 30 April 2021. 2020. URL: https://httpd.apache.org/.

[142] VideoLAN. *VLC media player*. Last accessed 30 April 2021. 2020. URL: https://www.videolan.org/vlc/index.html.

1

[1] The LaTeX template can be found at the following link.